Analysis of Multimode Low-Probability-of-Intercept (LPI) Communications With Atmospheric Effects

THESIS

Ala Ghordlo
Captain, Royal Jordanian Air Force

AFIT/GE/ENG/96D-03

19970113 057

DEPARTMENT OF THE AIR FORCE
AIR UNIVERSITY
AIR FORCE INSTITUTE OF TECHNOLOGY

Wright-Patterson Air Force Base, Ohio

DISTRIBUTION STATEMENT A
Approved for public release;
Distribution Unlimited

DTIC QUALITY INSPECTED 1

AFIT/GE/ENG/96D-03

Analysis of Multimode Low-Probability-of-Intercept (LPI)

Communications With

Atmospheric Effects

THESIS

Ala Ghordlo
Captain, Royal Jordanian Air Force

AFIT/GE/ENG/96D-03

Approved for public release; distribution unlimited

The views expressed in this thesis are those of the author and do not reflect the official policy or position of the Department of Defense or the U. S. Government.

AFIT/GE/ENG/96D-03

Analysis of Multimode Low-Probability-of-Intercept (LPI) Communications With Atmospheric Effects

THESIS

Presented to the Faculty of the School of Engineering

of the Air Force Institute of Technology

Air University

In Partial Fulfillment of the

Requirements for the Degree of

Master of Science in Electrical Engineering

Ala Ghordlo, B.ENG

Captain, Royal Jordanian Air Force

December, 1996

Approved for public release; distribution unlimited

Acknowledgements

First of all I would like to thank the Royal Jordanian Air Force (RJAF) for giving me this chance to come to AFIT and enhance my knowledge at this great institution. In addition, I would like to thank my advisor Maj. Gerald Gerace for his support guidance and continuous feedback. Also I would like to thank my committee members Dr. A. Terzuoli and Dr. V. Pyati (Thank you for taking me on so late and at short notice). And I would like to thank Maj. Robert Mills for helping me put my ideas together and his exceptional knowledge in LPI communications.

I would like to thank my family for their moral support, prayers and their solid belief in me giving me the courage and dedication to get through AFIT. And most of all I would like to thank my wife Lamia for her support and patience and trying to make life as comfortable as possible for me throughout my stay here at AFIT. Of course, the best thanks are for my son Lom for the joyful breaks (intended or unintended) he gave me releasing some of the pressure of work.

Ala Ghordlo

Table of Contents

Page

List of Figures

Figure | Page

List of Tables

List of Abbreviations and Symbols

Abbreviations	*Description*
AWGN	Additive White Gaussian Noise
BPF	Band Pass Filter
BPSK	Binary Phase Shift Keying
CDMA	Code Division Multiple Access
DS	Direct Sequence
DS-SS	Direct Sequence Spread Spectrum
EIRP	Effective Isotropic Radiated Power
FH-SS	Frequency Hopping Spread Spectrum
GHz	Gigahertz
I	Interceptor
INFOSEC	Information Security
ITS	Institute of Telecommunication And Science
kHz	Kilohertz
km	Kilometers
kPa	KiloPascal
LPI	Low-Probability-of-Intercept
MALPI	Multiple Access Low-Probability-of-Intercept
MHz	Megahertz
MPM	Millimeteric Propagation Model
PSD	Power Spectral Density
PSK	Phase Shift Keying
R_x	Receiver

RH .... Relative Humidity

SNR .... Signal-To-Noise Ratio

SS .... Spread Spectrum

T_x .... Transmitter

TH-SS .... Time Hopping Spread Spectrum

TRANSEC .... Transmission Security

VHF .... Very High Frequency

WWII .... Second World War

Symbols — *Description*

$\mathbf{A}_e$ .... antenna effective area

$\mathbf{A}_{er}$ .... effective area of receiving antenna

$\mathbf{ATM}_c$ .... atmospheric conditions in communication link

$\mathbf{ATM}_i$ .... atmospheric conditions in interception link

a .... range power index for ground-to-air propagation

$\mathbf{B}_c$ .... receiver bandwidth

$\mathbf{B}_i$ .... interceptor bandwidth

$\mathbf{B}_{mod}$ .... modulated signal bandwidth

$\mathbf{B}_{ss}$ .... spread spectrum bandwidth

c .... speed of light in free space

d .... wideband radiometer detectability factor

E .... Electric field strength

$\mathbf{E}_b$ .... bit energy

e .... partial pressure of water vapor

$\mathbf{f}$ .... carrier frequency

$\mathbf{F}_c$ .... receiver noise figure

$\mathbf{F}_i$ .... interceptor noise figure

$\mathbf{G}$ .... antenna gain

$\mathbf{G}_{ct}$ .... receiver gain in transmitter direction

$\mathbf{G}_{it}$ .... interceptor gain in transmitter direction

$\mathbf{G}_p$ .... processing gain

$\mathbf{G}_t$ .... transmitter antenna gain

$\mathbf{G}_{tc}$ .... transmitter antenna gain in receiver direction

$\mathbf{G}_r$ .... receiver antenna gain

$\mathbf{G}_{ti}$ .... transmitter antenna gain in interceptor direction

$\mathbf{g}_{cm}$ .... adaptive interference suppression factor for receiver

$\mathbf{g}_{cn}$ .... null steering antenna factor for receiver

$\mathbf{g}_{in}$ .... adaptive interference suppression factor for interceptor

$\mathbf{g}_{im}$ .... null steering antenna factor for interceptor

$\mathbf{H}_0$ .... hypothesis that no signal is present

$\mathbf{H}_1$ .... hypothesis that signal is present

$\mathbf{H_2O}$ .... chemical symbol for water

$\mathbf{h}_i$ .... interceptor height above ground level

$\mathbf{h}_r$ .... receiver height above ground level

$\mathbf{h}_t$ .... transmitter height above ground level

$\mathbf{J}_{nmc}$ .... the jamming power from *nth* jammer in *mth* frequency at receiver input

$\mathbf{J}_{nmi}$ .... the jamming power from *nth* jammer in *mth* frequency at the interceptor input

$\mathbf{k}$ .... Boltzmann constant

$\mathbf{k}_g$ .... air-to-ground propagation constant

$\mathbf{k}_r$ .... coefficient of imaginary refractivity of rain

$\mathbf{L}_{ATM}$ .... atmospheric loss

$\mathbf{L}_c$ .... atmospheric losses in communication link

$\mathbf{L}_i$ .... atmospheric losses in interception link

$\mathbf{L}_p$ .... antenna pattern loss

$\mathbf{L}_{pp}$ .... Hata model total propagation loss

$\mathbf{L}_t$ .... transmission line loss

$\mathbf{L}_{urban}$ .... Hata model propagation loss in urban areas

M .... mode quality factor in decimals

m .... meters

$\mathbf{M}_f$ .... number of frequencies

N .... dispersive part of refractivity of medium

$\mathbf{N}'$ .... real part of N

$\mathbf{N}''$ .... imaginary part of N

n .... refractive index of medium

$\mathbf{N}_c$ .... water-vapor continuum contribution

$\mathbf{N}_d$ .... dry air nonresonant refractivity

$\mathbf{N}_j$ .... number of jammers and jamming directions

$\mathbf{N}_{jc}$ .... jammers PSD at receivers input

$\mathbf{N}_{ji}$ .... jammers PSD at interceptor input

$\mathbf{N}_l$ .... moist air resonance contribution to N

$\mathbf{N}_n$ .... total noise

$\mathbf{N}_o$ .... thermal noise PSD

$\mathbf{N}_{oc}$ .... thermal noise at receiver input

$\mathbf{N}_{oi}$ .... thermal noise at interceptor input

$\mathbf{N}_{ol}$ .... nondispersive part of refractivity

$\mathbf{N}_r$ .... refractivity of rain

$\mathbf{N}_{sc}$ .... total noise plus interference PSD at the receiver input

$\mathbf{N}_{si}$ .... total noise plus interference PSD at the interceptor input

$\mathbf{N}_t$ .... total refractivity

$\mathbf{N}_w$ .... suspended water droplet refractivity

$\mathbf{O}_2$ .... chemical symbol for oxygen

$\mathbf{P}$ .... transmitted signal carrier power

$\mathbf{P}_d$ .... probability of detection

$\mathbf{P}_e$ .... probability of error

$\mathbf{P}_f$ .... probability of false alarm

$\mathbf{P}_m$ .... probability of miss

$\mathbf{P}_t$ .... transmitter output power

$\mathbf{P}_l$ .... barometric pressure as input for Liebe model

$\mathbf{P}_{lc}$ .... barometric pressure in communication link

$\mathbf{P}_{li}$ .... barometric pressure in intercept link

$\mathbf{P}_r$ .... received power

$\mathbf{p}$ .... partial pressure of dry air

$\mathbf{Q}_{ANT}$ .... antenna quality factor

$\mathbf{Q}_{ATM}$ .... atmospheric quality factor

$\mathbf{Q}_{IS}$ .... interference suppression quality factor

$\mathbf{Q}_{LPI}$ .... LPI quality factor

$\mathbf{Q}_M$ .... mode quality factor

$\mathbf{Q}_{MOD}$ .... modulation quality factor

$\mathbf{R}$ .... range

$\mathbf{R}_b$ .... signal bit rate

$\mathbf{R}_c$ .... communication range

$\mathbf{R}_d$ .... direct range

$\mathbf{R}_i$ .... interception range

$\mathbf{R}_l$ .... rainfall rate as input for Liebe model

$\mathbf{R}_{lc}$ .... rainfall rate in communication link

$\mathbf{R}_{li}$ .... rainfall rate in interception link

$\mathbf{R}_r$ .... reflected range

S .... signal power

$\mathbf{SNR}_{av}$ .... Available SNR

$\mathbf{SNR}_{conv}$ ... required SNR for interception with transmitter employing conventional modulation

$\mathbf{SNR}_c$ .... required SNR for receiver to receive the signal

$\mathbf{SNR}_i$ .... required SNR for interceptor to detect the signal

$\mathbf{SNR}_{req}$ .... conventionally required SNR by a system

$\mathbf{SNR}_{ss}$ .... required SNR for interception with transmitter employing SS techniques

$\mathbf{S}_c$ .... received signal power at the receiver

$\mathbf{S}_i$ .... received signal power at the interceptor

t .... time

$\mathbf{T}_{ac}$ .... receiver antenna temperature

$\mathbf{T}_{ai}$ .... interceptor antenna temperature

$\mathbf{T}_d$ .... signal propagation delay

$\hat{T}_d$ .... receiver estimate of signal propagation delay

$\mathbf{T}_i$ .... interceptor observation time

$\mathbf{T}_l$ .... ambient temperature of atmosphere as input for Liebe model

$\mathbf{T}_{lc}$ .... ambient temperature of atmosphere in communication link

$\mathbf{T}_{li}$ .... ambient temperature of atmosphere in intercept link

$\mathbf{T}_o$ .... ambient temperature

$\mathbf{U}_l$ .... relative humidity as input for Liebe model

$\mathbf{U}_{lc}$ .... relative humidity of atmosphere in communication link

$\mathbf{U}_{li}$ .... relative humidity of atmosphere in intercept link

$\mathbf{V}_T$ .... decision threshold

$\mathbf{W}_l$ .... water droplet concentration of atmosphere as input for Liebe model

$\mathbf{W}_{lc}$ .... water droplet concentration of atmosphere in communication link

$\mathbf{W}_{li}$ .... water droplet concentration of atmosphere in interception link

$\mathbf{w}$ .... radian carrier frequency

Γ .... reflection coefficient

α .... wave attenuation constant

α_c .... communication link loss due to the atmosphere in dB/km

α_i .... interception link loss due to the atmosphere in dB/km

β .... wave phase dispersion constant

γ .... complex wave propagation constant

δR .... path difference

ϵ .... medium permittivity

ϵ' .... real part of permittivity

ϵ'' .... imaginary part of permittivity

ϵ_o .... absolute permittivity

ϵ_r .... relative permittivity

η ... the ratio of resultant power to direct power at the receiver in ground-to-ground propagation

θ .... grazing angle

λ .... signal transmitted signal wavelength

μ .... medium permeability

μ' .... real part of permeability

μ'' .... imaginary part of permeability

μ_o .... absolute permeability

μ_r .... relative permeability

τ .... dispersive delay

ϕ .... received signal random phase

ϕ_c .... spreading code phase

ϕ_d .... modulating data phase

ψ_p phase difference between direct and reflected wave due to path difference in ground-to-ground propagation

ψ_r .... phase shift of reflected wave in ground-to-ground propagation

ψ_t .... total phase difference between direct and reflected wave in ground-to-ground propagation

Abstract

This research expanded Low-Probability-of-Intercept (LPI) communications analysis in two areas. First, multimode communication was included to account for ground-to-ground and air-to-ground links in addition to the standard air-to-air links traditionally used in LPI analysis. The propagation equations for the three modes of interest were derived and included in LPI analytic models in the form of a *mode quality factor* to account for multimode LPI scenarios. This new quality factor was used in studying several communication and interception link combinations. Variations due to differences between the communication and interception modes were presented graphically.

Second, atmospheric conditions were included to account for atmospheric attenuation. Previously, both links were assumed to be under the same atmospheric conditions. This assumption limits LPI analysis to scenarios where the receiver and interceptor are are located close to each other. Therefore, the *atmospheric quality factor* had to be expanded to include scenarios where the communication link and the interception link are experiencing different and possibly fluctuating atmospheric conditions. The atmospheric propagation losses were accounted for by using the Liebe atmospheric propagation model to estimate atmospheric attenuation in dB/km for any practical atmospheric conditions. The atmospheric quality factor was then applied to the analysis of various scenarios for communication and interception links under similar and different atmospheric conditions. The results were represented graphically emphasizing the changes in LPI quality due to atmospheric conditions. It was apparent from the simulations, that LPI analysis was greatly enhanced by including the atmospheric quality factor.

Finally, using both the mode and the atmospheric quality factors along with all the standard quality factors, a comprehensive LPI analysis was performed for many possible LPI scenarios. The results were presented graphically to show variations due the mode and atmospheric quality factors on LPI analysis. In all scenarios considered, theoretical models for the three different propagation

modes and estimates of atmospheric attenuation using the Liebe model were used in simulations with binary phase shift key (BPSK) signals and a wideband radiometer as the interceptor. Similarly, analysis of the mode quality factor indicates certain combinations of communication and interception modes may provide an advantage to the communication link, such as in the case of air-to-ground communications with ground-to-ground interception. Analysis of the atmospheric quality factor indicates different atmospheric conditions in each link may provide an advantage for the communication link such as in the case of air-to-air communication in dry air with air-to-air interception under 100 mm/h rain. Alternatively, the mode and the atmospheric conditions could degrade overall LPI quality if the above situations were reversed. The results clearly showed that the mode and atmospheric quality factors play a dramatic role in LPI analysis.

Analysis of Multimode Low-Probability-of-Intercept (LPI)
Communications With
Atmospheric Effects

I. Introduction

1.1 Background

The prime goal of communications planners is to transfer information between a transmitter and a receiver as securely as possible. This goal is of prime importance because in military communications scenarios it is inevitable that the enemy would attempt to disrupt or intercept sensitive information. In order to prevent information compromise, several methods have been employed either to conceal the communications signals or to prevent the enemy from extracting usable information from these signals. These methods are divided into two categories: information security (INFOSEC), and transmission security (TRANSEC) [1].

The first category INFOSEC, aims to conceal the information contained in the signal, not the signal itself, in order to prevent the interceptor from extracting information from the signal. An example of INFOSEC is the well-known method of cryptography. In cryptography the message is transformed into a form that prevents the disclosure of its content by the interceptor [2]. The second category TRANSEC, which aims to hide communication signals while making them less susceptible to jamming and interception. To prevent interception, TRANSEC aims to lower the probability of detection by unfriendly receivers through reduction of the signal-to-noise ratio (SNR) of the signal at the intended receiver; at the unintended receiver the probability that the signal will be detected and exploited is greatly reduced. This type of TRANSEC signal is called Low-Probability-of-Intercept (LPI) communications, a type of communication that is fundamental for secure and

survivable communications [2]. LPI is defined as the design of the most efficient communication system that maximizes performance and minimizes detectability by unintended receivers [3].

In order to achieve the goal of secure communications, various technologies are exploited, some of which are adaptive antennas, spread spectrum communications, interference suppression filters, and error control coding [3]. The use of these technologies, coupled with the effect of several interfering factors, results in the design of LPI quality factors.

Although these factors are a good reference and means of design assessment, they do not fully analyze LPI communications. Specifically, there are *two important limitations* that stand out. *First*, the LPI quality factors were derived for air-to-air communications mode and do not consider others, such as air-to-ground and ground-to-ground. However, all modes of communications are employed to transfer information in military operations. *Second*, the traditional LPI quality factors are based on free space communications and, usually, do not address atmospheric effects properly. And if atmospheric effects are considered, it is assumed that the receiver and transmitter are in the same atmosphere and nearly at the same distance from the transmitter. However, in most situations, communications are not conducted under free space conditions, but actually under variable atmospheric conditions. Also the standard assumption of same atmospheric conditions and same distance, on both the communication and interception links, is not always true. Although several models of the atmosphere have been developed, none were used to study and incorporate the atmospheric effects on LPI communications. Therefore, when it comes to situations other than free space air-to-air communications, the traditional LPI quality factors do not accurately assess LPI communications. Consequently, there is a need to analyze LPI quality factors to include other modes of communications. Further, it is important to include real time atmospheric effects in LPI analysis by using one of the atmospheric models. This analysis will result in a better assessment and understanding of the covertness and effectiveness of LPI communications.

1.2 Problem Statement

Communication security and survivability are very crucial to the success of military operations, especially if they are conducted in hostile territory. The measure of communications covertness can be quantified through the LPI quality factors. To make these quality factors more accurate and general the two limitations mentioned above should be addressed more carefully. Therefore, this research will tackle the two limitations by exploring means to quantify their effects and include the results in the LPI analysis. First, the LPI quality factors will be re-derived to be valid for three modes of communications commonly used in information transfer; air-to-air, air-to-ground, and ground-to-ground. This can be achieved by including another factor to the current LPI quality factors to account for the communication modes employed by the communication and interception links. Second, this research will examine atmospheric effects on LPI communication links by using the Liebe model of the atmosphere to quantify atmospheric effects on the LPI communication links. Also study what effect changing the atmospheric conditions on both links have on LPI analysis.

1.3 Summary of Current Knowledge

1.3.1 **LPI Communications.** The main objective of LPI is to reduce the intercept range with respect to the communication range. Achieving this goal forces intercepter to move closer to allow detection of communication signals. Generally, the LPI concept started with a simple form of LPI systems which focused on reducing the transmitted power and maintain close communications. This resulted in limiting the communication range but reduced the possibility of interception. An example of such a system is the ARC-164 airborne communication system which is installed on most aircrafts built by western countries. The ARC-164 has a switch which changes the transmitted power between 5 and 10 dBw. The 5 dBw position is for secure communications and the 10 dBw position is for normal communications. Recently, there was an attempt to study this subject in

depth and establish some metrics to aid in the design of LPI systems. Glenn Prescott[1], Lawrence Gutman[2] and Robert Mills[3] are currently considered leading LPI researchers. Their work resulted in design and performance metrics for LPI communication systems called the LPI quality factors.

These quality factors are LPI, antenna, interference suppression, modulation, and atmospheric quality factors. The LPI quality factor, Q_{LPI}, is a measure of the relation between the communication and interception ranges. The antenna quality factor, Q_{ANT}, compares the gains of the antennas in the system. The interference suppression quality factor, Q_{IS}, compares the sensitivities of the receiver and interceptor to noise. The modulation quality factor, Q_{MOD}, compares the SNR required by the receiver to receive the signal and the interceptor to detect the signal. The atmospheric quality factor, Q_{ATM}, compares the atmospheric losses in both the interception and communication links. The full details and derivation of these quality factors is discussed in section 2.1, the main formulas are given as [3]

$$20 \log \left(\frac{R_c}{R_i} \right) = 10 \log \left(\frac{G_{tc} G_{ct}}{G_{ti} G_{it}} \right) + 10 \log \left(\frac{N_{si}}{N_{sc}} \right) + 10 \log \left(\frac{S_i / N_{si}}{S_c / N_{sc}} \right) + 10 \log \left(\frac{L_i}{L_c} \right) \quad (1.1)$$

$$Q_{LPI} = Q_{ANT} + Q_{IS} + Q_{MOD} + Q_{ATM}. \quad (1.2)$$

However, it is known that using the air-to-air propagation equation for other modes is very optimistic since the air-to-air mode suffers much less losses than the air-to-ground and ground-to-ground modes. Therefore, it is important to investigate the propagation modes in more detail and include the results in the LPI analysis. Also the atmospheric quality factor, which is dependent on the losses due to the atmosphere in the communication and intercept paths, was not clearly studied and was assumed to be negligible. These losses are a function of frequency, atmospheric conditions, and the ranges in the intercept and communication paths. However, in the past, the

[1] University of Kansas Telecommunication and Information Science Laboratory
[2] Wright Research and Development Center, Wright Patterson AFB
[3] Air Force Institute of Technology faculty during part of this research

intercept and communication ranges and losses are assumed to be nearly the same. Obviously, this assumption is in conflict with the main objective of LPI communications, the desire to increase the communication range as much as possible with respect to the intercept range. The next two sections give a brief discussion of the atmosphere and propagation modes.

1.3.2 **Communication Modes.** Mainly, there are three communication modes air-to-air, air-to-ground, and ground-to-ground. These modes have different propagation characteristics which results in different amount of propagation losses. The air-to-air and ground-to-ground propagation modes are well defined and formulated [15] [16]. But there is no conclusive formulation for air-to-ground propagation. Actually, it is generally assumed that the air-to-ground propagation losses are a function of the range to the power of a number in the range of 2 to 4 [10] [29]. Since air-to-air and ground-to-ground propagation modes represent a lower and upper bounds for propagation losses, it is reasonable to consider the air-to-ground loss as an intermediate loss between them. Another issue to point out is the presence of several propagation models such as the Data model that predict propagation losses for a given scenario [27]. But such propagation models have several disadvantages to be used in LPI analysis as will be discussed in section 2.2

1.3.3 **The Atmosphere.** The main part of the atmosphere that affects most communication systems is the lower section known as the troposphere (about 0 - 10 km above ground level). Knowledge of the effects of the troposphere on communication signals is essential to system analysis because the atmosphere is within the troposphere where some of the propagating wave energy is absorbed by molecules, mainly water and oxygen, present in the atmosphere [6]. Experimenters became aware of the effects of the troposphere on wave propagation as early as the 1930s [25]. At that time, research was developed on transmission in the VHF band of frequencies. Of course, one of the major catalysts for the communication field development was WWII, during which a lot of research and development of communication principles and techniques were established and equipment built [4]. After WWII, an unprecedented advance in technology, knowledge and appli-

cations of communications began to take place. This advance resulted in an increased demand on exploiting more and more of the higher range of the frequency spectrum.

However, the use of higher frequencies exposes communication signals to atmospheric effects which are more pronounced as frequency increases [5]. Although a lot of research is still being done on the atmosphere, no conclusive formulation has been achieved, primarily since atmospheric characteristics are extremely variable. Consequently, much of the design and planning of communication links depends on empirical information based on extensive observation of electromagnetic waves propagation characteristics. Also, some researchers have introduced models of the atmosphere that can be used to give real time references [6].

One of the well-established models is the Liebe Model, also called the Millimeter-wave Propagation Model (MPM) first developed by The Institute for Telecommunication Science (ITS). The model gives a practical means to simulate the atmosphere and predict signal attenuation, delay and phase dispersion (0 - 30 km altitude). The Liebe Model input variables are barometric pressure, temperature, relative humidity, frequency, suspended water droplet concentration, and rainfall rate [7]. Although the Liebe Model involves some approximations, the results obtained are in good agreement with the theoretical values. Therefore, this model is effective for studying the atmospheric effects on communication links.

The calculation of range is commonly performed by assuming that electromagnetic waves propagate with velocity c, about 2.9979×10^8 m/s, which corresponds to the speed of light in free space. However in most applications, waves do not propagate in free space, but actually travel in the troposphere. Thus, the wave velocity in this medium is less than c. This implies that calculated ranges which assume free space are optimistic because received power calculation is based on assuming free space losses, and this power is used to predict the range. But actual received power is lower due to the losses being higher, resulting in a lower true range. Although in most applications the inaccuracy of computing ranges is not important, there are situations that

require accuracy in range measurement [9]. One such situation is LPI communications, in which range computations are important for assessing the effectiveness and covertness of communication systems.

1.4 Assumptions

In this research the following assumptions apply:

- All analyses are done in the far field. Since in typical communication scenarios the vast majority of communication links are established over a range of tens of kilometers, which are basically in the far field for the frequencies of interest.
- Earth surface is assumed to be quasi-smooth and flat to limit the research to propagation effects and avoid terrain effects.
- For the purpose of calculations and simulations antennas are assumed to be omni-directional. The antennas gains are accounted for in the antenna quality factor which is also an important factor in LPI link analysis.
- The Liebe Model of the atmosphere gives a reasonably correct measure of atmospheric effects on signal propagation. This assumption should be valid since the model is based on many years of meticulous laboratory experimentation and has been extensively reviewed by propagation scientists and engineers in the related discipline. And the results obtained are in good agreement with theoretical and experimental values.

1.5 Scope

This research examined three modes of communications air-to-air, air-to-ground, and ground-to-ground to give LPI metrics that apply to these modes. Also the analysis included atmospheric effects on the communication modes being studied. In addition, situations in which atmospheric

conditions in the communication and intercept paths are different was addressed for various atmospheric conditions such as rain, fog, and moist air. The analysis of these situations shed a light on the possible use of the atmosphere to the communicators advantage, enhancing LPI systems utilization. The propagation and atmospheric effects were studied employing a binary phase shift key (BPSK) signal and wideband radiometer as an interceptor. The effects of jamming and other forms of interference were not considered.

1.6 Approach

The research was conducted in the following order:

- The initial knowledge of LPI communication systems and quality factors was gathered by acquiring and reading the available literature on LPI communications, wave propagation, and on atmospheric modeling.
- Propagation equations for air-to-air, air-to-ground, and ground-to-ground communications were derived.
- The LPI quality factors were re-derived to account for air-to-air, air-to-ground, and ground-to-ground communication modes. This was achieved by using the derived propagation equations in the same analysis used in the derivation of the original LPI quality factors. Also to distinguish between the propagation modes and in turn the communication modes, boundaries are established.
- The new LPI metrics were programmed into a MATLAB® [registered trademark of Mathworks] code to be used in the analysis. The MATLAB® code asks for the heights and other system parameters for the transmitter, receiver, and interceptor and based on these inputs the modes of the communication and interception links is determined by the code. Also it gives the propagation losses for each link.

- The Liebe Model of the atmosphere was programmed into a MATLAB® code to be used in the analysis. This code has input variables that account for the following atmospheric parameters temperature, barometric pressure, relative humidity, frequency, suspended water droplet concentration, and rainfall rate.
- A MATLAB® code was written to test the degradation of communication signals passing through the atmosphere (The Liebe Model) for various atmospheric conditions.
- A graphic representation of the analysis showing LPI effectiveness in various modes of communication, and showing effect of the atmosphere on these modes of communication was produced to clarify the importance of including communication modes and atmospheric effects in LPI system analysis.

1.7 Material and Equipment

The MATLAB® software available in the AFIT (Air Force Institute of Technology) Computer Sun Workstation was used for performing the required analysis of LPI links, and graphic representation of the results.

1.8 Thesis Organization

This thesis consists of six chapters. Chapter I is this introduction. Chapter II introduces LPI communications theory, link analysis, quality factors, and discrepancies in current LPI analysis. In addition, it explains interception and wideband radiometer intercept receiver. Also it discusses multimode propagation and atmospheric effects issues. Furthermore, it presents the concept of Spread Spectrum (SS) communications and its advantages for LPI communications. Chapter III presents the propagation equations for air-to-air, air-to-ground, and ground-to-ground propagation modes. In addition, it introduces the boundaries between these propagation modes which are used in the scenarios studied in chapter IV.

Chapter IV presents the possible LPI scenarios. And using the propagation equations for the three modes of communication the scenarios are analyzed presenting an overall multimode LPI quality equation. As a result, a new quality factor called *the mode quality factor* is introduced. Chapter V presents and discusses the results obtained for propagation and atmospheric effects on LPI links for the various scenarios discussed in chapter IV showing possible enhancements and vulnerabilities. Also it discusses and graphically presents mode and atmospheric attenuation effects on LPI links and possible utilization of atmospheric conditions to enhance covertness. Chapter VI summarizes the thesis and provides recommendations that would further improve LPI analysis.

II. Theory

2.1 LPI Communications

The objective of LPI communications is to reduce, as much as possible, the range at which the signal can be intercepted by unfriendly receivers while at the same time maintaining, or even improving, the communication range of the intended receiver. A graphical representation of this objective is shown in figure 2.1 a and b. Figure 2.1a, illustrates the case of a typical conventional

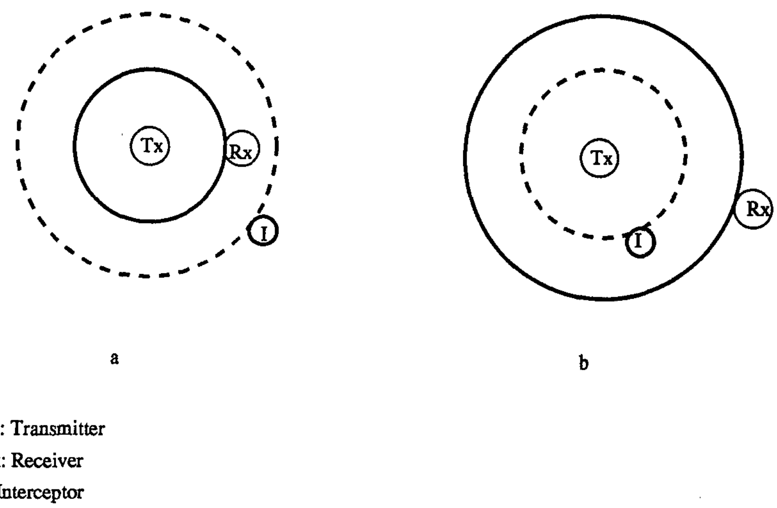

Figure 2.1 Illustration of LPI objective

communications situation where the intercept receiver can detect the signal at a distance larger than the communication receiver because interceptors usually require lower signal-to-noise ratio (SNR) to detect the presence of a signal. However, when LPI techniques are employed, the interceptor needs to move closer to detect the signal or the communication receiver can increase its range and still be able to receiver the signal as shown in figure 2.1 b.

The communication system designer can work towards achieving information transfer between the transmitter and the receiver while reducing the probability of being intercepted, which is the goal of LPI communications, by employing a variety of techniques that help reduce the probability of interception. Some of these techniques are high gain directional antennas, adaptive nulling

antennas, adaptive interference suppression filters, and custom waveform design [1]. A well-known waveform design technique is spread spectrum which based on using a transmission bandwidth that is much greater than the minimum bandwidth required for the signal.

A typical air-to-air communication and interception communications scenario is shown in figure 2.2.

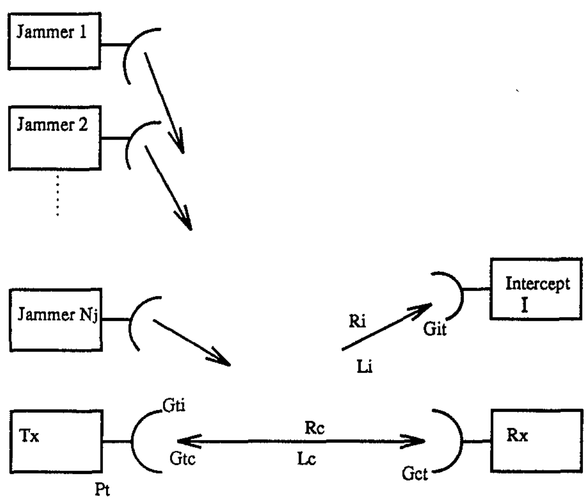

Figure 2.2 Typical LPI scenario

where

- T_x is the transmitter
- R_x is the receiver
- I is the interceptor
- R_i is the interception range
- R_c is the communication range
- L_i is atmospheric losses in interception link
- L_c is atmospheric losses in communication link
- G_{tc} is transmitter antenna gain in receiver direction

- G_{ct} is receiver antenna gain in transmitter direction
- G_{ti} is transmitter antenna gain in interceptor direction
- G_{it} is interceptors antenna gain in transmitter direction

In this environment the transmitter is attempting to convey information to the intended receiver, and the intercept receiver is trying to detect the signal, and maybe extract information. At the same time, several jammers are aiming to disrupt the information transfer to the intended receiver, which of course will result in the same effect on the intercept receiver. In order to understand the relationship between the various parameters of the systems in figure 2.2, a complete link analysis is performed in the following subsections.

2.1.1 **LPI communication link analysis.** The performance of each element in the LPI communications system is governed by several performance parameters, giving an overall measure of the LPI quality of the system. For example the jammer is characterized by its transmitted power, bandwidth and antenna gain; the transmitter is characterized by its transmitted power, antenna gain and type of modulation employed; the interceptor is characterized by its antenna gain, noise bandwidth and acceptable probabilities of detection (P_d) and false alarm (P_f); and the receiver is characterized by its antenna gain, noise bandwidth, system noise figure, modulation type employed, and minimum bit energy to noise power spectral density (PSD), E_b/N_o required to maintain a desired bit error probability. P_e. The last parameter is the most important from the communicator's point of view. Thus. the performance requirement is the bit error probability, P_e. The bit energy to noise ratio, E_b/No. can be related to the signal-to-noise PSD ratio by

$$\frac{S_c}{N_{sc}} = R_b \frac{E_b}{N_{sc}} \tag{2.1}$$

where

- S_c is the received signal power in *watts*

- R_b is the signal bit rate in *bits/second*
- E_b is the bit energy in *joules*
- N_{sc} is the noise plus interference power spectral density (PSD) at the receiver input in *watts/hz.*

Now going to the basic link budget equation, the power at the receiver input is [11] [10]

$$S_c = \frac{P_t G_{tc} G_{ct}}{(4\pi R_c/\lambda)^2 L_c(R_c, ATM_c)} \tag{2.2}$$

where

- P_t is transmitter output power in *watts*
- G_{tc} is transmitter antenna gain in the receivers direction
- G_{ct} is receiver antenna gain in transmitter direction
- R_c is the communication range in *km*
- $L_c(R_c, ATM_c)$ accounts for the losses due to the atmosphere and is explicitly dependent on R_c, the communication range. and ATM_c, atmospheric conditions in communication link.

The atmosphere, in turn, depends on the following parameters

$$ATM_c = f(T_{lc}, U_{lc}, W_{lc}, R_{lc}, f, P_{lc}) \tag{2.3}$$

where

- T_{lc} is ambient temperature, of atmosphere in communication link, in $°C$
- U_{lc} is relative humidity, of atmosphere in communication link, in $\%RH$
- W_{lc} is water droplet concentration, of atmosphere in communication link, in g/m^3
- R_{lc} is rainfall rate, of atmosphere in communication link, in mm/h

- f is carrier frequency in Ghz
- P_{lc} is the barometric pressure, of atmosphere in communication link, in kPa.

And noise plus interference(intentional and nonintentional) PSD at receiver input is [11]

$$N_{sc} = N_{oc} + N_{jc} \tag{2.4}$$

$$N_{sc} = kT_{ac} + kT_o(F_c - 1) + \sum_{n=1}^{N_j}\sum_{m=1}^{M_f} g_{cn}g_{cm}\frac{J_{nmc}}{B_c} \tag{2.5}$$

where

- N_{oc} is thermal noise PSD, at receiver input, in $watts/hz$
- N_{jc} is jammers PSD, at receiver input, in $watts/hz$
- k is Boltzmann constant 1.38×10^{-23} $watt/K - hz$ or J/K
- T_{ac} is communication receiver antenna temperature in K
- T_o is ambient temperature in K
- F_c is noise figure for communication receiver
- N_j is the number of jammers and jamming directions
- M_f is the number of frequencies
- g_{cn} is null steering antenna
- g_{cm} is adaptive interference suppression
- J_{nmc} is the jamming power from nth jammer in mth frequency, at receiver input, in $watts$
- B_c is communications receiver bandwidth in hz

The double summation term represents the summing the effect of jamming on each frequency component by all jammers, which counts for N_j jammers transmitting from N_j directions, jamming M_f frequency components. The next step is to compute the signal power to noise plus interference PSD ratio at receiver input which is achieved by dividing equation 2.2 by N_{sc} resulting in the following [11] [10]

$$\frac{S_c}{N_{sc}} = \frac{P_t G_{tc} G_{ct}}{(4\pi R_c/\lambda)^2 N_{sc} L_c(R_c, ATM_c)}. \tag{2.6}$$

Then rearranging this equation gives an expression for the communication range, R_c, as

$$R_c^2 = \frac{P_t G_{tc} G_{ct}}{(4\pi/\lambda)^2 N_{sc} L_c(R_c, ATM_c)} \left(\frac{1}{S_c/N_{sc}}\right) \tag{2.7}$$

where L_c is the losses due to the atmosphere in the communication path, and is a function of the range and atmospheric conditions imposed on the path.

2.1.2 **Interception Link.** The interceptor is required to maintain a desired probability of detection, P_d, and probability of false alarm, P_f. Therefore, the desired performance is governed by the received signal power to noise plus interference PSD ratio, S_i/N_{si}, which determines P_d and P_f. The intercept link is analyzed in similar fashion using intercept parameters. This gives power at interceptor input as [11] [10]

$$S_i = \frac{P_t G_{ti} G_{it}}{(4\pi R_i/\lambda)^2 L_i(R_i, ATM_i)} \tag{2.8}$$

where

- S_i is the intercepted signal power in *watts*
- G_{ti} is transmitter antenna gain in interceptor direction
- G_{it} is interceptor antenna gain in transmitter direction

- R_i is the interception range in km
- L_i accounts for atmospheric losses due to the atmosphere in the intercept link
- ATM_i is atmospheric conditions in the intercept link

And noise plus interference (intentional and nonintentional) PSD at interceptor input is

$$N_{si} = N_{oi} + N_{ji} \tag{2.9}$$

or

$$N_{si} = kT_{ai} + kT_o(F_i - 1) + \sum_{n=1}^{N_j} \sum_{m=1}^{M_f} g_{in} g_{im} \frac{J_{nmi}}{B_i} \tag{2.10}$$

similarly giving a signal power to noise plus interference PSD at interceptor input of

$$\frac{S_i}{N_{si}} = \frac{P_t G_{ti} Git}{(4\pi R_i/\lambda)^2 N_{si} L_i(R_i, ATM_i)}. \tag{2.11}$$

Then rearranging this equation gives an expression for the interception range, R_i, gives [10]

$$R_i^2 = \frac{P_t G_{ti} G_{it}}{(4\pi/\lambda)^2 N_{si} L_i(R_i, ATM_i)} \left(\frac{1}{S_i/N_{si}} \right) \tag{2.12}$$

similarly, L_i is losses due to the atmosphere and is explicitly dependent on intercept range and atmospheric conditions imposed on the intercept path.

2.1.3 **LPI Quality Factors.** The next step is to establish a meaningful relationships between the receiver and interceptor parameters that would provide an insight on how to interpret these relationships to be able to give a measure of the covertness of the system. Using equations

2.7 and 2.12 for the communication and intercept ranges. Dividing equation 2.7 by 2.12 gives

$$\left(\frac{R_c}{R_i}\right)^2 = \left(\frac{G_{tc}G_{ct}}{G_{ti}G_{it}}\right)\left(\frac{N_{si}}{N_{sc}}\right)\left(\frac{S_i/N_{si}}{S_c/N_{sc}}\right)\left(\frac{L_i}{L_c}\right). \tag{2.13}$$

Then converting to decibels

$$20\log\left(\frac{R_c}{R_i}\right) = 10\log\left(\frac{G_{tc}G_{ct}}{G_{ti}G_{it}}\right) + 10\log\left(\frac{N_{si}}{N_{sc}}\right) + 10\log\left(\frac{S_i/N_{si}}{S_c/N_{sc}}\right) + 10\log\left(\frac{L_i}{L_c}\right). \tag{2.14}$$

Which is defined as the *LPI* quality factors equation given as

$$Q_{LPI} = Q_{ANT} + Q_{IS} + Q_{MOD} + Q_{ATM}. \tag{2.15}$$

As can be seen equation 2.14 relates similar parameters in one factor which are defined in the following sections.

2.1.3.1 **LPI Quality Factor.** This main quality factor, according to this derivation, defines the relationship between the communication and intercept ranges and is given by

$$Q_{LPI} = 20\log\left(\frac{R_c}{R_i}\right). \tag{2.16}$$

It is desired for LPI communications to make its quality factor, Q_{LPI}, as large as possible. From communicator's stand point large Q_{LPI} means a larger range of communications or lower system requirements for some given range. As for the interceptor, large Q_{LPI} means a smaller intercept range or higher system requirements for some given range.

2.1.3.2 **Antennas Quality Factor.** This quality factor highlights the effect of the antennas gains. Mainly, it defines the relation between gains of the antennas in the system. It is

defined as

$$Q_{ANT} = 10 \log \left(\frac{G_{tc} G_{ct}}{G_{ti} G_{it}} \right). \tag{2.17}$$

To improve performance or covertness, it is required to make Q_{ANT} as high as possible, which in turn improves Q_{LPI}. The increase in Q_{ANT} can be achieved by using directional antennas with high gain in desired direction and small side lobes or nulls in interceptor direction. This requires large G_{tc} and G_{ct}, and small G_{ti}. As for G_{it} it is the interceptors requirement to make it as large as possible. But the interceptor is limited by how much G_{it} can be increased since increasing G_{it} means a narrower antenna beam resulting in reducing probabilities of intercepting the transmission in the right direction at the right time.

2.1.3.3 **Interference Suppression Quality Factor.** This factor is basically a design comparison of how well can the receiver and interceptor suppress interference at their inputs. That is, how much interference (intentional or nonintentional) the system can withstand and still be able to receive the signal and distinguish it from interference for both the receiver and interceptor. It is defined as

$$Q_{IS} = 10 \log \left(\frac{N_{si}}{N_{sc}} \right) \tag{2.18}$$

where N_{si} is the total interference present at the interceptor input and N_{sc} is the total interference present at the receiver input. Therefore, improving interference suppression properties of the receiver with respect to the interceptor results in improving Q_{LPI}.

2.1.3.4 **Modulation Quality Factor.** This is the most important factor since it is the essence of the system performance. It is defined as

$$Q_{MOD} = 10 \log \left(\frac{S_i/N_{si}}{S_c/N_{sc}} \right) \tag{2.19}$$

where S_i/N_{si} is the signal power to noise plus interference PSD Ratio required by the interceptor to intercept the signal, and S_c/N_{sc} is the signal power to noise plus interference PSD Ratio required by the communication receiver to receive the signal and extract information from it. Q_{MOD} is independent of the other LPI quality factors and is design dependent based upon the receiver and interceptor design parameters P_e, P_d, and P_f. These parameters are based on signal design (modulation, bandwidth, and detection techniques). Therefore, any measures that aim to decrease the required PSD by the receiver and increase the required PSD by the interceptor results in increasing Q_{MOD} and inturn Q_{LPI}.

2.1.3.5 **Atmospheric Quality Factor.** This factor, even though assumed negligible in traditional LPI analysis, it could prove useful. The atmospheric quality factor is expressed as

$$Q_{ATM} = 10 \log \left(\frac{L_i}{L_c} \right) = \alpha_i R_i - \alpha_c R_c \tag{2.20}$$

where α_i is the loss due to the atmosphere in the intercept path in dB/km, and α_c is the loss due to the atmosphere in the communication path in dB/km. This quality factor is a function of the communication and interception ranges, and the atmospheric conditions in these links. As a result, it is desired to make α_i and R_c as large as possible, and α_c and R_i as small as possible. It can be noticed that there is a direct relationship between α_i and R_c, therefore increasing α_i results in increasing R_c for a fixed α_c and R_i. The eventual result desired is a large Q_{ATM} which in turn increases Q_{LPI}. The traditional LPI analysis basically ignores atmospheric effects under the

assumption that the receiver and the interceptor are both under the same atmospheric conditions and are at nearly the same range. *But this assumption is in contradiction with the way LPI quality factors are defined.* Because according to LPI analysis the atmospheric quality factor is a function of the ranges ratio and having the same atmospheric conditions and being at nearly the same range means that $\alpha_c = \alpha_i$ and $R_c = R_i$. However the LPI quality factor is also a function of the ranges ratio and when they are equal then the LPI quality factor will always be 0 dB even if other parameters in the links are changed. This result means that the whole LPI analysis is useless. Therefore, it is important to address atmospheric effects more clearly.

Generally, LPI research evolved gradually starting with point-to-point communication links, consisting, basically, of a transmitter-receiver pair, one or more jammers, and an interceptor. Then it was expanded to include multiple access networks which are termed Multiple Access LPI (MALPI) which is defined as "a collection of users sharing a radio frequency channel such that the detectability of the overall network is minimized" [11]. Although LPI research has advanced considerably in the last few years, all LPI research have over looked two important issues. First, these researches based their link analyses on free-space propagation equation, which is only valid for air-to-air communications. Second, they tend to weakly address the effect of the atmosphere, mainly atmospheric attenuation.

Therefore it is important to address propagation modes other than air-to-air since communications, especially military communications, involve all modes of communications. In this research the focus was on studying air-to-air, air-to-ground, and ground-to-ground communication modes and establishing an LPI formulation that is valid for these three modes and compatible with the already available LPI quality factors mentioned in chapter two. Also atmospheric effects were considered to study how much degradation it causes on LPI links, and how we can capitalize on atmospheric conditions to the communicators advantage, which will be discussed also in chapter III.

2.2 Propagation Models And Atmospheric Models

There are several propagation models, mainly, developed for point-to-point mobile communications. These propagation models are based on experimental results and are interested in closing the communication links. Also there are some atmospheric models which are based on statistical averages. To give more detail of propagation and atmospheric models one of the most known propagation models, called the Hata Model, and one of the most prominent atmospheric models, called the Liebe Model, are discussed in the next two sections followed by a discussion if their is a potential for using either one in LPI analysis.

2.2.1 **The Hata Model.** The Hata Model evolved from the Okumura method, which is a method for predicting propagation mean path loss based on extensive experimental studies. However, since Okumura's method requires extracting results from a family of curves it is not practical for use in system planning [27]. Therefore, Hata put Okumura's results in formulas, using curve fitting techniques, to simplify Okumura's results and make them easy to apply [26].

Hata established empirical formulas to give the predicted path loss in the form $K(R_c)^{-r}$, where K is a constant dependent on the situation parameters (antennas heights, frequency, and range), and r a constant in the range of 2 to 4. This model is applicable for frequency range of 150 to 1500 Mhz, transmitter height of range 30 to 200 m, receiver height range of 1 to 10 m, and communication range of 1 to 20 km. The mathematical form of the Hata model, for quasi-smooth open area, is given by [16] [27]

$$L_{pp} = L_{urban} - 4.78(\log f)^2 + 18.33\log f - 40.94 \qquad dB \qquad (2.21)$$

$$L_{urban} = 69.55 + 26.16\log f - 13.82\log h_t - a(h_r) + (44.9 - 6.55\log R_c \quad dB \qquad (2.22)$$

$$a(h_r) = (1.1\log f - 0.7)h_r - (1.56\log f - 0.8) \qquad m \qquad (2.23)$$

where

- L_{pp} is total propagation loss in dB
- L_{urban} is urban areas propagation loss in dB
- f is the carrier frequency in Mhz
- h_t is transmitter antenna height in m
- h_r is receiver antenna height in m
- R_c is communication range in km.

This expression is much easier to use to predict propagation path loss than Okumura's curves. For more detail on the Hata model see [27]

2.2.2 **The MPM Model.** As discussed in chapter I it is desired to explore higher frequencies of the spectrum, but atmospheric propagation limitations dominate any steps of moving towards higher frequencies. Generally, the power transmitted from an antenna is attenuated as it travels away from the transmitter due to two independent effects:

1. The transmitted wave spreads out from the antenna.
2. The wave power is absorbed and scattered by the medium it travels in.

The first phenomenon can only be dealt with by using receive antennas with large effective area. As for the second phenomenon the signal power lost can not be captured or recovered since it is lost before it reaches the receiver. For the purpose of this research the focus will be on the second phenomenon, which deals with molecular absorption due to atmospheric gases (O_2 and H_2O), and absorption and scattering by liquid and solid particles in the atmosphere (fog and rain) [13].

To be able to predict system performance in a given atmospheric condition it is required to have a model that effectively predicts how the atmosphere will attenuate signals. Of course, exact prediction is very difficult but it is possible to get very close by taking into account the largest possible number of observable phenomenon to assess atmospheric attenuation on signals [7][8]. One

of the well-established models of atmospheric attenuation is the MPM Model (For more detail on the MPM Model see appendix A).

The MPM Model was developed by The Institute for Telecommunication Science (ITS). It provides practical means to simulate the atmosphere and predict signal attenuation, delay, and phase dispersion due to the atmosphere (0 - 30 km altitude). The MPM Model input variables are barometric pressure, temperature, relative humidity, frequency, suspended water droplet concentration and rainfall rate [7]. Although the MPM Model involves some approximations the results obtained are in good agreement with theoretical and experimental values. Therefore, this model is good for studying atmospheric effects on communication links. The derivation of propagation losses in terms of attenuation and phase dispersion is achieved by using the electromagnetic and propagation theory. Where the complex propagation constant γ contains the attenuation and phase dispersion factors α and β, which are generally real, given by [24]

$$\gamma = \alpha + j\beta \tag{2.24}$$

which is also defined as a function of wave propagation electromagnetic parameters by [22]

$$\gamma = jw\sqrt{\mu\epsilon'}\frac{\sqrt{\epsilon' - j\epsilon''}}{\sqrt{\epsilon'}} \tag{2.25}$$

where $j = \sqrt{-1}$ the complex operator. $w = 2\pi f$ is the radian frequency, μ is the medium permeability, ϵ' is the real part of the medium permittivity, and ϵ'' is the imaginary part of the medium permittivity. These terms are defined as

$$\begin{aligned} \mu &= \mu' - j\mu'' = \mu_o\mu_r \qquad \text{H/m} && (2.26) \\ \epsilon &= \epsilon' - j\epsilon'' = \epsilon_o\epsilon_r \qquad \text{F/m} && (2.27) \end{aligned}$$

where μ' is the real part of the medium permeability, μ'' is the imaginary part of the medium permeability, μ_r is the relative permeability, μ_o is the absolute permeability, ϵ_r is the relative permittivity, and ϵ_o is the absolute permittivity. These parameters define the speed of light, c, and the refractive index, n, by

$$c = \frac{1}{\sqrt{\mu_o \epsilon_o}} \tag{2.28}$$

$$n = \sqrt{\mu_r \epsilon_r} \tag{2.29}$$

The variations in the value of the refractive index are usually small, therefore a more convenient measure of the refractive properties of the atmosphere is introduced, which is called the refractivity, N_t, defined as [25]

$$N_t = N_{ol} + N = N_{ol} + N' - jN'' = (n-1)10^6 \tag{2.30}$$

where N_{ol} is the nondispersive part of refractivity, N' is the real part of dispersive refractivity , and N'' is the imaginary part of dispersive refractivity. Using the above definitions of the variables in equation 2.25 simplifies to

$$\gamma = jw\sqrt{\mu\epsilon} = jw\sqrt{\mu_o \mu_r \epsilon_o \epsilon_r} \tag{2.31}$$

$$= \frac{jw}{c} n \tag{2.32}$$

$$= \frac{jw}{c}\left(\frac{N}{10^6} - 1\right) \tag{2.33}$$

$$= \alpha + j\beta = \frac{jw}{c}\left(\frac{N' - jN''}{10^6} + 1\right). \tag{2.34}$$

Then equating the real and imaginary parts gives

$$\alpha = \left(\frac{w}{c}\right)\left(\frac{N''}{10^6}\right) \qquad \text{Np/m} \tag{2.35}$$

$$\beta = \left(\frac{w}{c}\right)\left(\frac{N'}{10^6}+1\right) \qquad \text{rad/m} \tag{2.36}$$

And using the conversion factor [22]; from Np/m to dB/m of 8.69, and from rad/m to deg/m of 57.296. which are then converted to dB/km and deg/km results in [7]

$$\alpha = 0.1820 f N'' \qquad \text{dB/km} \tag{2.37}$$

$$\beta = 3.36 f N'. \qquad \text{deg/km} \tag{2.38}$$

The following figures give examples of the results obtained by the MPM Model showing the amount of attenuation suffered by electromagnetic waves, propagating through the atmosphere, as a function of frequency and atmospheric conditions.

Figure 2.3, shows atmospheric attenuation in dB/km with respect to frequency in varying humidity levels in the atmosphere. Figure 2.4, shows atmospheric attenuation , dB/km, with respect to frequency in varying rain levels. And figure 2.5 presents atmospheric attenuation, dB/km, with respect to frequency for different fog levels. In conclusion, we define better or favorable atmospheric conditions as the conditions when the atmospheric losses get lower and worse atmospheric conditions when losses get higher. Atmospheric losses increase when atmospheric parameters increase such as rainfall rate, barometric pressure, fog level, and humidity.

2.2.3 **Discussion of Models.** The Hata propagation loss model presented in previous sections, similar models, have some short comings which can be summarized in the following three points. First, atmospheric effects are implicitly included in the experimental results and the con-

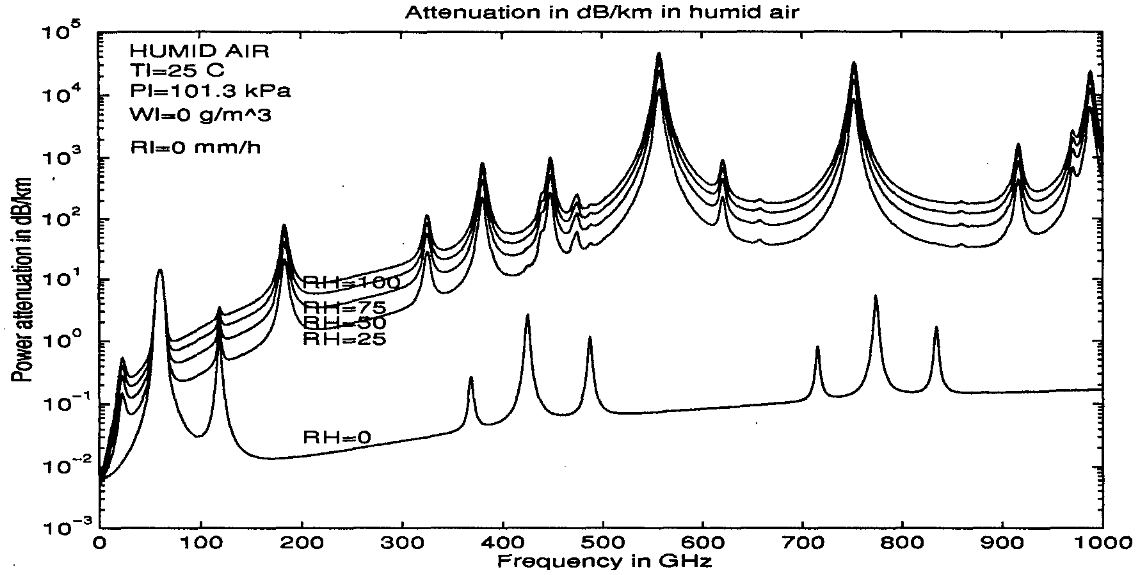

Figure 2.3 MPM model attenuation in humid air for five values of relative humidity, U_l, ($U_l = 0$, 25, 50, 75 and 100 $\%RH$)

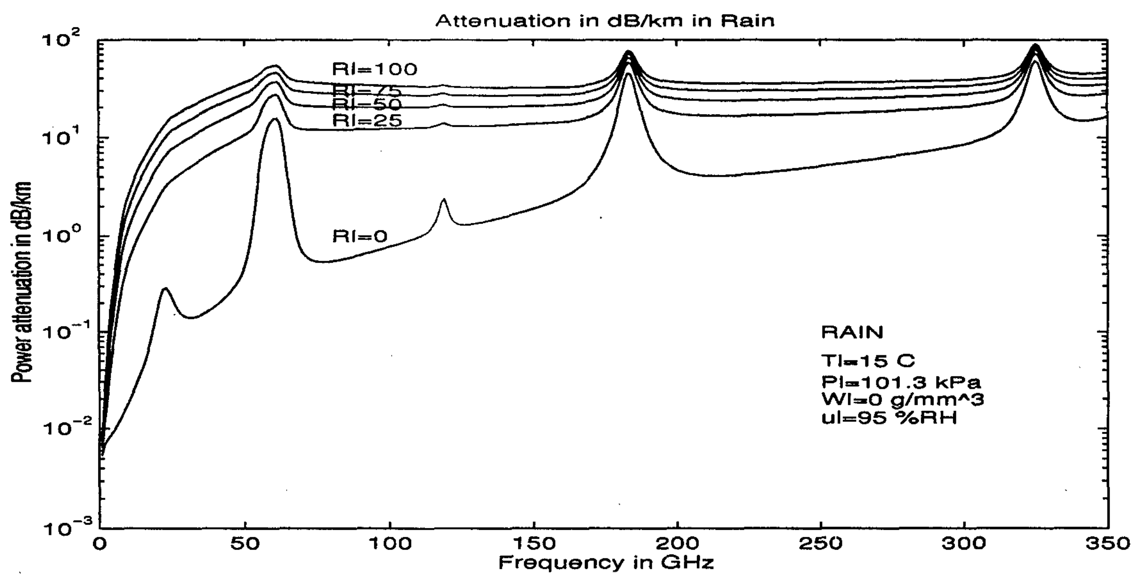

Figure 2.4 MPM Model attenuation in rain for five values of rainfall rate, R_l, (R_l =0, 25, 50, 75 and 100 mm/h)

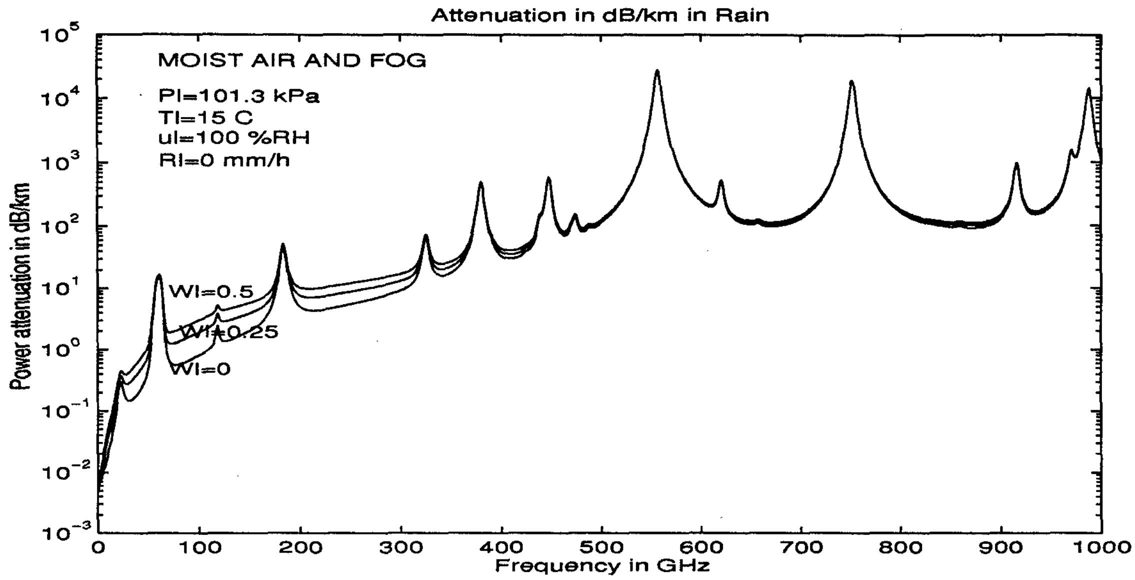

Figure 2.5 MPM Model Attenuation in Fog for three levels of water droplet concentration, W_l, (W_l =0, 0.25 and 0.5 g/mm^3)

sequent formulas can not be used to extract the LPI quality factors separately. However, in LPI analysis it is desirable to be able to consider atmospheric losses and mode effects separately and utilize either one or both to enhance covertness. Second, this model and others similar in format and derivation (such as Allbrook's, Blomquist-Ladell, and Edward-Durkin models [16] [18]) are based on experimental results obtained in a certain area or location under certain atmospheric conditions [18]. Consequently, these results do not necessarily apply to other areas. Third, they tend to mix air-to-ground and ground-to-ground propagation modes and do not have distinct boundaries between them. Therefore, it is not practical or useful to use a propagation model in LPI analysis. As for the Liebe model of the atmosphere, it gives a great degree of flexibility in being able to give the atmospheric attenuation for any weather conditions. In addition, it gives the atmospheric attenuation in dB/km which directly fits in the atmospheric quality factor in LPI analysis by α_c and α_i for any given atmospheric conditions. Therefore, the Liebe model can be merged in LPI analysis to create a useful atmospheric quality factor.

The previous discussions showed that more work is needed to put the propagation modes into perspective. On the other hand, the Liebe model gives a very good and practical means of measuring atmospheric losses under any weather conditions. Before going any farther, since the main objective of LPI is to make R_c and R_i comparatively small. And since the antennas are assumed to be omnidirectional (unity gain) the only possible quality factor that can be employed to achieve the LPI objective (ignoring the atmospheric quality factor and the modes) in the traditional LPI analysis is modulation quality factor, Q_{MOD}. Popular techniques to increase Q_{MOD} are spread spectrum (SS) techniques. Spread spectrum is used to compensate for mode losses or atmospheric losses or both by increasing transmitting power to maintain the communication link by maintaining the required postspreading SNR while reducing the SNR received by the interceptor. The use of SS in LPI is discussed in more detail in chapter V. The next section gives a brief discussion of these techniques.

2.3 Spread Spectrum (SS) Communications

As mentioned in chapter I one of the methods to achieve jam resistant and LPI communications is Spread Spectrum (SS) techniques. This section presents spread spectrum theory and its benefits to LPI communications.

In spread spectrum the modulated information is modulated (spread) a second time, not dependent on the information first modulation, to expand the bandwidth of the transmitted signal and make it larger than the original information bandwidth [23]. This process makes the signal power spectral density (PSD) resemble additive white Gaussian noise (AWGN) which makes the signal appear noise like or random at the intercept receiver. At the intended receiver the signal is deterministic and detectable since the intended receiver has prior knowledge of the spreading technique employed by the transmitter [2]. Spread spectrum techniques have the following main properties [14]

1. The transmitted signal bandwidth is greater than the minimum bandwidth required by the modulated information.

2. The modulated information is spread by using a spreading code signal that is independent of the modulated information.

3. the intended receiver despreads the received signal by correlating it with a replica of the spreading code signal employed by the transmitter. Then the modulated information is demodulated using conventional demodulation techniques.

Spread Spectrum (SS) has several applications and desirable advantages such as improvement of signal interference rejection capabilities, code division multiple access (CDMA) applications, and enhanced Low-Probability-of-Interception (LPI) capabilities [23]. There are three primary spread spectrum techniques [1]:

1. Direct Sequence Spread Spectrum (DS-SS) in which the modulated information is spread by modulating the modulated information with a digital code sequence called Direct Sequence (DS).

2. Frequency Hopping Spread Spectrum (FH-SS) in which the modulated information is shifted over a larger bandwidth divided into a number of cells of bandwidth equal to that of the information bandwidth. The shifting is controlled by a code sequence.

3. Time Hopping Spread Spectrum (TH-SS) in which bursts of the modulated information are transmitted at time intervals dictated by a code sequence.

In this research only one result of SS is of interest which is the processing gain, G_p. Therefore, to obtain the processing gain DS-SS is discussed briefly in the next section.

2.3.1 **Direct Sequence Spread Spectrum.** Direct sequence spread spectrum randomly, using a pseudo-random code sequence, varies the modulated information phase prior to transmission [1]. This results in spreading, randomly, the transmitted power over the entire SS

bandwidth reducing the power spectral density, PSD, level [26]. At the other end of the communication link the receiver is required to perform two additional steps compared with the conventional receiver. First, it must learn the code sequence that was employed by the transmitter to spread the signal, this process is called acquisition. Then continue to reproduce this code sequence, this process is called tracking. The acquisition and tracking processes together are called synchronization. Second, the receiver is also required to return the received signal to its modulated information bandwidth by removing the SS bandwidth. The SS bandwidth is removed by multiplying the received signal with a replica of the spreading code used by the transmitter. This process is called carrier despreading [2]. After the despreading the signal is in its standard modulated information form which can be conventionally demodulated to extract the information transmitted.

A conceptual diagram of a typical DS-SS system is shown in figure 2.6 [23].

The digital binary baseband information, $d(t)$, is phase shift key (PSK) modulated by the first modulator giving the modulated waveform $s(t)$ by

$$s(t) = \sqrt{2P}\cos(w_o t + \phi_d(t)) \tag{2.39}$$

where w_o is the carrier frequency. P is the carrier power, and $\phi_d(t)$ is the data phase modulation. Then multiplying $s(t)$ by the spreading code gives the transmitted signal as

$$y(t) = \sqrt{2P}\cos(w_o t + \phi_d(t) + \phi_c(t)) \tag{2.40}$$

where $\phi_c(t)$ is the spreading code phase modulation.

The binary Phase Shift Keying (BPSK) is achieved by making the spreading code and information signals have an instantaneous phase change of π radians; that is, they are both antipodal

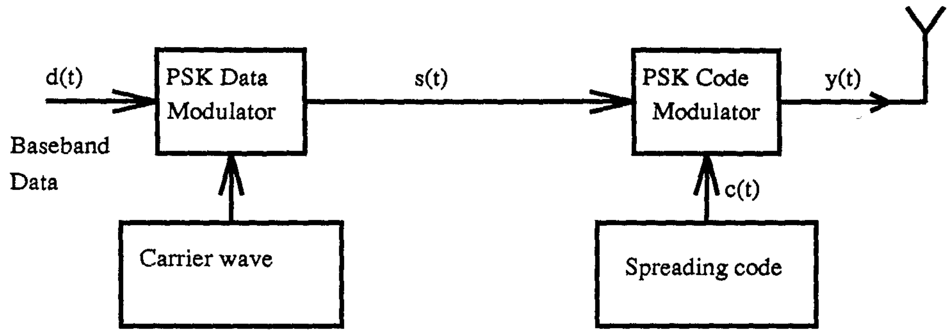

Transmitter

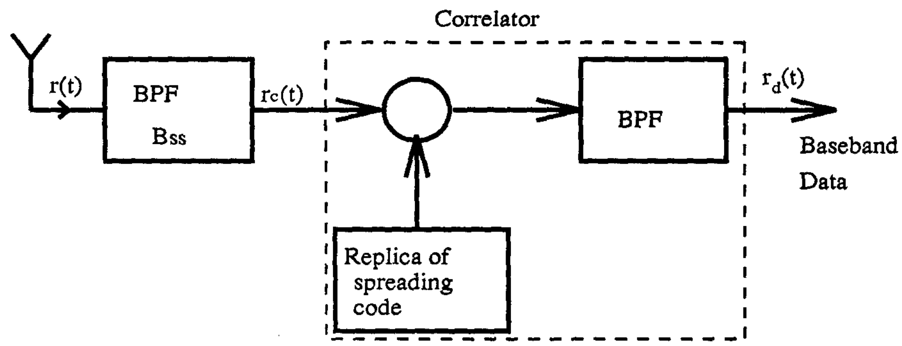

Receiver

Figure 2.6 Direct Sequence Spread Spectrum (DS-SS) Transmitter and Receiver

pulse streams with pulse values of +1 or −1. This reduces equation 2.40 to

$$y(t) = \sqrt{2P}d(t)c(t)\cos(w_o t). \tag{2.41}$$

The signal reaches the receiver with propagation delay, T_d, and random phase, ϕ, in the range 0 to 2π radians. Then the input to the receiver is

$$r(t) = \sqrt{2P}d(t - T_d)c(t - T_d)\cos(w_o(t - T_d) + \phi) \tag{2.42}$$

the receiver estimate of the propagation delay is $\hat{T}_d$ consequently delays the spreading code replica by that amount of time. Then the received signal is multiplied by the delayed spreading code replica giving the despread signal as

$$r_c(t) = \sqrt{2P}c(t - T_d)c(t - \hat{T}_d)\cos(w_o(t - T_d) + \phi). \tag{2.43}$$

Now if the receiver estimate of the propagation delay is correct, that is $T_d = \hat{T}_d$ then

$$c(t - T_d)c(t - \hat{T}_d) = c^2(t) = 1 \tag{2.44}$$

resulting in the following despread signal

$$r_c(t) = \sqrt{2P}\cos(w_o(t - T_d) + \phi). \tag{2.45}$$

This is similar to the modulated information but has a time delay of T_d and a random phase of ϕ. The despread signal is then demodulated with a conventional BPSK demodulator and the baseband information is recovered [23] [26] [14].

As mentioned earlier the important factor in SS of interest in LPI communications is the processing gain, G_p. It is a measure of the effectiveness of the spreading process and is defined by

$$G_p = \frac{B_{ss}}{B_{mod}} \tag{2.46}$$

where B_{ss} is the spread signal bandwidth and B_{mod} is the modulated signal bandwidth which equals the receiver's bandwidth, B_c. The processing gain is of prime importance in improving signal covertness for LPI communications, because the transmitted power is spread over the entire SS bandwidth, B_{ss}, giving a PSD of P_t/B_{ss}. At the receiver the spreading effect is removed by the despreading process. For the interceptor, the interception bandwidth, B_i, is much smaller than

B_{ss}. This results in reducing the received SNR at the interceptors input, so if in conventional communication the required SNR for interception is SNR_{conv} and in SS communications the required SNR for interception is SNR_{ss} then they can be related by [10]

$$SNR_{ss} = \frac{SNR_{conv}}{G_p} \tag{2.47}$$

where SNR_{conv} is the SNR required by the interceptor if conventional modulation is employed by the communication link, and SNR_{ss} is the SNR required if the communication link employed SS techniques. Equation 2.47 indicates that the intercept signal SNR is reduced by a factor of $1/G_p$ compared with conventional modulation resulting in lowering the interception effectiveness. Also the signal power to noise plus interference PSD at the interceptor input is also reduced by a factor of $1/G_p$. Therefore, the interceptor is required to move closer to increase the received power level to detect signals or reduce the system requirements in terms of probabilities of detection and false alarm to detect the signal at the same distance. Also the processing gain has an upper limit with current design and hardware technologies available and is in the order of about 10 Mhz [2]. And as the processing gain gets larger the transmitter and receiver become more complex and expensive.

It is also important to consider the interception process to more fully understand what happens on both the communication and interception links in LPI communications. Next interception basics are presented followed by a discussion of the worst case interceptor.

2.4 Interception

The objective of LPI, as mentioned earlier, is to minimize the probability of detection by the unintended receiver (interceptor) while maximizing reception by the intended receiver. Therefore, it is important to know how intercept receivers work to assess their performance characteristics for LPI analysis. The intercept receiver is characterized by its probability of detection, P_d, and probability of false alarm, P_f. These two probabilities determine the required intercept receiver

decision threshold, V_T, which determines the required signal-to-noise ratio (SNR), at the intercept receiver input, for detecting the presence of a signal at the receivers input [26] [12]. This is achieved through statistical analysis and decision theory. The intercept receiver generates a test statistic and compares it with the decision threshold, V_T. If the result of the test statistic is lower than the threshold then hypothesis H_o is declared (no signal is present). And if the result of the test statistic is higher than the threshold then hypothesis H_1 is declared (signal is present).

Putting it all together, any of the following situations could take place. First, hypothesis H_o could be declared when a signal was actually present. This is considered a miss. Second, hypothesis H_1 could be declared when a signal is present. This is a detection. Third, hypothesis H_1 could be declared when no signal was present. This is considered a false alarm. These cases in mathematical form are as follows: the probability of detection is

$$P_d = \int_{V_T}^{\infty} f_{V|H_1}(v|H_1))dv \tag{2.48}$$

the probability of false alarm is

$$P_f = \int_{V_T}^{\infty} f_{V|H_o}(v|H_o)dv \tag{2.49}$$

and the probability of miss is

$$P_m = 1 - P_d \tag{2.50}$$

were $f_{V|H_o}$ and $f_{V|H_1}$ are the hypotheses conditional probability density functions [1] [28].

For the intercept link any type of interceptor could be used. To present a worst case situation the wideband radiometer is used, which is discussed next.

2.4.1 **Wideband Radiometer.** The Wideband Radiometer shown in figure 2.7, also known as The Energy Detector, is the simplest intercept receiver. The energy received in a given bandwidth, B_i, and an observation time, T_i, is estimated then compared with the decision threshold.

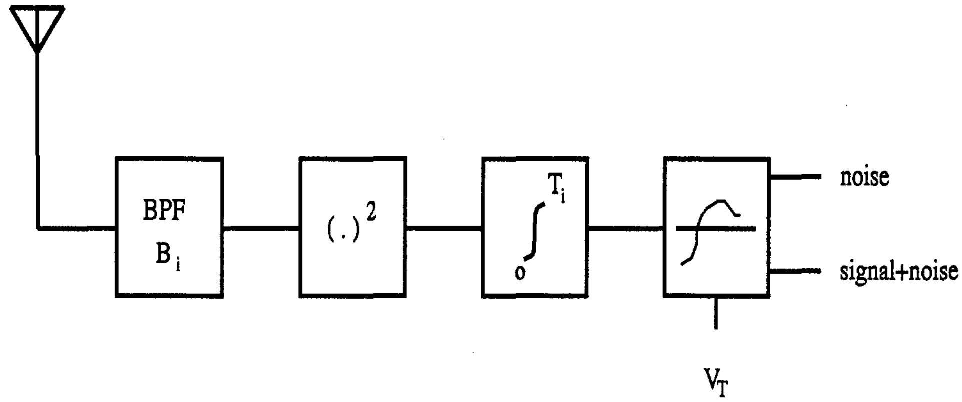

Figure 2.7 Radiometer Block Diagram for detection of unknown signals

If the estimated energy is above the threshold then a signal is declared present. And if the estimate is below the threshold it declares no signal is present [26]. The relationship of the Radiometer parameters (P_d, P_f, T_i and B_i) to the signal-to-noise ratio required to intercept is given by

$$SNR_{req} = \frac{d}{\sqrt{T_i B_i}} \qquad , T_i B_i > 100 \tag{2.51}$$

where the detectability factor, d, is defined as

$$d = \left[Q^{-1}(P_f) - Q^{-1}(P_d)\right] \tag{2.52}$$

where Q^{-1} is the inverse error function. And since noise, N_n, is defined by

$$SNR = \frac{S}{N_n} \tag{2.53}$$

where S is the signal power and N_n is the total noise power given by

$$N_n = N_o B_i. \tag{2.54}$$

In terms of signal-to-noise PSD equation 2.51 becomes

$$\left(\frac{S}{N_o}\right)_{req} = d\sqrt{\frac{B_i}{T_i}}. \tag{2.55}$$

This is known as the Edell Model [12], and provides the interception part of the modulation quality factor, Q_{MOD} in LPI analysis. For a complete derivation of the Edell Model, see appendix B.

This chapter introduced the LPI communications and quality factors, propagation models, and an atmospheric model. The LPI quality factors do not address communication and interception modes of communication and effectively ignore realistic propagation losses on each path. Furthermore, the models available for ground-to-ground communications are not suitable for LPI analysis. Also the Liebe model highlights the importance of considering atmospheric attenuation especially in certain weather conditions such as rain. In addition, Spread spectrum was discussed introducing the processing gain and how it plays an important role in LPI communications. Also interception was introduced and intercept variables were related to LPI analysis. Towards obtaining a mode quality factor, the next chapter introduces formulas for air-to-air, air-to-ground, and ground-to-ground propagation modes. Also the issue of determining or defining the boundaries between these modes is discussed to create a foundation for understanding multimode propagation.

III. Propagation Modes

As discussed earlier the present LPI quality factors only consider the air-to-air mode of communications. Therefore, it is essential to establish or improve the LPI analysis to take into account air-to-ground and ground-to-ground modes of communication. For the purpose of including other modes of communications it was important to revisit the LPI link analysis taking into consideration the multimode communications issue. This requires deriving the propagation or link equations for the three modes of communication concerned.

3.1 Propagation Equations

On one hand, the air-to-air mode is widely used and is well defined in literature [15] [14] [13]. On the other hand, the ground-to-ground mode is not widely used, and ground-to-air mode is not clearly defined. But they are all some how related as we will see later. Also since there are three modes, the boundaries between these modes must be established. Next we look at each mode separately then we try to link them with each other.

3.1.1 Air-to-Air.

The fundamental derivation starts with the assumption that the antenna is omnidirectional or an *isotropic radiator* (G= 0 dB) [21] [15]. As shown in figure 3.1 the power density as a function of distance. $P(d)$, is related to the transmitted power, P_t, by

$$p(R) = \frac{P_t}{4\pi R^2} \qquad watts/m^2. \tag{3.1}$$

The received power, P_r, intercepted by the receiving antenna is given by [19] [15]:

$$P_r = \frac{P_t}{4\pi R^2} A_{er} \qquad watts \tag{3.2}$$

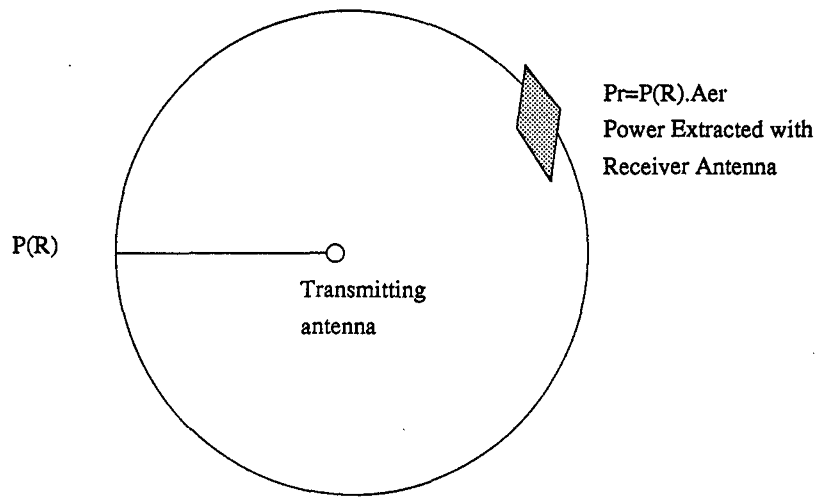

Figure 3.1 Power Density as a Function of Distance For Isotropic Antenna

where A_{er} is the effective area of the receiving antenna. Now taking into consideration a non-isotropic antenna gain, P_t is replaced with the EIRP (Effective Isotropic Radiated Power), which is defined as

$$EIRP = P_t G_t \tag{3.3}$$

where G_t is the transmitting antenna gain. This gives the received power as

$$P_r = \frac{EIRP}{4\pi R^2} A_{er} \tag{3.4}$$

But the effective area of the antenna is generally defines as [20]

$$A_e = \frac{G\lambda^2}{4\pi} \tag{3.5}$$

where G is the antenna gain and λ is the wavelength of the carrier . The resulting equation for air-to-air mode is [14]

$$P_r = \frac{P_t G_t G_r \lambda^2}{(4\pi R)^2}. \tag{3.6}$$

Equation 3.6 presents only the very simple form of the air-to-air propagation equation, which is known as free-space equation. So in a more realistic scenario other losses need to be added resulting in [15]

$$P_r = \frac{P_t G_t G_r \lambda^2}{(4\pi R)^2 L_t L_p L_{ATM}} \tag{3.7}$$

where L_t is transmission line loss, L_p is antenna pattern loss, and L_{ATM} is atmospheric losses. For this research only atmospheric losses are considered. Therefore the equation that will be used is

$$P_r = \frac{P_t G_t G_r \lambda^2}{(4\pi R)^2 L_{ATM}} \tag{3.8}$$

Next the ground-to-ground mode will be considered.

3.1.2 **Ground-to-Ground.** For distances in the order of tens of kilometers it is acceptable to assume a flat earth rather than round earth. Also it is assumed that we have a small grazing incidence angle so that the reflection coefficient is $\Gamma = -1$. First it is worth mentioning that this derivation is based on specular reflection and other factors are not included [16] [17]. Also the issue of rough terrain is ignored in this analysis. The pertinent geometry is shown in figure 3.2.

where

- R_d is the direct range between transmitter and receiver
- R_r is the reflected or indirect range between transmitter and receiver

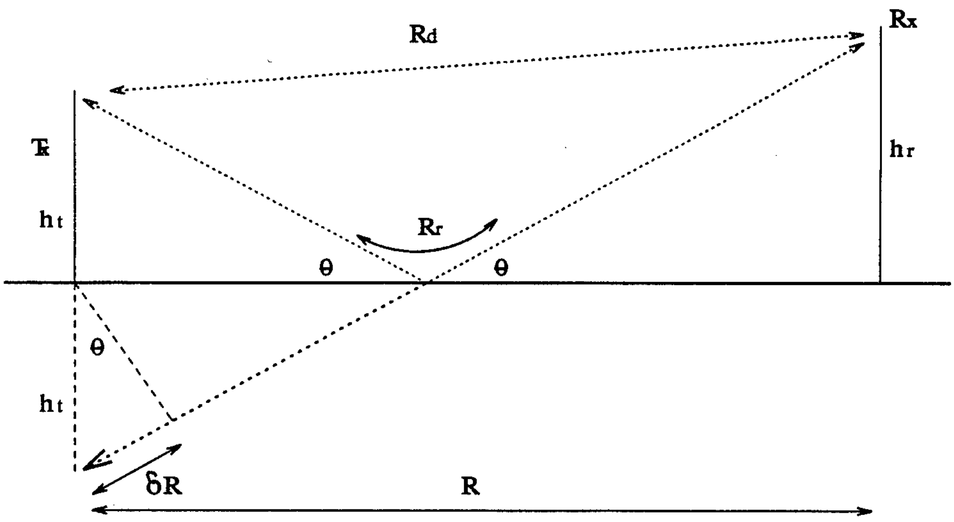

Figure 3.2 Propagation over a plane earth

- δR is the path difference between R_d and R_r
- R is the azimuth range between the transmitter and receiver
- h_t is the transmitter height above ground level
- h_r is the receiver height above ground level
- θ is the grazing angle
- T_x is the transmitter
- R_x is the receiver

The received signal will consist of two components, the direct wave, R_d, and the ground reflected wave, R_r, with the assumption that this is the overall mean of all reflected waves. This assumption is based on the fact that the reflected waves before and after the reflection point considered will nearly cancel each other out. If it is assumed that the incidence angle is small, then the geometry implies that $R \gg h_t, h_r$ [16]. From geometry direct and reflected path lengths are

[21]

$$R_d = [R^2 + (h_r - h_t)^2]^{1/2} \approx R\left[1 + (1/2)\left[\frac{h_r - h_t}{R}\right]^2\right] \tag{3.9}$$

$$R_r = [R^2 + (h_r + h_t)^2]^{1/2} \approx R\left[1 + (1/2)\left[\frac{h_r + h_t}{R}\right]^2\right] \tag{3.10}$$

where the approximation are the result of keeping the first two terms of the binomial expression. Then the resulting path difference is [17] [30]

$$\delta R = R_r - R_d = \frac{2h_t h_r}{R}. \tag{3.11}$$

This path difference results in a phase difference of

$$\psi_p = \frac{2\pi}{\lambda}\frac{2h_t h_r}{R} \qquad radians. \tag{3.12}$$

the total phase difference, ψ_t, between the direct and reflected waves, is the sum of the path difference phase, ψ_p, and the phase due to reflection, ψ_r. The reflected wave phase shift is π radians since it was assumed that $\Gamma = -1$. The total phase difference is:

$$\psi_t = \psi_p + \psi_r = \frac{2\pi}{\lambda}\frac{2h_t h_r}{R} + \pi \tag{3.13}$$

Therefore, the resultant field of the two signals at the receiver, each of unity amplitude but with a phase difference of ψ_t, can be obtained in the following [15]:

$$E = 1 + \exp(-j\psi_t) \tag{3.14}$$

$$\mid E \mid = \mid 1 + \cos\psi_t - j\sin\psi_t \mid \tag{3.15}$$

$$= [(1 + \cos\psi_t)^2 + (\sin\psi_t)^2]^{1/2} \tag{3.16}$$

$$= \sqrt{2}\,[1 + \cos\psi_t]^{1/2} \tag{3.17}$$

$$= \sqrt{2}\,[1 - \cos\psi_p]^{1/2}. \tag{3.18}$$

Since power is proportional to the square of the field, E^2, then the ratio of the power at the receiver of resultant to direct signal is given by [15]

$$\eta = 2(1 - \cos\psi_p) = 4\sin^2\left(\frac{2\pi h_t h_r}{\lambda R}\right). \tag{3.19}$$

Now the received power is obtained by multiplying the free-space equation 3.6 by η [19]. giving:

$$P_r = \frac{P_t G_t G_r \lambda^2}{(4\pi R)^2} 4\sin^2\left(\frac{2\pi h_t h_r}{\lambda R}\right). \tag{3.20}$$

And for small angles $\sin\psi_p = \psi_p$, since $R \gg h_t h_r$, gives [17] [30]:

$$P_r = \frac{P_t G_t G_r \lambda^2}{(4\pi R)^2} \left(\frac{4\pi h_t h_r}{\lambda R}\right)^2 \tag{3.21}$$

or

$$P_r = P_t G_t G_r \left(\frac{h_t h_r}{R^2}\right)^2. \tag{3.22}$$

Adding atmospheric losses as in the air-to-air propagation case it becomes

$$P_r = \frac{P_t G_t G_r}{L_{ATM}} \left(\frac{h_t h_r}{R^2}\right)^2. \tag{3.23}$$

Equation 3.23 is known as the plane earth propagation equation [21]. There are two things to point out about this equation. First, the assumption of having a small grazing angle, θ, resulted in cancelling out the wavelength factor making the equation independent of frequency. Second the loss is a function of the fourth-inverse law with respect to range [16].

3.1.3 **Air-to-Ground.** In situations where part of the system, transmitter or receiver, is below a certain altitude and the other one is above that altitude, then it is in air-to-ground propagation mode. The altitude limit is discussed in the next section. It is desired to have a propagation equation for air-to-ground that is similar in structure to the air-to-air and ground-to-ground propagation equations. Therefore it is logical to base the air-to-ground propagation equation on the basic variables used in the other two propagation equations. Mainly, antennas gains, transmitter power, free space loss, and atmospheric attenuation. As is for the case of ground-to-ground, there needs to be another loss factor to account for other losses associated with one part of the system being close to the ground. It is generally known that air-to-air and ground-to-ground represent the lower and upper bounds on propagation losses, where air-to-ground and ground-to-air are assumed to have a loss that is somewhere between the above two limits [11]. A widely used equation for air-to-ground propagation is [23] [29]

$$P_r = \left(\frac{P_r G_t G_r}{(4\pi R/\lambda)^2 L_{ATM}} \right) \frac{k_g}{R^a} \qquad , 0 \leq a \leq 2 \tag{3.24}$$

where k_g is a constant that for this research, is set to unity. Second, for the variable a, air-to-ground losses are compared with ground-to-ground and air-to-air losses so as to make air-to-ground losses be close to the mean of ground-to-ground and air-to-air losses. This was done by curve fitting and the value of a that produce the best fit was extracted. Figure 3.3 shows the comparison between the modes losses and gives the value of $a = 0.5$ for air-to-ground losses being the median of air-to-air and ground-to-ground.

3.2 Boundaries Between Modes

In the previous section the propagation equations for the three propagation modes of interest were presented. The next logical step is to determine the boundaries between these modes. The boundaries between modes are important because, as seen in the previous section, the propagation

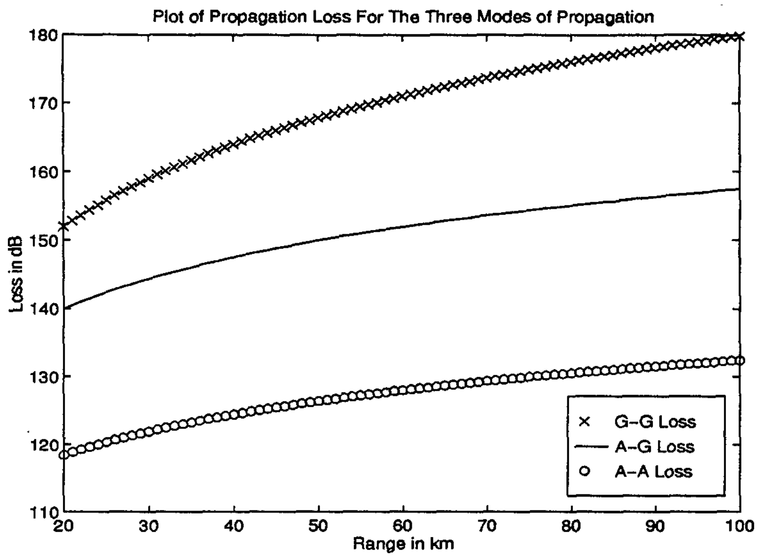

Figure 3.3 Plot of Losses For The Three Modes of Propagation

losses are dependent on the propagation mode. Therefore, the next three subsections describe the boundaries between the three propagation modes.

3.2.1 **Ground-to-Ground Boundary.** The boundary for this mode can be determined by computing the sine term in equation 3.20 for a given range (for this research a range of 50 *km* and a frequency of 5 *Ghz* are used) and various heights until the small angle approximation produces an error of greater than 0.1 *radians*. In figure 3.4 the approximated value begins to depart by more than 0.1 *radians* from the original value between 10 and 20 *meters*.

So the determining factor is the accuracy required in the assumption. In this case, with an accuracy of 0.1 *radians* the ground-to-ground communications boundary is about 15 *meters*. Obviously the boundary is range and frequency dependent. Thus, for different frequencies and ranges the value will change.

3.2.2 **Air-to-Ground Boundary.** As discussed earlier the air-to-ground mode is when the transmitter or receiver is below a certain altitude above the ground. This limit as shown in

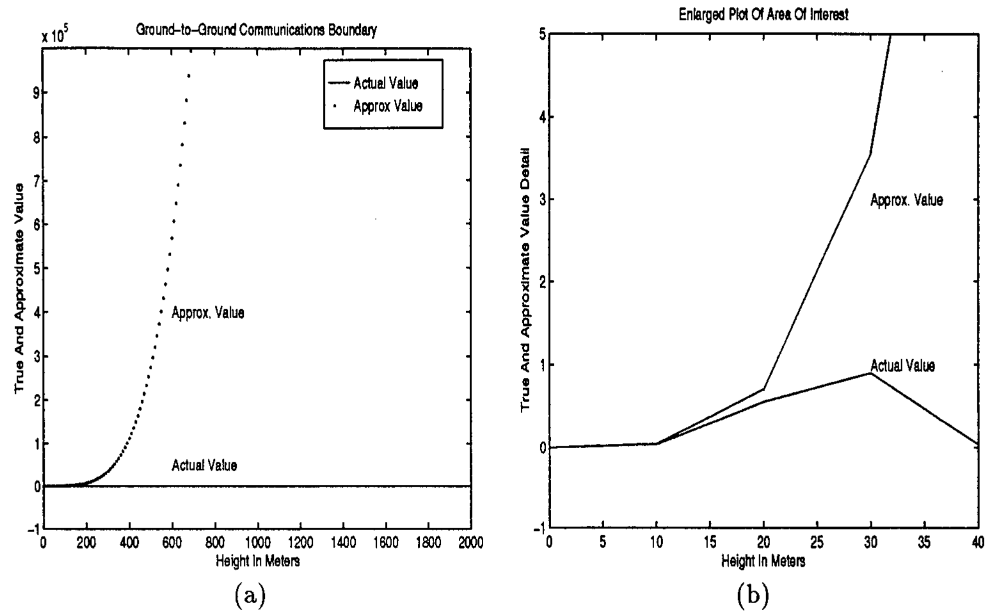

Figure 3.4 Ground-to-Ground Communication Boundary Based On The Small angle Approximation

the ground-to-ground boundary section was range and frequency dependent. Therefore if either the transmitter or receiver exceeds the ground-to-ground upper limit while the other unit is below that limit then the system is in air-to-ground mode of communication.

3.2.3 **Air-to-Air Boundary.** Now to complete the whole boundaries issue it seems logical to assume that if both transmitter and receiver are above the ground-to-ground boundary (15 *meters* high for f =5 Ghz and R =50 km) then the system is in the air-to-air mode of communications.

Now that all the necessary tools and equations are prepared the next step is to put these results together to analyze the possible situations that might be encountered. The following chapter presents the possible LPI scenarios and analyzes them using the equations and boundaries derived in this chapter.

IV. Possible LPI Scenarios

Now combining the analysis for the various types of links one can produce formulations for a variety of possible situations that might take place.

4.1 Air-to-Air Communications

The air-to-air communication link can be intercepted by either an airborne or ground based interceptor as shown in figure 4.1. The analysis for each case is slightly different because the functional dependence of the path loss on intercept distance is different for each case. Lets look at each situation in turn.

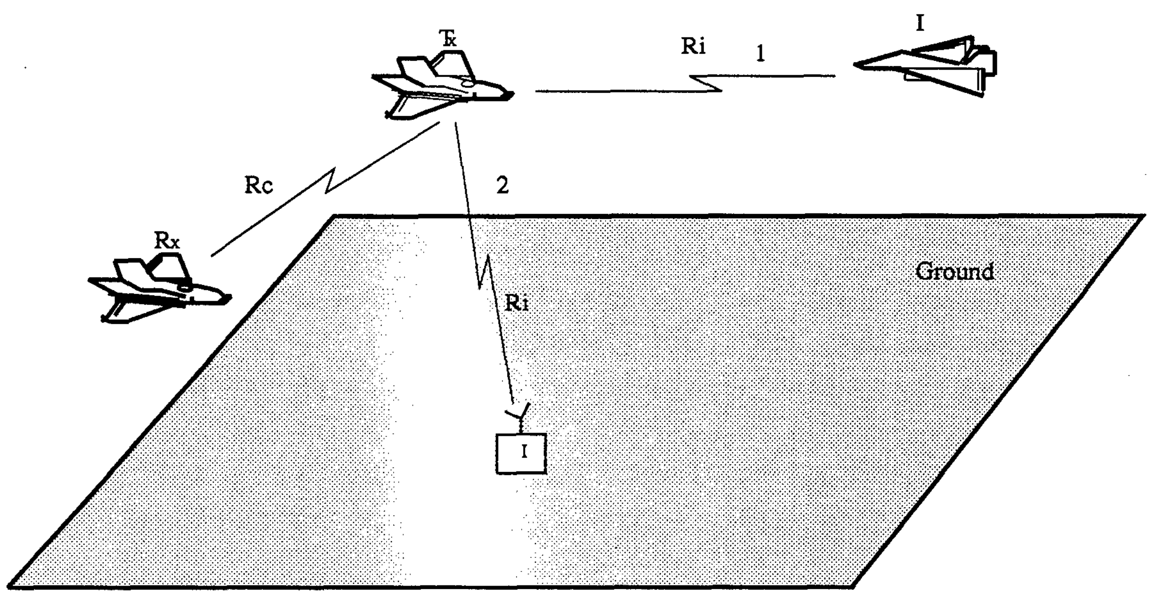

Figure 4.1 Interception Possibilities for Air-to-Air Communication Link

4.1.1 Air-to-Air interception.

The air-to-air interception situation is the typical one on which all the previous LPI work was focused. The results already obtained in section 2.1, show the LPI link quality factor is

$$\left(\frac{R_c}{R_i}\right)^2 = \left(\frac{G_{tc}G_{ct}}{G_{ti}G_{it}}\right)\left(\frac{N_{si}}{N_{sc}}\right)\left(\frac{S_i/N_{si}}{S_c/N_{sc}}\right)\left(\frac{L_i}{L_c}\right) \tag{4.1}$$

and converting to decibels become

$$Q_{LPI} = Q_{ANT} + Q_{IS} + Q_{MOD} + Q_{ATM} \tag{4.2}$$

where it is desired to make Q_{LPI} as large as possible providing a large communication range with a relatively smaller interception range. This is achieved through maximizing Q_{ANT}, Q_{IS}, Q_{MOD} and Q_{ATM}. These factors were discussed in details in section 2.1.3.

4.1.2 **Air-to-Ground Interception.** In the air-to-ground interception case we need to account for the difference in the propagation losses in the air-to-air communication channel and the air-to-ground interception channel. Using the same technique discussed in section 2.1, the LPI quality factors can be derived in the following manner. Using equation 3.8, the signal power to noise plus interference power spectral density (PSD) ratio for the communication link is:

$$\frac{S_c}{N_{sc}} = \frac{P_t G_{tc} G_{ct}}{(4\pi R_c/\lambda)^2 N_{sc} L_c(R_c, ATM_c)} \tag{4.3}$$

where $L_c(R_c, ATM_c)$ indicates a functional dependence on the communication distance (R_c) and the atmospheric losses per unit distance (ATM_C) along the communication path. Putting R_c^2, the communication distance, on the left side, one obtains

$$R_c^2 = \frac{P_t G_{tc} G_{ct}}{(4\pi/\lambda)^2 N_{sc} L_c(R_c, ATM_c)} \left(\frac{1}{S_c/N_{sc}}\right). \tag{4.4}$$

And similarly the signal power to noise plus interference PSD ratio for the interception link, using equation 3.24 is

$$\frac{S_i}{N_{si}} = \frac{P_t G_{ti} G_{it}}{(4\pi R_i/\lambda)^2 N_{si} L_i(R_i, ATM_i)} \left(\frac{1}{R_i^a}\right) \tag{4.5}$$

the functional dependence of ground-to-ground path loss on the fourth power of the range as was derived in equation 3.23. The following discusses the two possible interception situations.

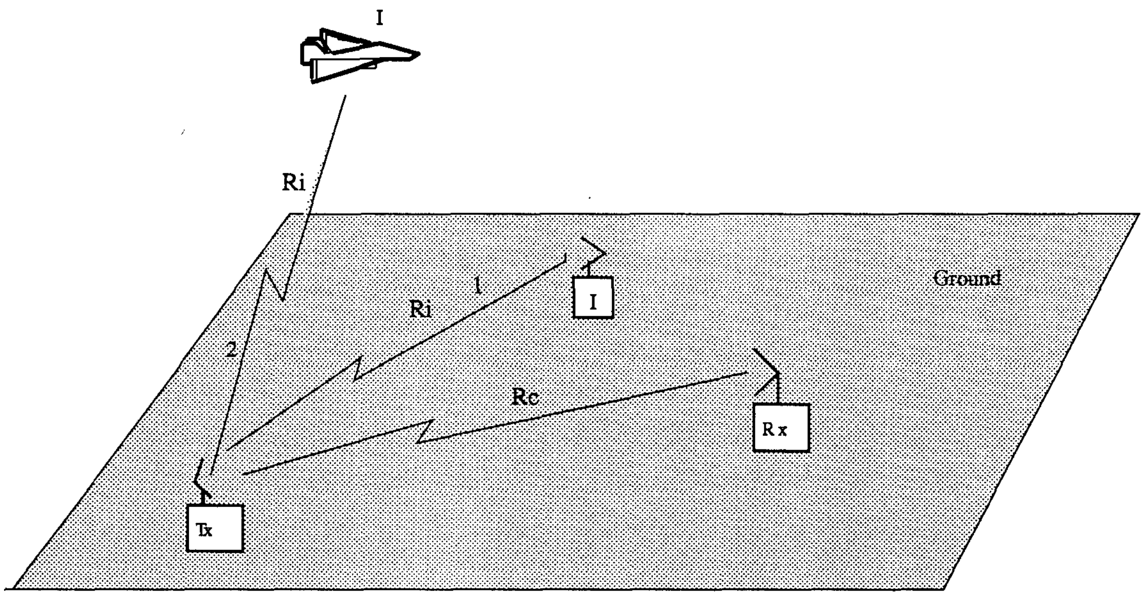

Figure 4.2 Ground-to-Ground Communications Interception Possibilities

4.2.1 **Ground-to-Ground Interception.** In the the ground-to-ground interception case the communicator and interceptor are both on the ground, using the same propagation mode. Therefore, this case is similar to the air-to-air interception case discussed in the section 4.1.1, but the losses in both paths are higher because the propagation loss in ground-to-ground propagation mode are higher as shown in equation 3.21. Using equation 3.21 the signal power to noise plus interference PSD ratio for the communication link is

$$\frac{S_c}{N_{sc}} = \frac{P_t G_{tc} G_{ct}}{(4\pi R_c/\lambda)^2 N_{sc} L_c(R_c, ATM_c)} \left(\frac{4\pi h_t h_c}{\lambda R_c}\right)^2 \tag{4.10}$$

which can be rearranged to obtain the following expression for the communication range

$$R_c^2 = \frac{P_t G_{tc} G_{ct}}{(4\pi/\lambda)^2 N_{sc} L_c(R_c, ATM_c)} \left(\frac{1}{S_c/N_{sc}}\right) \left(\frac{4\pi h_t h_c}{\lambda R_c}\right)^2 \tag{4.11}$$

Similarly the signal power to noise plus interference PSD ratio for the interception link results is

$$\frac{S_i}{N_{si}} = \frac{P_t G_{ti} Git}{(4\pi R_i/\lambda)^2 L_i(R_i, ATM_i)} \left(\frac{4\pi h_t h_i}{\lambda R_i}\right)^2 \tag{4.12}$$

with the following expression for R_i^2

$$R_i^2 = \frac{P_t G_{ti} G_{it}}{(4\pi/\lambda)^2 N_{si} L_i(R_i, ATM_i)} \left(\frac{1}{S_i/N_{si}}\right) \left(\frac{4\pi h_t h_i}{\lambda R_i}\right)^2 \tag{4.13}$$

To obtain a relationship between the two ranges equation 4.11 is divided by equation 4.13 giving

$$\left(\frac{R_c}{R_i}\right)^2 = \left(\frac{G_{tc} G_{ct}}{G_{ti} G_{it}}\right) \left(\frac{N_{si}}{N_{sc}}\right) \left(\frac{S_i/N_{si}}{S_c/N_{sc}}\right) \left(\frac{L_i}{L_c}\right) \left[\left(\frac{R_i}{R_c}\right)^2 \left(\frac{h_c}{h_i}\right)^2\right] \tag{4.14}$$

Again this equation is similar to the original LPI equation 4.1 with an additional term consisting of two parts the first is the inverse of the LPI factor which if moved to the left side of the equation will just increase the power of the LPI factor on the left side of the equation. The second part is a function of the transmitter and receiver heights above the ground, indicating that increasing the receiver height relative to the interceptor height improves LPI system performance. The requirements are the same as before where it is desired to increase (R_c/R_i) as much as possible by maximizing all the factors on the right side of equation 4.14.

4.2.2 **Ground-to-Air Interception.** The ground-to-air interception case, number two on figure 4.2 we need to account for the difference in the path losses in the ground-to-ground communication channel and ground-to-air interception channel. As in section 2.1, the LPI quality factors are derived in the following manner. Using the air-to-ground propagation equation 3.24 the signal power to noise plus interference PSD ratio is:

$$\frac{S_c}{N_{sc}} = \frac{P_t G_{tc} G_{ct}}{(4\pi R_c/\lambda)^2 N_{sc} L_c(R_c, ATM_c)} \left(\frac{4\pi h_t h_r}{\lambda R_c}\right)^2 \tag{4.15}$$

yielding the following expression for the communication range

$$R_c^2 = \frac{P_t G_{tc} G_{ct}}{(4\pi/\lambda)^2 N_{sc} L_c(R_c, ATM_c)} \left(\frac{1}{S_c/N_{sc}}\right) \left(\frac{4\pi h_t h_r}{\lambda R_c}\right)^2 \tag{4.16}$$

where the last term, $\left(\frac{4\pi h_t h_r}{\lambda R_c}\right)^2$, indicates an added loss factor along the communication path functionally dependent on the transmitter and receiver heights ($h_t and h_r$), wavelength (λ), and the communication range (R_c). And using equation 3.24 the interception link, signal power to noise plus interference PSD ratio is:

$$\frac{S_i}{N_{si}} = \frac{P_t G_{ti} Git}{(4\pi R_i/\lambda)^2 L_i(R_i, ATM_i)} \left(\frac{1}{R_i^a}\right) \tag{4.17}$$

with a corresponding expression for, R_i^2 the interception range

$$R_i^2 = \frac{P_t G_{ti} G_{it}}{(4\pi/\lambda)^2 N_{si} L_i(R_i, ATM_i)} \left(\frac{1}{S_i/N_{si}}\right) \left(\frac{1}{R_i^a}\right). \tag{4.18}$$

To obtain a relationship between R_c^2 and R_i^2 equation 4.16 is divided by equation 4.18 giving

$$\left(\frac{R_c}{R_i}\right)^2 = \left(\frac{G_{tc} G_{ct}}{G_{ti} G_{it}}\right) \left(\frac{N_{si}}{N_{sc}}\right) \left(\frac{S_i/N_{si}}{S_c/N_{sc}}\right) \left(\frac{L_i}{L_c}\right) \left[\frac{\left(\frac{4\pi h_t h_r}{\lambda R_c}\right)^2}{\left(\frac{1}{R_i^a}\right)}\right] \tag{4.19}$$

$$= \left(\frac{G_{tc} G_{ct}}{G_{ti} G_{it}}\right) \left(\frac{N_{si}}{N_{sc}}\right) \left(\frac{S_i/N_{si}}{S_c/N_{sc}}\right) \left(\frac{L_i}{L_c}\right) \left[\left(\frac{2\pi h_t h_r}{\lambda}\right)^2 \left(\frac{R_i^a}{R_c^2}\right)\right]. \tag{4.20}$$

Equation 4.20 is in the traditional LPI form with an additional term to accounts for difference in modes. This term is a function of the ranges, transmitter and receiver heights above the ground, and wavelength. To improve covertness it is desired to make this additional term as large as possible. Again note that both R_c and R_i appear on both sides of equation 4.20.

4.3 Ground-to-Air Communications

The ground-to-air communications can be intercepted either by ground based or airborne interceptor as shown in figure 4.3. Each case requires slightly different analysis because for the first case the ground based interceptor is attempting to intercept a signal transmitted by a ground based transmitter to an airborne receiver. The propagation losses for the first interception link are function of R_i^4 and communication link propagation losses are function of $R_c^{2.5}$. For the second case with an airborne interceptor the propagation losses for both links have the same functionality with respect to range ($R^{2.5}$). Lets look at the two situations in details.

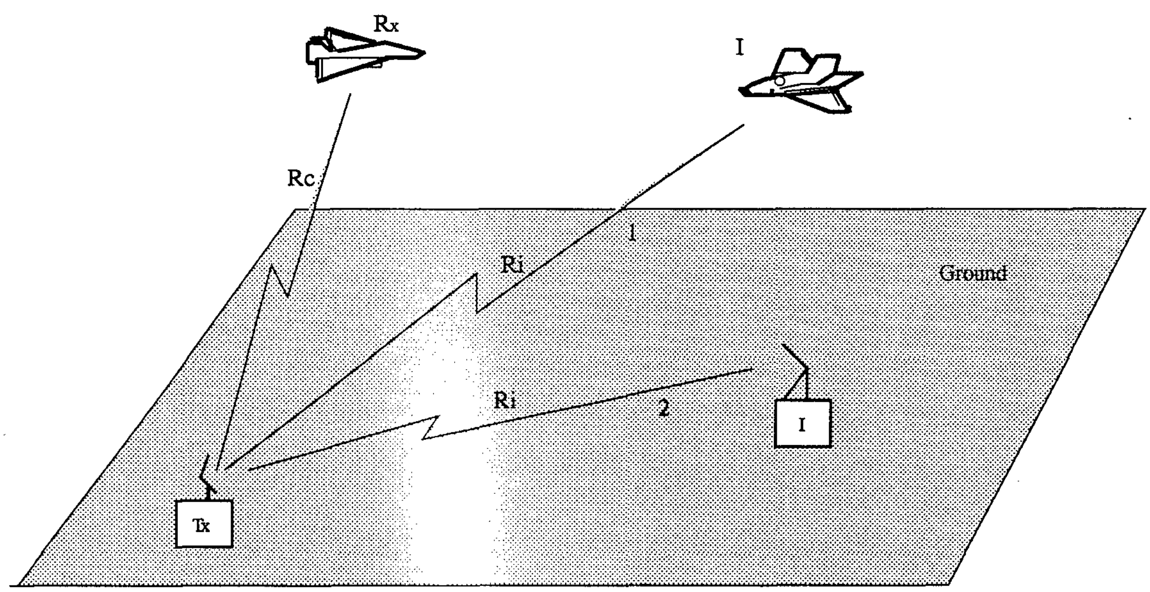

Figure 4.3 Ground-to-Air Communication Interception Possibilities

4.3.1 **Ground-to-Ground Interception.** The ground-to-ground situation is similar to section 4.2.1 for the interception link. For the communication link the receiver is airborne suffering less losses than the ground interceptor. Therefore, one must use ground-to-air propagation equation 3.24 for the communication link and ground-to-ground propagation equation 3.21 for the interception link. The signal power to noise plus interference PSD ratio for the communication link

is

$$\frac{S_c}{N_{sc}} = \frac{P_t G_{tc} G_{ct}}{(4\pi R_c/\lambda)^2 N_{sc} L_c(R_c, ATM_c)} \left(\frac{1}{R_c^a}\right) \tag{4.21}$$

with a corresponding expression for R_c^2, communication range, of

$$R_c^2 = \frac{P_t G_{tc} G_{ct}}{(4\pi/\lambda)^2 N_{sc} L_c(R_c, ATM_c)} \left(\frac{1}{S_c/N_{sc}}\right) \left(\frac{1}{R_c^a}\right). \tag{4.22}$$

The intercept signal power to noise plus interference PSD ratio is

$$\frac{S_i}{N_{si}} = \frac{P_t G_{ti} Git}{(4\pi R_i/\lambda)^2 L_i(R_i, ATM_i)} \left(\frac{4\pi h_t h_i}{\lambda R_i}\right)^2. \tag{4.23}$$

Solving for R_i^2, the interception range, one obtains

$$R_i^2 = \frac{P_t G_{ti} G_{it}}{(4\pi/\lambda)^2 N_{si} L_i(R_i, ATM_i)} \left(\frac{1}{S_i/N_{si}}\right) \left(\frac{4\pi h_t h_i}{\lambda R_i}\right)^2. \tag{4.24}$$

The relationship between the communication and interception ranges (R_c^2/R_i^2) is obtained by dividing equation 4.22 by equation 4.24

$$\left(\frac{R_c}{R_i}\right)^2 = \left(\frac{G_{tc} G_{ct}}{G_{ti} G_{it}}\right) \left(\frac{N_{si}}{N_{sc}}\right) \left(\frac{S_i/N_{si}}{S_c/N_{sc}}\right) \left(\frac{L_i}{L_c}\right) \left[\left(\frac{R_i^2}{R_c^a}\right) \left(\frac{\lambda}{4\pi h_t h_i}\right)^2\right]. \tag{4.25}$$

All the terms in equation 4.25 are the same as those discussed and explained in sections 4.1.1 and 4.1.2, except for the last term on the right side of the equation. This term is due to the different propagation modes used in the communication and interception links. It is a function of the transmitter's and interceptor's heights (h_t, h_i), Ranges (R_c, R_i), and wavelength (λ). This new term is desired to be as large as possible to improve LPI.

4.3.2 **Ground-to-Air Interception.** The ground-to-air interception involves involves a ground transmitter communicating with an airborne receiver while trying to prevent interception

by an airborne interceptor. Such situation is similar to sections 4.1.1 and 4.2.1 where the two links use the same propagation mode. This requires analysis of two ground-to-air links, using equation 3.24. Utilizing the same techniques used in section 4.1.2 the signal power to noise PSD ration for the communication link is:

$$\frac{S_c}{N_{sc}} = \frac{P_t G_{tc} G_{ct}}{(4\pi R_c/\lambda)^2 N_{sc} L_c(R_c, ATM_c)} \left(\frac{1}{R_c^a}\right). \tag{4.26}$$

Putting R_c^2 on the left side, one obtains

$$R_c^2 = \frac{P_t G_{tc} G_{ct}}{(4\pi/\lambda)^2 N_{sc} L_c(R_c, ATM_c)} \left(\frac{1}{S_c/N_{sc}}\right) \left(\frac{1}{R_c^a}\right) \tag{4.27}$$

The intercept link the signal power to noise PSD ratio is:

$$\frac{S_i}{N_{si}} = \frac{P_t G_{ti} Git}{(4\pi R_i/\lambda)^2 L_i(R_i, ATM_i)} \left(\frac{1}{R_i^a}\right); \tag{4.28}$$

solving for R_i^2 we obtain

$$R_i^2 = \frac{P_t G_{ti} G_{it}}{(4\pi/\lambda)^2 N_{si} L_i(R_i, ATM_i)} \left(\frac{1}{S_i/N_{si}}\right) \left(\frac{1}{R_i^a}\right). \tag{4.29}$$

Then the ratio of R_c^2/R_i^2 is:

$$\left(\frac{R_c}{R_i}\right)^2 = \left(\frac{G_{tc} G_{ct}}{G_{ti} G_{it}}\right) \left(\frac{N_{si}}{N_{sc}}\right) \left(\frac{S_i/N_{si}}{S_c/N_{sc}}\right) \left(\frac{L_i}{L_c}\right) \left(\frac{R_i^a}{R_c^a}\right). \tag{4.30}$$

Equation 4.30 is similar to the original LPI equation with an extra term (R_i^a/R_c^a) to account for the fact that the air-to-ground propagation suffers an added $1/R^a$ loss. Again R_c and R_i are on both sides of equation 4.30, therefore there is no explicit solution for R_c^2/R_i^2.

4.4 Air-to-Ground Communications

A typical representation of air-to-ground communication is shown in figure 4.4. There are two interception possibilities, airborne interceptor represented by link (1) and ground based interceptor represented by link (2) both in figure 4.4. The analysis is similar to section 4.3 but the transmitter and receiver exchange locations. Thus the interception propagation modes are different. The analysis of the two situations is discussed next.

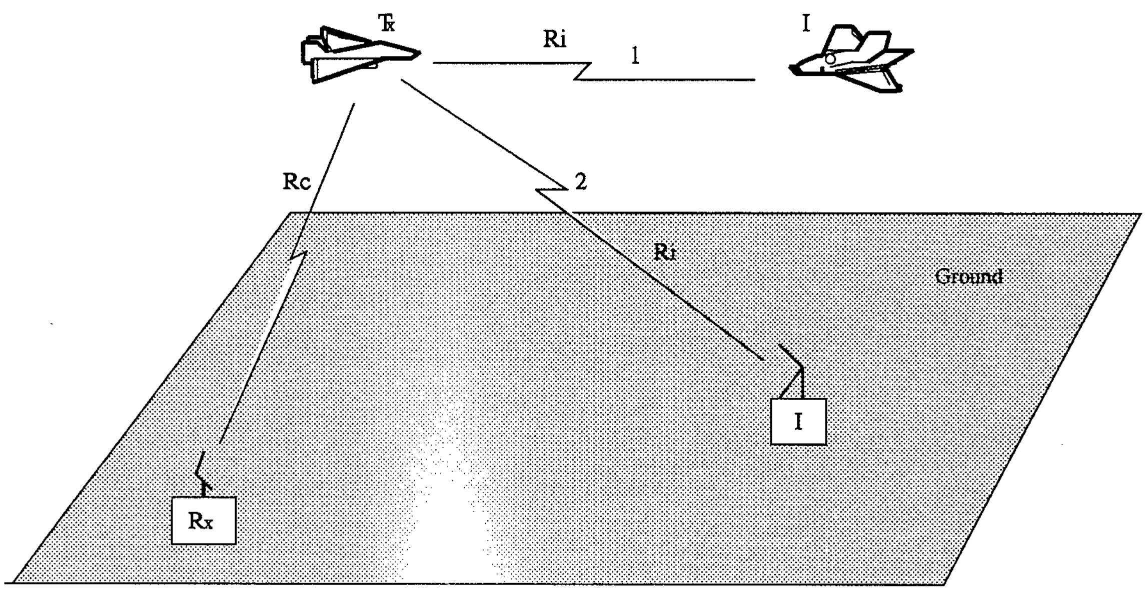

Figure 4.4 Air-to-Ground Communication Interception Possibilities

4.4.1 **Air-to-Air Interception.** The air-to-air interception involves an air-to-air interception link and a air-to-ground communication link. Therefore, we need to account for the difference in propagation losses in both paths. Following the same procedure used in all the previous sections of chapter IV. For the communication link the power to noise PSD ratio is given by

$$\frac{S_c}{N_{sc}} = \frac{P_t G_{tc} G_{ct}}{(4\pi R_c/\lambda)^2 N_{sc} L_c(R_c, ATM_c)} \left(\frac{1}{R_c^a}\right); \tag{4.31}$$

solving for R_c^2 one obtains

$$R_c^2 = \frac{P_t G_{tc} G_{ct}}{(4\pi/\lambda)^2 N_{sc} L_c(R_c, ATM_c)} \left(\frac{1}{S_c/N_{sc}}\right) \left(\frac{1}{R_c^a}\right). \tag{4.32}$$

Similarly for the interception link the signal power to noise PSD ratio is:

$$\frac{S_i}{N_{si}} = \frac{P_t G_{ti} Git}{(4\pi R_i/\lambda)^2 L_i(R_i, ATM_i)} \tag{4.33}$$

with the following expression for R_i^2

$$R_i^2 = \frac{P_t G_{ti} G_{it}}{(4\pi/\lambda)^2 N_{si} L_i(R_i, ATM_i)} \left(\frac{1}{S_i/N_{si}}\right). \tag{4.34}$$

Dividing R_c^2 by R_i^2 gives

$$\left(\frac{R_c}{R_i}\right)^2 = \left(\frac{G_{tc} G_{ct}}{G_{ti} G_{it}}\right) \left(\frac{N_{si}}{N_{sc}}\right) \left(\frac{S_i/N_{si}}{S_c/N_{sc}}\right) \left(\frac{L_i}{L_c}\right) \left(\frac{1}{R_c^a}\right). \tag{4.35}$$

Equation 4.35 is similar to the standard LPI equation 4.1 with an additional term that accounts for the difference in the propagation modes for the communication and interception links. This term is a function of the communication range (R_c^a). As in the traditional case the ratio R_c^2/R_i^2 is desired to be as large as possible. Therefore, the terms on the right of equation 4.35 need to be maximized but the extra term is always very small, less than one. This increases the requirements on the other factors to compensate for the losses due to the term $1/R_c^a$.

4.4.2 **Air-to-Ground Interception.** The air-to-ground interception situation involves an airborne transmitter communicating with a ground based receiver while trying to prevent interception by a ground based interceptor. Performing similar analysis as in all the previous cases of

chapter IV the signal power to noise PSD ratio for the communication link is:

$$\frac{S_c}{N_{sc}} = \frac{P_t G_{tc} G_{ct}}{(4\pi R_c/\lambda)^2 N_{sc} L_c(R_c, ATM_c)} \left(\frac{1}{R_c^a}\right); \tag{4.36}$$

solving for R_c^2 we obtain

$$R_c^2 = \frac{P_t G_{tc} G_{ct}}{(4\pi/\lambda)^2 N_{sc} L_c(R_c, ATM_c)} \left(\frac{1}{S_c/N_{sc}}\right) \left(\frac{1}{R_c^a}\right). \tag{4.37}$$

Similarly for th interception link the signal power to noise PSD ration is:

$$\frac{S_i}{N_{si}} = \frac{P_t G_{ti} Git}{(4\pi R_i/\lambda)^2 L_i(R_i, ATM_i)} \left(\frac{1}{R_i^a}\right); \tag{4.38}$$

solving for R_i^2 we obtain

$$R_i^2 = \frac{P_t G_{ti} G_{it}}{(4\pi/\lambda)^2 N_{si} L_i(R_i, ATM_i)} \left(\frac{1}{S_i/N_{si}}\right) \left(\frac{1}{R_i^a}\right); \tag{4.39}$$

dividing R_c^2 by R_i^2 gives

$$\left(\frac{R_c}{R_i}\right)^2 = \left(\frac{G_{tc} G_{ct}}{G_{ti} G_{it}}\right) \left(\frac{N_{si}}{N_{sc}}\right) \left(\frac{S_i/N_{si}}{S_c/N_{sc}}\right) \left(\frac{L_i}{L_c}\right) \left(\frac{R_i^a}{R_c^a}\right). \tag{4.40}$$

Equation 4.40 is similar to the standard LPI equation 4.1 with an extra term to account to the fact that the two links are using air-to-ground propagation mode. For LPI it is desired to make R_c^2/R_i^2 as large as possible.

4.5 Multimode LPI Equation

Obviously, to make the whole analysis of LPI scenarios for the various situations discussed they must be represented in one equation that can be used to analyze any particular scenario of

interest. To achieve that only the extra mode or scenario related terms need to be put into one single term with variables that are used to extract the desired form of the equation related to the desired situation. This is achieved in the following equation, where M is a variable dependent on the communication and interception modes as

$$\left(\frac{R_c}{R_i}\right)^2 = \left(\frac{G_{tc}G_{ct}}{G_{ti}G_{it}}\right)\left(\frac{N_{si}}{N_{sc}}\right)\left(\frac{S_i/N_{si}}{S_c/N_{sc}}\right)\left(\frac{L_i}{L_c}\right)(M). \tag{4.41}$$

Now converting to dBs it becomes

$$\begin{aligned} 10\log\left(\frac{R_c}{R_i}\right)^2 &= 10\log\left(\frac{G_{tc}G_{ct}}{G_{ti}G_{it}}\right) + 10\log\left(\frac{N_{si}}{N_{sc}}\right) + 10\log\left(\frac{S_i/N_{si}}{S_c/N_{sc}}\right) \\ &+ 10\log\left(\frac{L_i}{L_c}\right) + 10\log(M) \end{aligned} \tag{4.42}$$

which gives the equation in quality factors as

$$Q_{LPI} = Q_{ANT} + Q_{IS} + Q_{MOD} + Q_{ATM} + Q_M. \tag{4.43}$$

This equation is the same as the original LPI equation introduced in section 2.1.3 with an added term to account for the modes employed by the communication and interception links. This new term will be called *the LPI mode quality factor,* Q_M. The mode quality factor is presented in table 4.1 in decimals by the term M. And once the communication and interception modes are known the the mode quality factor can be extracted and put in equation 4.43, where $Q_M = 10\log M$.

The next step is to put the multimode LPI equation into a form that can be used to perform a logical analysis of the LPI situation and understand which parts can be utilized to improve the covertness of friendly communications and prevent interception by unfriendly listeners. Now that all the parts are put together the following chapter discusses a different approach to analyze the

M		*Communications Link*			
		Air-to-Air	Air-to-Ground	Ground-to-Air	Ground-to-Ground
Inter-	Air-to-Air	1	$\left(\frac{1}{R_c^a}\right)$	NA	NA
ception	Air-to-Ground	(R_i^a)	$\left(\frac{R_i^a}{R_c^a}\right)$	NA	NA
Link	Ground-to-Air	NA	NA	$\left(\frac{R_i^a}{R_c^a}\right)$	$\left(\frac{4\pi h_t h_r}{\lambda}\right)^2 \left(\frac{R_i^a}{R_c^2}\right)$
	Ground-to-Ground	NA	NA	$\left(\frac{\lambda}{4\pi h_t h_i}\right)^2 \left(\frac{R_i^2}{R_c^a}\right)$	$\left(\frac{h_c R_i}{h_i R_c}\right)^2$

Table 4.1 Mode Quality Factor Table, in Decimals, For Multimode LPI Communications (NA: Not Applicable)

LPI quality factors with graphical representation of various scenarios showing the importance of the atmospheric and mode quality factors in LPI analyses.

V. Results And Discussion

The propagation modes problem was solved by introducing the mode quality factor, Q_M (section 4.5). Also the atmospheric effects problem was solved by using the Liebe model of the atmosphere (section 2.2.2) to extract an accurate estimate of atmospheric attenuation in each link and used in the atmospheric quality factor, Q_{ATM} (section 2.1.3). The overall LPI quality factors equation obtained in section 4.5 is given by

$$Q_{LPI} = Q_{ANT} + Q_{IS} + Q_{MOD} + Q_{ATM} + Q_M; \tag{5.1}$$

putting the quality factors in terms of their respective variables Q_{LPI} becomes

$$\left(\frac{R_c}{R_i}\right)^2_{dB} = \left(\frac{G_{tc}G_{ct}}{G_{ti}G_{it}}\right)_{dB} + \left(\frac{N_{si}}{N_{sc}}\right)_{dB} + \left(\frac{S_i/N_{si}}{S_c/N_{sc}}\right)_{dB} + \left(\frac{L_i}{L_c}\right)_{dB} + (M)_{dB} \tag{5.2}$$

where $(L_i)_{dB} = \alpha_i R_i$ and $(L_c)_{dB} = \alpha_c R_c$ as explained in chapter II, and the subscript dB indicates taking ten times the logarithm to base ten of the value within the brackets. Also M is a variable representing the mode quality factor obtained from table 4.1 depending on the scenario under consideration. It is obvious that L_i and L_c are a function of their respective ranges. And M is mainly a function of the communication and interception ranges raised to similar or different powers. For example, in the case of ground-to-ground communication and ground-to-air interception equation 5.2 becomes

$$\left(\frac{R_c}{R_i}\right)^2_{dB} = \left(\frac{G_{tc}G_{ct}}{G_{ti}G_{it}}\right)_{dB} + \left(\frac{N_{si}}{N_{sc}}\right)_{dB} + \left(\frac{S_i/N_{si}}{S_c/N_{sc}}\right)_{dB} + \left(\frac{L_i}{L_c}\right)_{dB} + \left(\left(\frac{4\pi h_t h_r}{\lambda}\right)^2 \left(\frac{R_i^a}{R_c^2}\right)\right)_{dB} \tag{5.3}$$

where

$$\left(\frac{L_i}{L_c}\right)_{dB} = \alpha_i R_i - \alpha_c R_c \qquad \text{dB} \tag{5.4}$$

where α_c and α_i are the atmospheric attenuation for the communication and interception links respectively, obtained using the Liebe model of the atmosphere.

Also considering all other possible combinations it was noticeable that R_i and R_c are on both sides of the equation and there was no solution that will solve for R_c/R_i in a closed form. Therefore, to make the results comprehensive, a more practical and general approach was desired to perform the analysis. An appropriate and logical approach was to focus on the systems (transmitter,receiver and interceptor) design parameters; antennas gain, interference suppression capabilities, and required SNR for detection. Therefore, the system related parameters are defined as the system quality factor, Q_{SYS}, given by

$$Q_{SYS} = \left(\frac{G_{tc}G_{ct}}{G_{ti}G_{it}}\right)_{dB} + \left(\frac{N_{si}}{N_{sc}}\right)_{dB} + \left(\frac{S_i/N_{si}}{S_c/N_{sc}}\right)_{dB}. \tag{5.5}$$

This quality factor incorporates all of the design aspects of the communication and interception links. Now equation 5.2 becomes

$$Q_{SYS} = \left(\frac{R_c}{R_i}\right)^2_{dB} - (\alpha_i R_i - \alpha_c R_c) - (M)_{dB}. \tag{5.6}$$

Similar to the traditional LPI analysis it is desired to make Q_{SYS} as large as possible. The system quality factor can be simplified by considering the following: First, since no jamming was considered and it was assumed that the receiver and interceptor have the same noise at their respective inputs the interference suppression quality factor, Q_{IS}, was considered to be 0 dB. Second, as it was assumed at the outset for this research, the antennas are omnidirectional with unity gain giving the value of the antenna quality factor, Q_{ANT}, as 0 dB. Omnidirectional antennas are preferred because in most aircrafts and mobile communication units omnidirectional antennas are used due to their versatility, and lower cost and weight compared with other types of antennas. Therefore, omnidirectional antennas were used in this research to provide flexibility and mobility of the links

components. Under these considerations, for this research, $Q_{SYS} = Q_{MOD}$. And the LPI equation becomes

$$Q_{MOD} = \left(\frac{R_c}{R_i}\right)^2_{dB} + (\alpha_i R_i - \alpha_c R_c) - (M)_{dB}\,. \tag{5.7}$$

The modulation quality factor, Q_{MOD}, is the main design factor of the LPI system and is given by

$$Q_{MOD} = 10\log\left(\frac{(S_i/N_{si})_{req}}{(S_c/N_{sc})_{req}}\right) \tag{5.8}$$

where $(S_i/N_{si})_{req}$ is the required signal power to noise PSD ratio for the interceptor to intercept the signal for a given P_d and P_f, $(S_c/N_{sc})_{req}$ is the required signal power to noise PSD ratio for the receiver to receive the signal with a given P_e. This quality factor can be increased by utilizing spread spectrum design techniques. The transmitter 'attenuates' the signal power to noise PSD ratio of the transmitted signal by spreading it over a much larger bandwidth using a spreading code known to the receiver. The receiver is able to 'amplify' the received signal power to noise PSD ratio by despreading the received signal and reducing the bandwidth to the original information bandwidth. Equation 5.8 can be expressed as a function of the receiver and interceptor parameters as

$$Q_{MOD} = \frac{\zeta_i(P_d, P_f, T_i, B_i)}{\zeta_c(P_e, R_b)} \tag{5.9}$$

where $\zeta_i(P_d, P_f, T_i, B_i)$ is the signal power to noise PSD ratio required by the interceptor as a function of interceptor probability of detection, P_d, interceptor probability of false alarm, P_f, interceptor observation time, T_i, and interceptor bandwidth, B_i. And $\zeta_c(P_e, R_b)$ is the prespreading signal power to noise PSD ratio required by the receiver as a function of the desired reception probability of bit error, P_e, and given bit rate, R_b.

Using DS-SS signals equation 5.8 becomes [2]

$$Q_{MOD} = \left[\frac{SNR_i\, G_p}{SNR_c}\right] \tag{5.10}$$

$$Q_{MOD} = \left[\frac{\frac{S_i}{N_{si} B_i} G_p}{\frac{S_c}{N_{sc} B_{mod}}} \right] \tag{5.11}$$

where SNR_i is the required signal-to-noise ratio (SNR) for the interceptor to detect the signal without the use of SS by the transmitter, SNR_c is the required SNR for the receiver to receive the signal, S_i/N_{si} is the required signal-to-noise PSD ratio for the interceptor to detect the signal without the use of SS by the transmitter, S_c/N_{sc} is the signal-to-noise PSD ratio required at the receiver to receive the signal, and $\frac{S_i}{N_{si}} G_p$ is the required signal to noise PSD for the interceptor to detect the signal at the same distance, with the use of SS by the transmitter. For worst case interception we assume $B_i = B_{mod}$ and equation 5.11 becomes

$$Q_{MOD} = \left[\frac{\frac{S_i}{N_{si}} G_p}{\frac{S_c}{N_{sc}}} \right]. \tag{5.12}$$

For a wideband radiometer it was found in chapter II that the required signal power to noise plus interference PSD ratio is

$$\left(\frac{S_i}{N_{si}} \right)_{req} = d \sqrt{\frac{B_i}{T_i}} \tag{5.13}$$

where d is the detectability factor, B_i is the interceptor bandwidth, and T_i is the interceptor observation time. And for BPSK, using conventional modulation, it is also known that the postspeading signal power to noise PSD ratio is

$$\left(\frac{S_c}{N_{sc}} \right)_{req} = \frac{E_b R_b}{N_{sc}} = \frac{E_b B_{mod}}{N_{sc}}. \tag{5.14}$$

Therefore, using equations 5.13 and 5.14, equation 5.12 becomes

$$Q_{MOD} = 10 \log \left[\frac{\left(d \sqrt{\frac{B_i}{T_i}} G_p \right)}{\left(\frac{E_b}{N_{sc}} R_b \right)} \right]. \tag{5.15}$$

Also the processing gain can be defined in decibels as the difference between the required SNR, for interception and available SNR, at interception distance, as

$$(G_p)_{dB} = \left((SNR_{av})_{dB} - (SNR_{req})_{dB}\right) \tag{5.16}$$

where SNR_{av} is the available signal-to-noise ratio (SNR) for the interceptor with the transmitter employing SS techniques. This indicates that the conventionally required SNR_{req} by the interceptor is reduced by a factor of G_p. Consequently, the interceptor either moves closer to increase intercepted power or increases its sensitivity.

The factors of interest in this research are the communication range, R_c, intercept range, R_i, and system quality factor, Q_{SYS}. Through out this research, the following receiver and interceptor parameters are set, $P_e = 1 \times 10^{-4}$, $P_f = 1 \times 10^{-3}$, $P_d = 0.7$, $T_i = 1$ sec, $N_o = 1 \times 10^{-18}$, f=5 Ghz, and B_i=B_c=B_{mod}=20 khz. These values were chosen because they are commonly used in communications. Also they were not changed because changing them only changes the performance of the systems but not the effect on LPI analysis except for the bandwidths B_i and B_c are made equal to present a worst case scenario. And to make comparison between scenarios easier. The next step is to introduce the effect of the new mode quality factor without the atmosphere present. Then examine the effects of the atmosphere. Finally, the results with both parameters together as in equation 5.6 are shown by emphasizing how the atmospheric and mode quality factors interact and affect the analysis.

5.1 Mode Quality Factor, Q_M

The mode quality factor is introduced to account for the difference in the communication and interception links modes. This quality factor is a measure of loss due to the communication and interception modes employed. The mode quality factor is explained by presenting and discussing all the possible scenarios , with no atmospheric effects, graphically in the following subsections.

5.1.1 **Air-to-Air Communication And Interception.** This is the traditional LPI scenario with the propagation losses a function of the range squared, R^2, in both links. The contour lines of Q_{SYS} are shown in figure 5.1. These lines are used to decide the required Q_{SYS} for a specific communication range, R_c, and intercept range, R_i. In addition, the lines are straight and the 0 dB line represents a reference since moving to the left of this line means the interceptor is gaining, whereas moving right means the communicator is gaining. For example, if one wants to

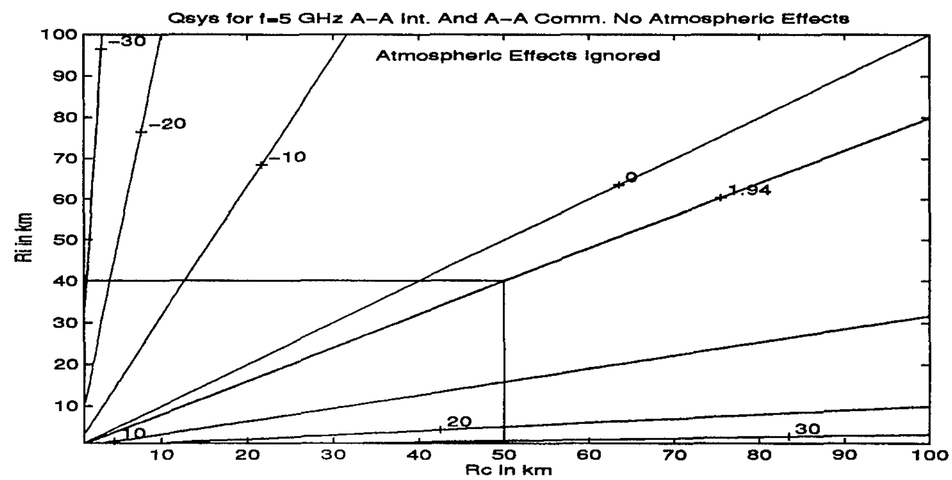

Figure 5.1 Q_{SYS} Contour Lines For Air-to-Air Communication And Interception, No Atmosphere

restrict the interception range to 40 km while maintaining a 50 km communication range, then a Q_{SYS} of about 1.94 dB is required, determined using equation 5.6. This was achieved by making G_p equal 26.63 dB, determined using equation 5.16.

5.1.2 **Air-to-Ground Communication And Interception.** This can also be called ground-to-air communication and interception scenario since from a propagation stand point they are the same. This case is similar to the case of air-to-air communications and interception discussed above. But it suffers higher losses in both links since the air-to-ground propagation, equation 3.24, losses are function of the range to the power 2.5, $R^{2.5}$, resulting in the Q_{SYS} contour lines being more dense compared with previous scenario as shown in figure 5.2. this increase in density indicates

an increased loss as a function of distance for the whole system since losses for this scenario are function of the range to power 2.5 ($R^{2.5}$). But it is desired to have R_c larger compared with R_i resulting in higher losses in the communication link. For example, for R_c of 50 *km* and R_i of 40 *km* then Q_{SYS} of about 2.5 *dB* is required.

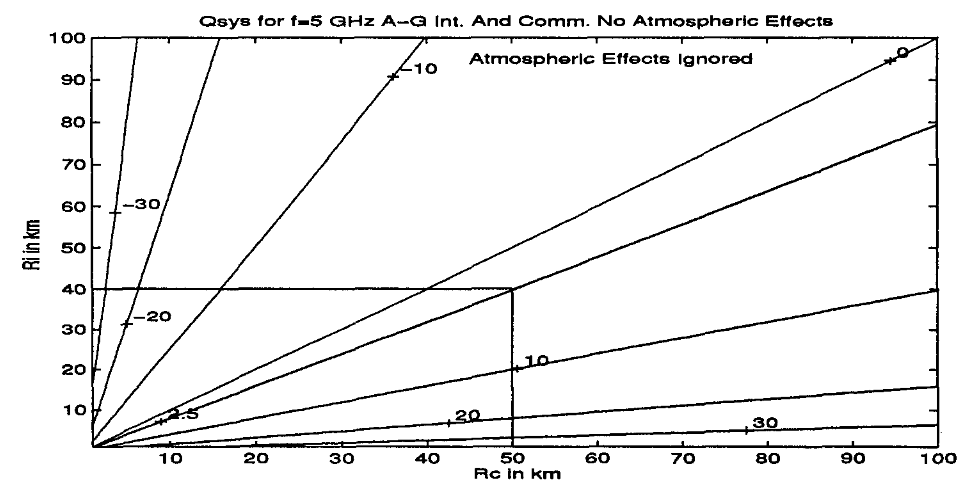

Figure 5.2 Q_{SYS} Contour Lines For Air-to-Ground Communication And Interception, No Atmosphere

5.1.3 **Ground-to-Ground Communication And Interception.** The Q_{SYS} contour lines are shown in figure 5.3. Also the contour lines are even more dense compared with air-to-air and air-to-ground propagation cases. This indicates more propagation losses as a function of distance because the ground-to-ground propagation losses are a function of the range to power 4 (R^4). And again since it is desired to have R_c larger than R_i, the propagation losses are higher in the communication link resulting in higher requirements on the communication link to establish the desired LPI measure. For example, for R_c of 50 *km* and R_i of 40 *km* then Q_{SYS} of about 4 *dB* is required.

5.1.4 **Air-to-Air Communication And Air-to-Ground Interception.** The contour lines of Q_{SYS} for this scenario are shown in figure 5.4. In this case the propagation losses in the communication and interception links are function of the range squared, (R^2), and the range to

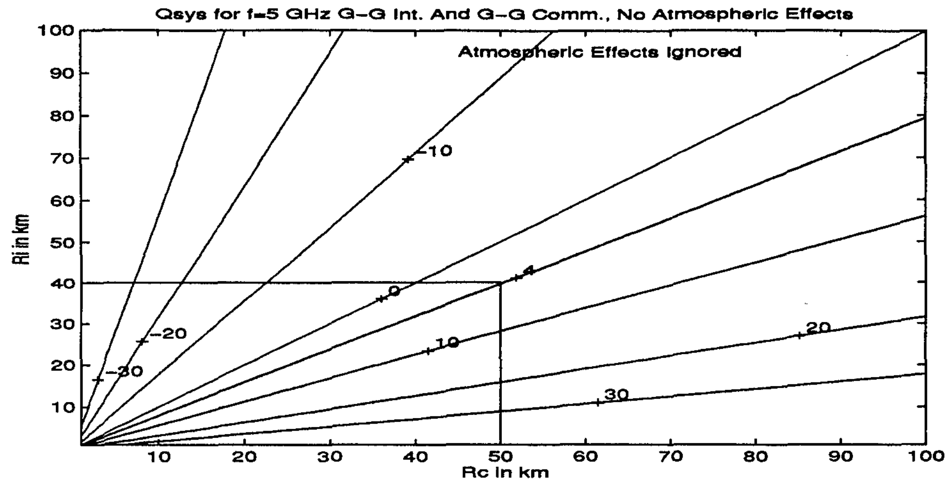

Figure 5.3 Q_{SYS} Contour Lines For Ground-to-Ground Communication And Interception, No Atmosphere

the power 2.5 ($R^{2.5}$), respectively. Therefore, the losses as a function of distance are higher for the communication link compared with relatively lower losses in the interception link. This is clarified by looking at the 0 dB line which is biased towards the communication range axis indicating that the communication link is having a better LPI quality due to lower propagation losses. Also the contour lines have some curvature and are not straight any more because the intercept link suffers more losses than the communication link even if the ranges are the same. For example, for R_c of 50 km and R_i of 40 km, using figure 5.4 the communication link is required to provide a Q_{SYS} of -21.1 dB, determined using equation 5.6. This was achieved by establishing G_p of 2.97 dB. The negative value for Q_{SYS} indicates that it is much easier for the communication link to establish LPI communications because the processing requirements are comparatively lower as seen by the value of G_p.

5.1.5 **Air-to-Ground Communication And Air-to-Air Interception.** Figure 5.5 shows Q_{SYS} contour lines for this scenario. This is the opposite of the case of air-to-air communication and air-to-ground interception discussed above where the situation was switched to the interceptor's advantage. The consequence of this case are the opposite of section 5.1.4 because

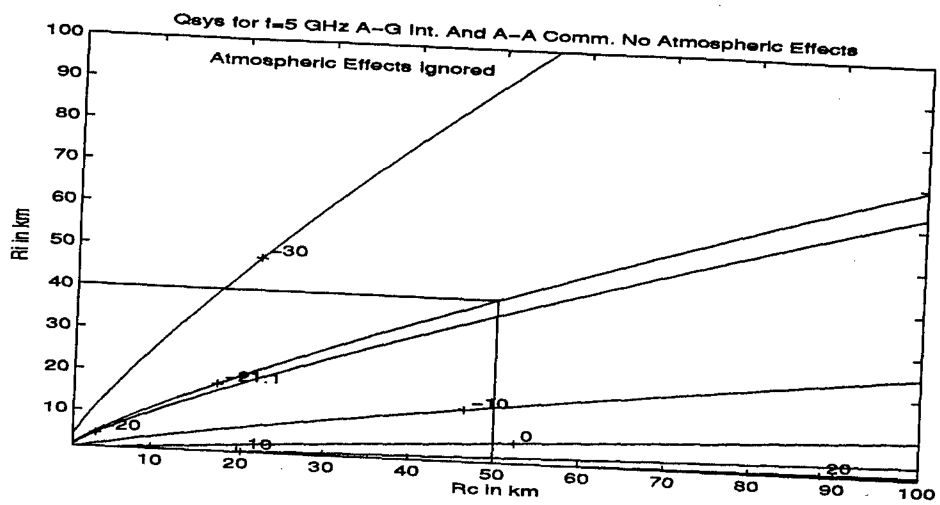

Figure 5.4 Q_{SYS} Contour Lines For Air-to-Air Communication And Air-to-Ground Interception, No Atmosphere

the communication link is required to provide a Q_{SYS} of 25.5 dB for the same communication range of 50 km and interception range of 40 km. This was achieved by making G_p equal 49.76 dB, increasing the requirements on the communication link.

5.1.6 **Ground-to-Air Communication And Ground-to-Ground Interception.** In this scenario the ground-to-ground propagation losses are a function of the range to the power 4, R^4, compared with the ground-to-air losses a function of $R^{2.5}$. Therefore, the communication link suffers less propagation losses, consequently the system is biased towards the communication link indicated by the condensation of the contour lines near the communication range axis as shown in figure 5.6. For the same R_c and R_i, Q_{SYS} required is about -100 db and G_p is -75.7 dB. This result means that the system can achieve LPI not only with out SS but it can also increase R_c and still maintain covertness of communications. The negative value for G_p means no SS is needed since the value of G_p must be positive, then going back to equations 5.6 and ??, G_p can be set to 0 dB and Q_{LPI} increased.

5.1.7 **Ground-to-Ground Communication And Ground-to-Air Interception.** Figure 5.7 represents the contour lines for Q_{SYS} which can be seen to be the opposite of the

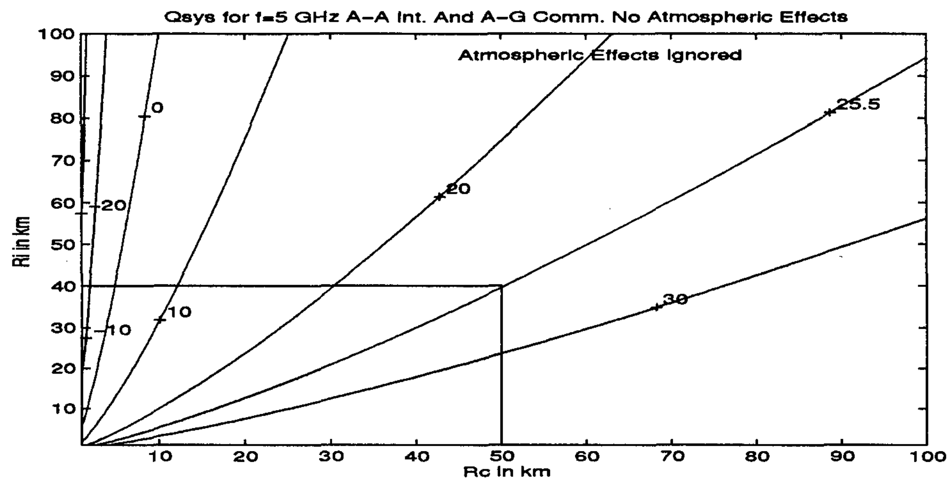

Figure 5.5 Q_{SYS} Contour Lines For Air-to-Ground Communication And Air-to-Air Interception, No Atmosphere

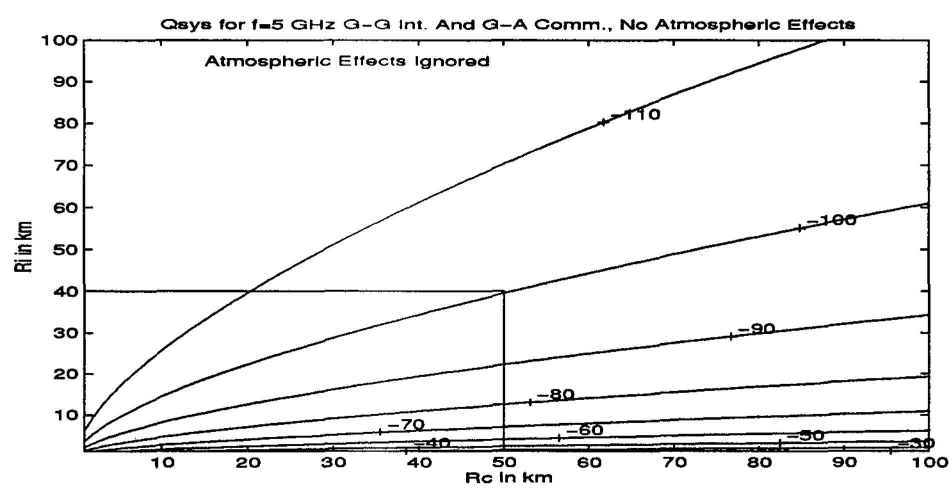

Figure 5.6 Q_{SYS} Contour Lines For Ground-to-Air Communication And Ground-to-Ground Interception, No Atmosphere

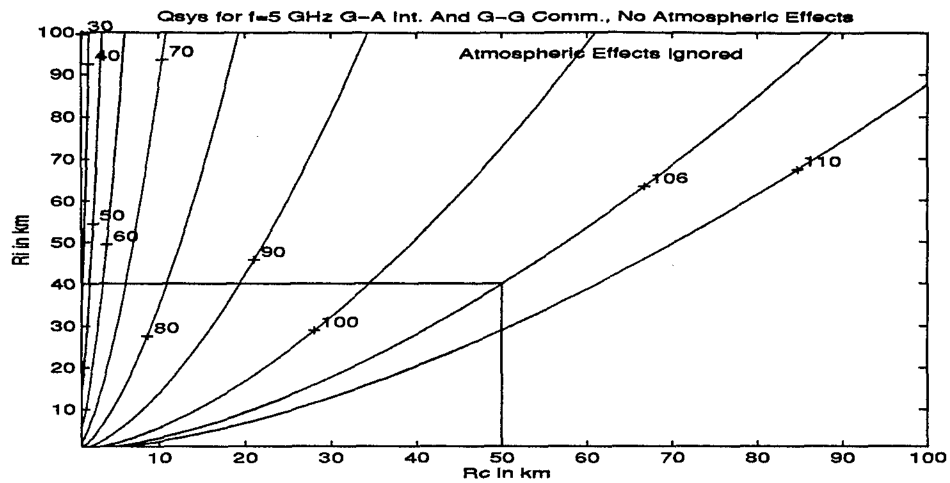

Figure 5.7 Q_{SYS} Contour Lines For Ground-to-Ground Communication And Ground-to-Air Interception, No Atmosphere

case of ground-to-air communication and ground-to-ground interception discussed above where the interceptor is in a better situation than the receiver. This result means that the requirements on the communication link are very high to achieve some measure of LPI.

The presentation of all of the above scenarios indicate that the 0 dB line can be used as a reference to indicate which link the whole system is biased towards. Next the atmospheric quality factor, Q_{ATM} is discussed.

5.2 Atmospheric Quality Factor, Q_{ATM}

The atmospheric effect is discussed using air-to-air communication and interception because the air-to-air propagation mode has the lowest propagation losses G giving a more distinct display of the effect atmospheric losses. The results for the atmospheric attenuation can viewed through figures 5.8 and 5.9. Figure 5.8 shows the contours for the system quality factor, Q_{SYS}, according to the assumption of the traditional LPI equation which assumes that the atmospheric quality factor, Q_{ATM}, is 0 db. On figure 5.8 to achieve a communication range of 50 km with an intercept range of 40 km (or R_c/R_i of 5/4), the communication link is required to have a transmission

power of 11.76 dBw determined using equation 3.8 ignoring atmospheric losses. Also for LPI the required Q_{SYS} is 1.94 dB, using equation 5.6, this requires a processing gain,G_p, of 26.63 dB, using equation 5.16. As can be seen, the contour lines are straight. But when atmospheric attenuation is considered for both links under 100 mm/h rain, figure 5.9 shows that to achieve the same R_c and R_i, first the transmitted power need to be increased to 31.85 dBw, determined using equation 3.8 with atmospheric losses. Second, it is required to increase Q_{SYS} to 5.95 dB and G_p to 41.7 dB. Note that the contour lines are not straight. This indicates that the interceptor gained an advantage because the requirements on the communication link became relatively higher. It can be concluded for the case of the communication and interception links in the same atmosphere that as the atmospheric conditions get worse the interceptor gains with respect to the receiver. The reason for that is because the goal of LPI is to make R_c as large as possible compared with R_i, this results in higher losses in the communication link and as a result the transmitter is required to increase the transmitted power to mate up for these losses. But the interceptor losses are lower and increase in transmitted power makes it possible for the interceptor to increase its range. Therefore, Q_{ATM} is very important and should be considered in the analysis and can not be assumed to be zero, except in the case of having the receiver and interceptor at the same range as seen by the 0 dB contour line in both figures 5.8 and 5.9.

Another important case is when the communication and interception links are in different atmospheric conditions. It was concluded that if the atmospheric conditions in the communication link are worse than those in the interception link then the interceptor gains and vice versa. The two figures 5.10 and 5.11 graphically shows these results. Figure 5.10 shows a situation in which the communication link was in dry air and the interception link was in 100 mm/h rain. Considering the same R_c = 50 km and R_i = 40 km discussed earlier the transmitted power was reduced to P_t = 12.18 dBw, determined using equation 3.8, and required Q_{SYS} reduced to -13.7 dB, determined using equation 5.6 which reduced G_p to 22.06 dB, determined using equation 5.16. Also as can be seen from figure 5.10 as R_c increases R_i only increases by a small amount compared

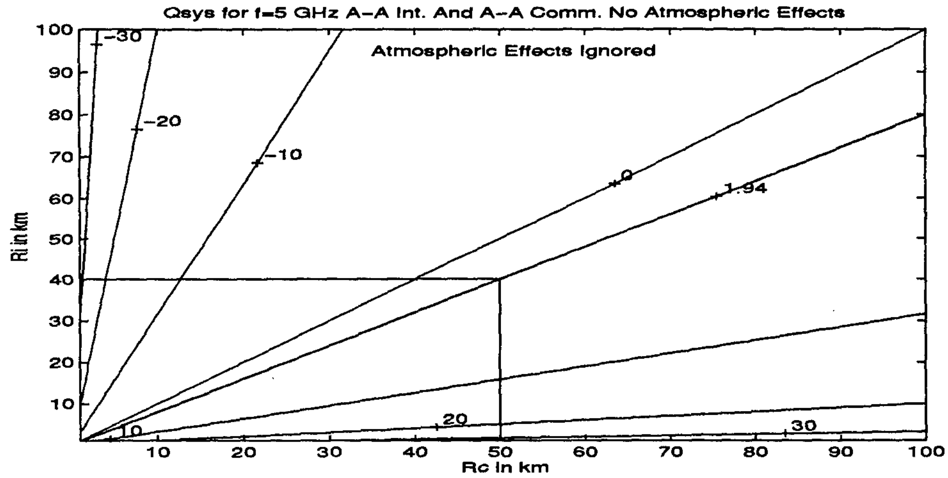

Figure 5.8 Contours For Q_{SYS} Ignoring Q_{ATM}, For Air-to-Air Communication And Interception

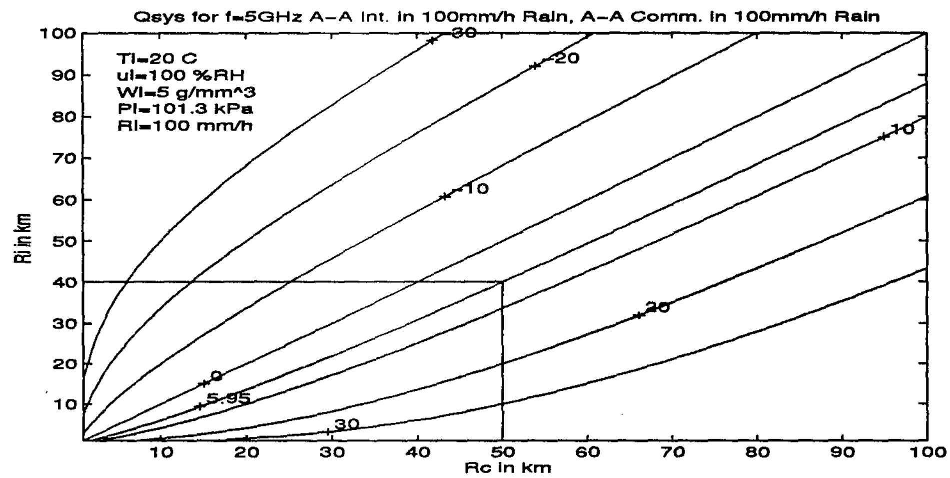

Figure 5.9 Contours For Q_{SYS} Considering Q_{ATM}, For Air-to-Air Communication And Interception, And The Same Atmospheric Conditions As Shown For Both The Communication and Interception Links

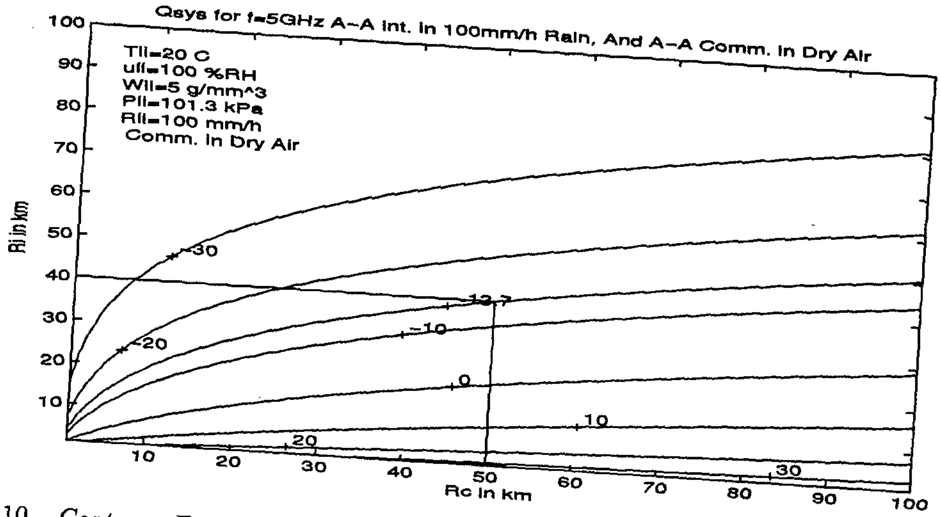

Figure 5.10 Contours For Q_{SYS} Considering Q_{ATM} For Air-to-Air Communication And Interception And Different Atmospheric Conditions As Shown For Both Communication And Interception Links

to R_c. But when the situation was reversed as shown in figure 5.11, the interceptor has an advantage over the receiver. Therefore, for an R_c of 50 km and an $R_i = 40$ km, the transmitted power must be increased to 31.85 dBw to maintain the communication link, using the air-to-air propagation equation 3.8. To force the interceptor to $R_i = 40$ km, Q_{SYS} was increased to 21.7 dB, using equation 5.6, which increased G_p to 57.50 dB by equation 5.16. This means that the requirements on the communication link are very high to maintain an LPI link. Consequently, this will be at the expense of a more expensive and complicated transmitter and receiver. The available means of achieving this objective is to increase G_p. Also it can be seen that as R_c increases R_i increases more rapidly giving the interceptor a bigger advantage.

The figures discussed above clearly indicate the importance of the atmospheric quality factor. Also it shows that if the two links are in different atmospheric conditions, then the 0 dB contour line moves towards the link that is under better atmospheric conditions (this term was explained in section 2.2.2). The contributions of Q_{SYS} and Q_M so far were considered separately. It turned out that combining the contributions of the two together in the overall analysis proved even more

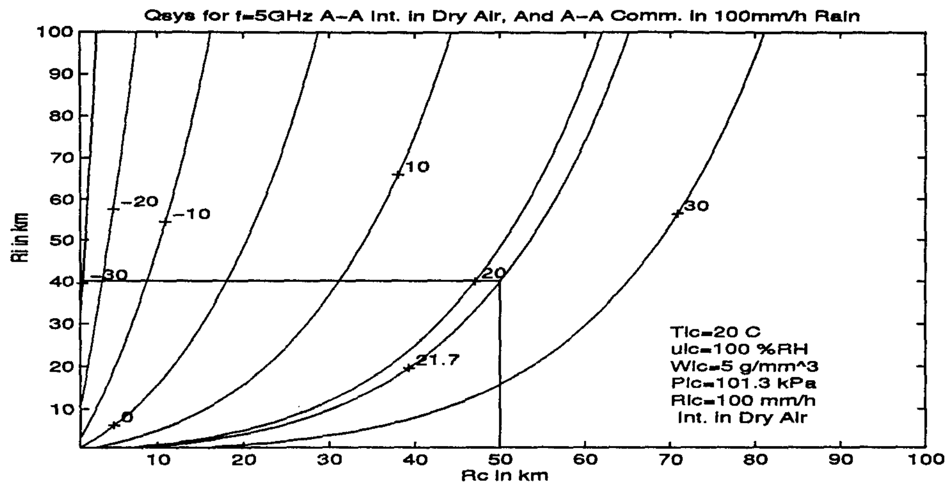

Figure 5.11 Contours For Q_{SYS} Considering Q_{ATM} For Air-to-Air Communication And Interception And Different Atmospheric Conditions As Shown For Both Communication And Interception Links

interesting. Therefore, some of the previously discussed scenarios are presented again but this time both the modes used by each link, and the atmospheric conditions in each link were different.

5.3 Mode Quality Factor Q_M And Atmospheric Quality Factor, Q_{ATM}

The combined effect of the mode and atmospheric quality factors were studied in two ways. First, the communication and interception links were put under the same atmospheric conditions for all the possible scenarios and Q_{SYS} contour lines were plotted for R_c and R_i in the range of 0 to 100 *km*. Second, the two links were put under different atmospheric conditions and investigated. Then the atmospheric conditions were interchanged between the two links and the results were compared with the previous case. Also in each case the transmitted power was increased or reduced to maintain the communication link for the desired communication range. Consequently, the focus was on the how Q_{SYS} changes reflecting gain or loss inflicted on each link.

5.3.1 **Same Communication and Interception Modes.** There are four cases to consider but since air-to-ground and ground-to-air are the same only air-to-ground will be discussed.

In all scenarios under consideration the two links were put under the same atmospheric conditions of T_l=20 $°C$, U_l=100 $\%RH$, W_l=5 g/mm^3, P_l=101.3 kPa, and R_l=100 mm/h.

5.3.1.1 **Air-to-Air.** This situation is the traditional LPI scenario on which the original LPI equation (equation 2.14) was based. The plot of Q_{SYS} as a function of R_c and R_i was presented in figures 5.8 and 5.9 to illustrate the difference between ignoring and considering the atmospheric quality factor while the mode quality factor, Q_M, is 0 dB (i.e. same propagation mode for both links). In addition, when the two links were under different atmospheric conditions, the 0 dB Q_{SYS} contour line moved towards the link that was under more favorable atmospheric conditions (this term was explained in section 2.2.2) giving it an advantage over the other link.

5.3.1.2 **Air-to-Ground.** In this case the mode quality factor added some attenuation due to the difference in ranges with the zero contour line similar to that in the air-to-air case. It can be seen from figure 5.12 that the contour lines are similar to those in figure 5.9 but they are more condensed. That is, to achieve the same R_c=50 km and R_i=40 km it was required to increase Q_{SYS} to 6 dB. The reason is that the main goal of LPI is to increase R_c with respect to R_i. Therefore, the intercept link suffers less mode losses than the communication link resulting in an advantage for the interceptor.

5.3.1.3 **Ground-to-Ground.** In the ground-to-ground scenario, the additional attenuation was exacerbated by the difference in ranges. Since the changes in the transmitter, receiver and interceptor heights was in the order of meters, the major cause of attenuation was the difference in ranges which was in the order of kilometers. Figure 5.13 shows Q_{SYS} contour lines for of this scenario where the heights of the receiver and interceptor were 1 *meter*. Again the 0 dB Q_{SYS} contour line is the same as the previous cases but the other lines are even more condensed than the previous two cases. In addition, for R_c=50 km and R_i=40 km, Q_{SYS} was increased to 8

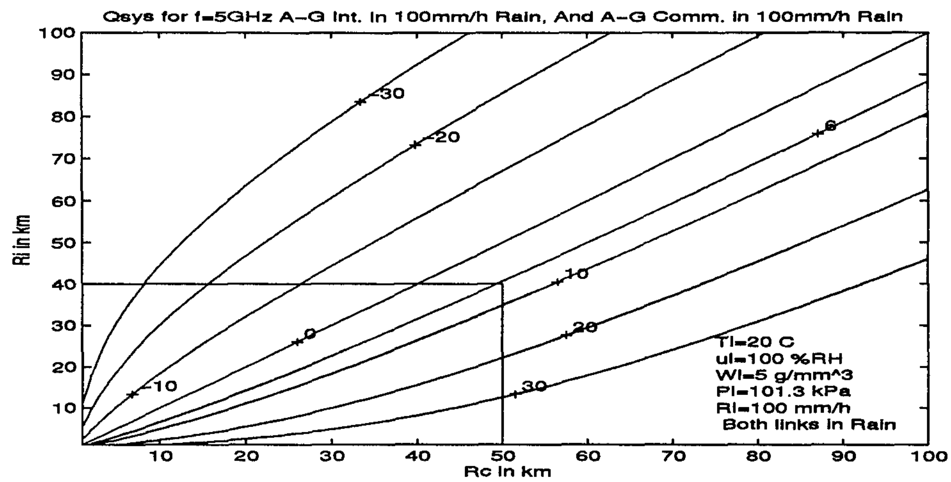

Figure 5.12 Contours For Q_{SYS} for Air-to-Ground Communication and Interception Links Under The Same Atmospheric Conditions As Shown

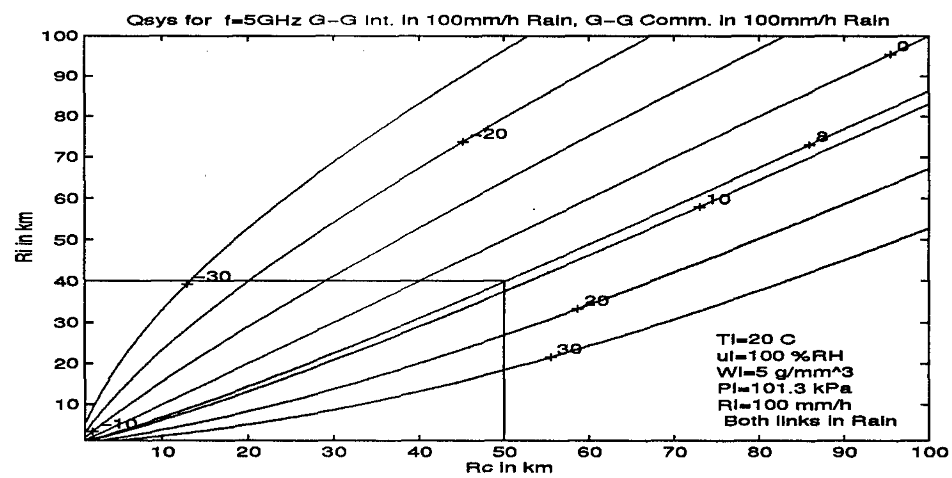

Figure 5.13 Contours For Q_{SYS} for Ground-to-Ground Communication and Interception Links Under Atmospheric Conditions Shown

dB where as in the air-to-ground case, it was 6 dB resulting in an increase of 2 dB due to both the mode and atmospheric losses.

The contour lines in the above three cases become denser as the mode goes from air-to-air to air-to-ground to ground-to-ground. Also the lines are not straight any more but are curved due to the losses in both links being a function of the range to power 4 (R^4) and the added losses due to the atmosphere made the curves nonlinear.

5.3.2 **Different Communication and Interception Modes.** The mode and atmospheric quality factors were discussed fully in isolation in the previous two section. This section addresses cases with different modes and different atmospheric conditions. In the case of different modes for the communication and intercept links, the situation became better or worse for the communication link depending on the mode of propagation and the atmospheric conditions imposed on the communication link. In the following cases for a given communication and interception mode, different atmospheric conditions were set then interchanged and the results compared. The two atmospheric conditions considered for all the following scenarios were: 1) rain with T_l=20 $°C$, U_l=100 $\%RH$, W_l=5 g/mm^3, P_l=101.3 kPa, and R_l=100 mm/h; 2) dry air with T_l=20 $°C$ and the rest of the atmospheric parameters set to zero.

5.3.2.1 **Air-to-Air Communication And Air-to-Ground Interception.** The two cases are shown graphically in figures 5.14 and 5.15 shows. First, figure 5.14 shows the results for an air-to-air communication link in rain with an air-to-ground intercept link in dry air. The shift of the 0 dB line towards the intercept range axis indicates that even though the communication link was in air-to-air mode the atmospheric losses in the communication link were so high that the intercept link had an advantage over the communication link. For example, for R_c=50 km and R_i=40 km required Q_{SYS}=-1.5 dB compared to -21.1 dB for the same case ignoring atmospheric effects as discussed in section 5.1.4. Second, when the atmospheric conditions were reversed, the situation was reversed giving the advantage to the communication link as shown in figure 5.15. As

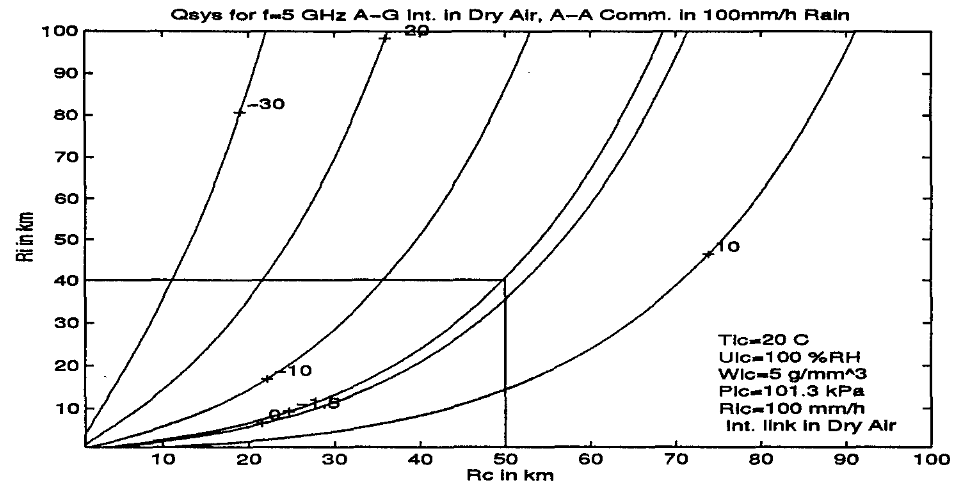

Figure 5.14 Air-to-Air Communications in Rain With Air-to-Ground Interception in Dry Air

a result, for R_c=50 km and R_i=40 km, the requirements on the communication link were much less and Q_{SYS} was reduced to -37 dB.

5.3.2.2 **Air-to-Ground Communication And Air-to-Air interception.** In this case the communication link is under rain while the interception link is in dry air. This was compared to the same mode situation but with the atmospheric conditions reversed. The results of the two scenarios are shown in figures 5.16 and 5.17.

Figure 5.16 shows, as in section 5.3.2.1 that the requirements on the communication link were increased due to being under worse atmospheric conditions. For the same R_c and R_i relationship as before (i.e. $R_c = 50\ km$ and $R_i = 40\ km$) the required Q_{SYS} was 45 dB. Again reversing the atmospheric conditions resulted in reversing the advantage as shown in figure 5.17 where Q_{SYS} is 10 dB.

5.3.2.3 **Ground-to-Air Communication And Ground-to-Ground Interception.** The same atmospheric conditions used before were applied in this scenario giving the results shown in figures 5.18 and 5.19. Figure 5.18 shows that even though the communication link was in rain it was still able to easily establish LPI. This occurs because the propagation losses in

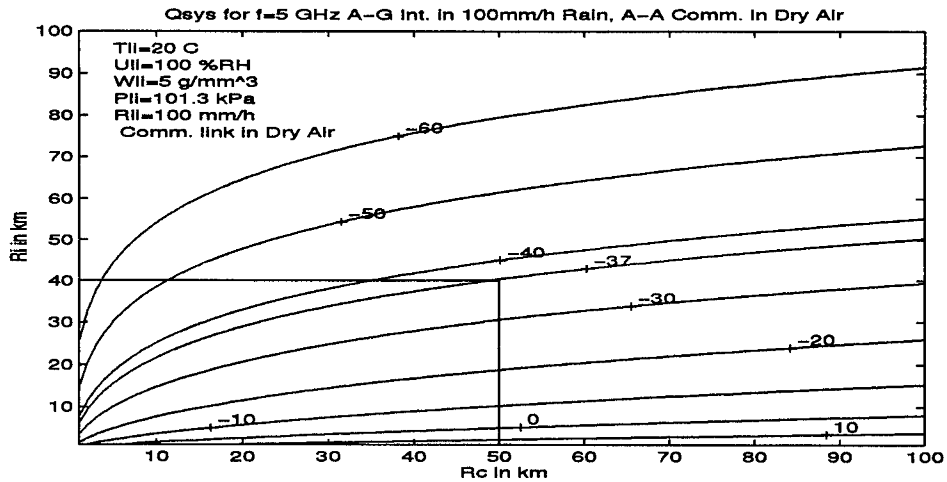

Figure 5.15 Air-to-Air Communications in Dry Air With Air-to-Ground Interception in Rain

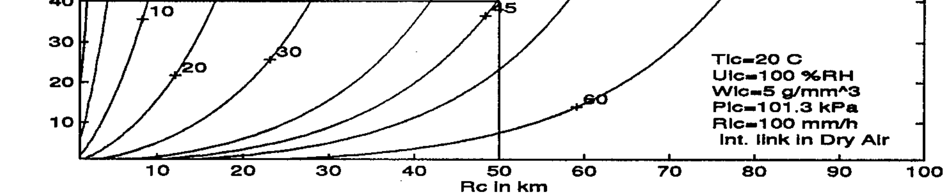

Figure 5.16 Air-to-Ground Communications in Rain With Air-to-Air Interception in Dry Air

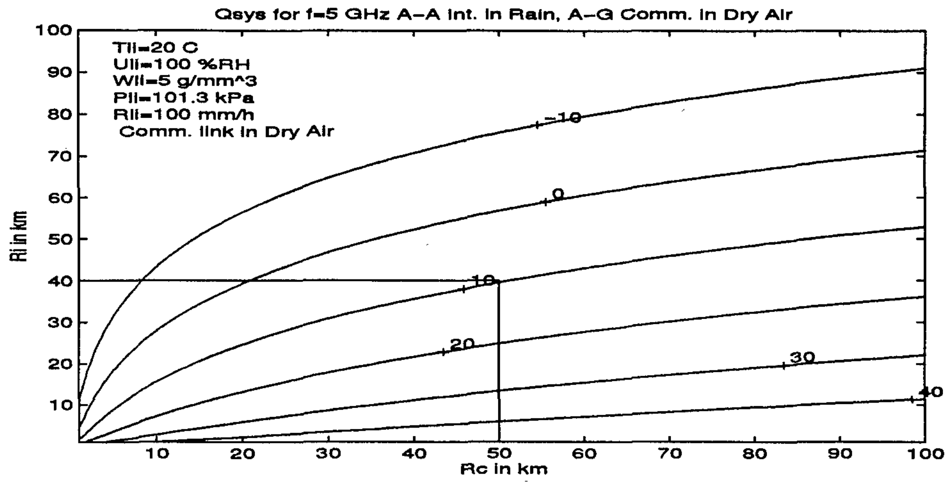

Figure 5.17 Air-to-Ground Communications in Dry Air With Air-to-Air Interception in Rain

the ground-to-ground interception link were large compared with the atmospheric and propagation losses in the communication link. In figure 5.19, interchanging atmospheric conditions resulted in making it easier for the communication link to be covert because the interception link was suffering from both high propagation losses and high atmospheric losses. Consequently, in such situations it is very difficult, if not impossible, for the interceptor to intercept the communications signal.

5.3.2.4 Ground-to-Ground communication And Ground-to-Air Interception.

Again the same atmospheric conditions were used. The results are shown in figures 5.20 and 5.21. This case is the opposite of the previous one because the modes were switched around. Figure 5.20 indicates a clear advantage for the interception link since the communication link was suffering from the high ground-to-ground propagation losses. In figure 5.21, it is shown that even when the atmospheric conditions were interchanged, the interception link still had a large advantage over the communication link despite the rain on the interception link.

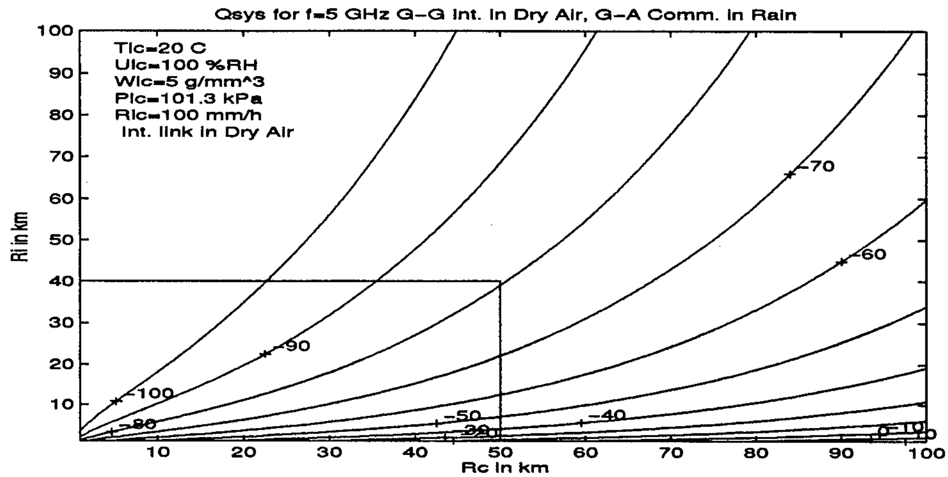

Figure 5.18 Ground-to-Air Communications in Rain With Ground-to-Ground Interception in Dry Air

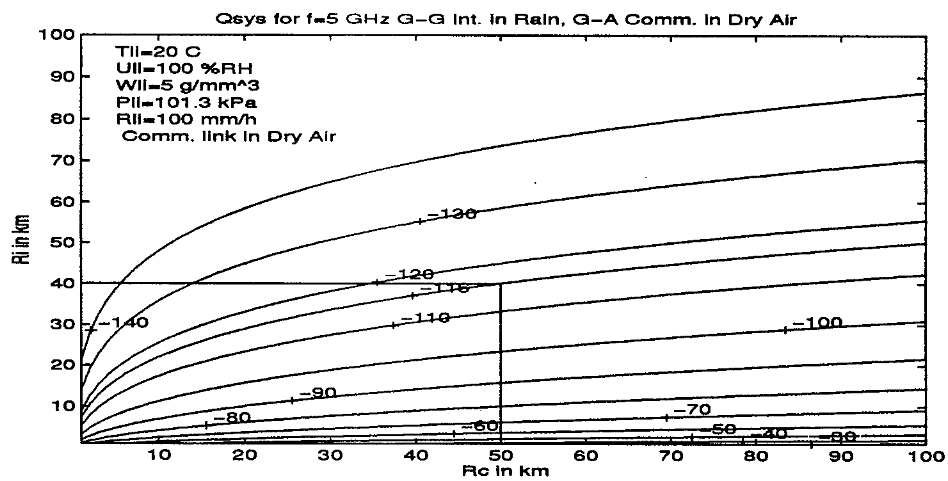

Figure 5.19 Ground-to-Air Communications in Dry Air With Ground-to-Ground Interception in Rain

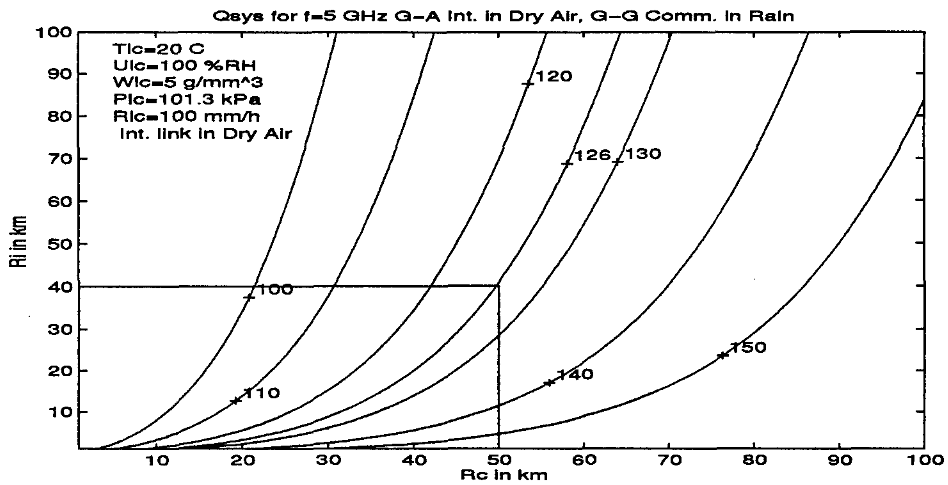

Figure 5.20 Ground-to-Ground Communications in Rain With Ground-to-Air Interception in Dry Air

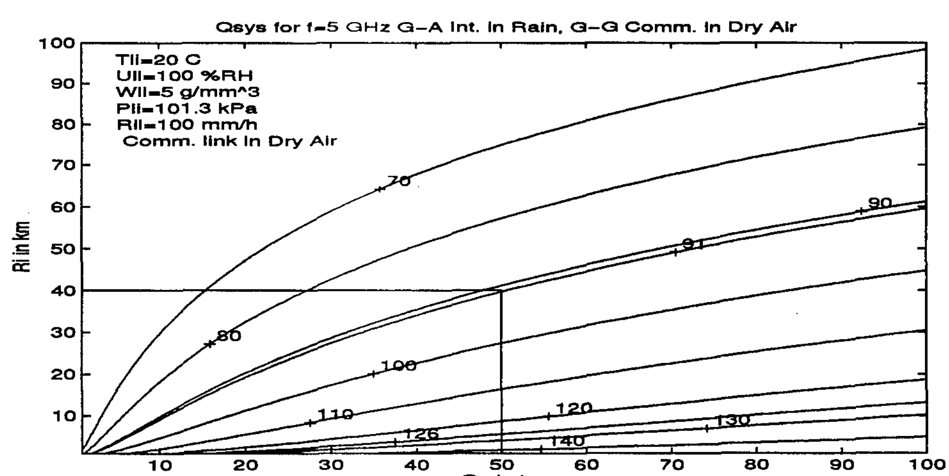

Figure 5.21 Ground-to-Ground Communications in Dry Air With Ground-to-Air Interception in Rain

5.4 Summary of Results

In conclusion, the results obtained in this research emphasize the importance of both the mode and atmospheric quality factors. These two factors should not be ignored in LPI analysis. On the contrary, they could prove very useful for determining ways to enhance covertness while reducing the design requirements on the communication link. In addition, the results indicated that the mode quality factor is very crucial for the communication link, especially in ground-to-ground communications mode because the ground-to-ground propagation mode the losses are the highest being a function R^4 compared to $R^{2.5}$ and R^2 for the air-to-ground and ground-to-ground modes respectively. Also the atmospheric effects become more severe if higher frequencies were employed as was shown in the Liebe model. Therefore, in Multimode Low-Probability-of-Intercept (MLPI) communication system analysis both should be considered. The results for this chapter are summarized in table 5.1.

	Communication	Interception	
Case	T_x-R_x	T_x-I	Results
1	A-A	A-A	Both links suffer same losses but since R_c is desired to be larger, loss in the communication link is higher and both are function of R^2. Atmospheric conditions add losses to both links and link under added better conditions will have an added advantage over the other link. See figures 5.1, 5.9, 5.10 and 5.11
2	A-A	A-G	Loss in interception link is higher and function of $R^{2.5}$ and loss in communication link is lower and function of R^2. If interception link is in worse atmospheric conditions it becomes easier for communication link to establish LPI communications. If the communication link is under worse atmospheric conditions atmospheric conditions then as these conditions get worse the advantage for interception link increases. See figures 5.4, 5.14 and 5.15
3	A-G	A-A	Communication link loss function of $R^{2.5}$ and interception link loss function of R^2. Gain for interception link. If communication link under worse atmospheric conditions, requirements increase to establish LPI. If interception link under worse atmospheric conditions communication link gains as atmospheric conditions get worse. See figures 5.5, 5.16 and 5.17.
4	A-G	A-G	Similar to case 1, but propagation losses in both links are function of $R^{2.5}$. See figures 5.2 and 5.12.
5	G-A	G-G	Communication link propagation loss function of $R^{2.5}$. Interception link propagation loss function of R^4. Communication link under better atmospheric conditions it makes it easier to establish LPI. If interception link is under better atmospheric conditions interception capabilities improves depending on how bad are the atmospheric conditions in the communication link. See figures 5.6,5.18 and 5.19.
6	G-A	G-A	Similar to case 4.
7	G-G	G-G	Similar to cases 1, 4 and 6. But losses in both links function of R^4. See figures 5.3 and 5.13
8	G-G	G-A	The opposite of case 5. The communication link loss function of R^4. Interception link loss function of $R^{2.5}$. See figures 5.7, 5.20 and 5.21.

Table 5.1 Summary Of Results (I: interceptor; R_x: receiver; T_x: transmitter; A: Airborne; G: ground based).

VI. Conclusions and Recommendations

6.1 Conclusions

6.1.1 **Summary.** The objective of this research was to improve Low-Probability-of-Intercept (LPI) communications analysis. Two areas were considered: 1) The expansion of the LPI analysis to include air-to-ground, ground-to-air, and ground-to-ground communication modes because in practical applications and especially in military operations all modes of communication are employed instead of air-to-air communications; 2) The clarification of the role of atmospheric effects on LPI link analysis and the invalid assumption used in the literature that having the same atmospheric conditions in both the communication and interception links allows the analysis to ignore the atmospheric quality factor, Q_{ATM}. The overall results for this research are summarized in table 5.1 in section 5.4. This table gives a very quick and brief reference for the results. The mode and atmospheric effects are discussed independently in the following sections.

6.1.2 **Modes Quality Factor,** QM. The inclusion of the three propagation equations in LPI analysis resulted in the introduction of the *mode quality factor*, Q_M, which was added to the already existing LPI quality factors. This quality factor expanded LPI analysis, to include air-to-ground, ground-to-air, and ground-to-ground propagation modes. Consequently, the LPI analysis was expanded, from just being applicable to air-to-air scenarios, to include all the possible scenarios that might be considered by the combination of the three propagation modes. Which was called Multimode LPI (MLPI).

6.1.3 **Atmospheric Quality Factor,** Q_{ATM}. The results obtained in this research clearly showed that the assumption of ignoring the atmospheric quality factor is not valid whether the communication and interception links are under the same or different atmospheric conditions. In addition, it was noticed that the atmospheric quality factor can be advantageous or disadvantageous, from the communicators stand point, depending on the weather conditions in both links. Generally,

the link, communication or interception, that is under worse atmospheric conditions suffer more losses resulting in the reduction in its LPI capabilities in terms of covertness for the communication link or interception for the interception link.

Another important point concluded was that using spread spectrum techniques is not always a feasible or acceptable solution to achieve the LPI result desired because the processing gain, G_p, has an upper limit and increasing G_p increases the system complexity and cost. In addition, if spread spectrum does achieve desirable results it will be at the cost of very high processing gain which in turn means more expensive, complicated, and heavier communication equipment. Therefore, in scenarios where the requirements on the communication link are very high to achieve covertness, other means need to be exploited in conjunction with spread spectrum techniques. Some of these means are directional antennas and null steering antennas.

6.2 Recommendations

It was concluded that other means might be required in some scenarios to obtain some measure of LPI. Directional antennas and null steering antennas are a feasible solution provided they do not add to system complexity, in terms of high processing time and cost, or other undesirable effects. These two techniques greatly improve covertness while reducing the requirements on signal and system design. Therefore, a good follow up research project would be to study the feasibility of including these techniques in the MLPI analysis in a meaningful way. Also since the results in this research were based on the assumption of the earth being quasi-smooth and flat (flat earth assumption is valid for a range of about 50 km) another quality factor could be added to the analysis to account for terrain effects. Therefore, additional research on LPI Quality Factors can be very useful in enhancing MLPI analysis and improving the accuracy of LPI estimates.

Appendix A. The Liebe Model

The Liebe Model, also known as The Millimetric Propagation Model (MPM), was developed by Dr. Hans Liebe of the Institute for Telecommunication Science (ITS). It was based on years of laboratory work by simulating atmospheric variables and monitoring their effect on electromagnetic waves for frequencies up to 1000 GHz. The results were studied and equations generated to fit these results. Over time, refinement of the experiments resulted in adjustments to the equations to yield a closer agreement with the experimental data.

A.1 Introduction

A major obstacle in using millimeter wave frequencies over an atmospheric channel is signal attenuation and distortion due to atmospheric elements such as rain, fog, snow, and suspended water particles [25]. The MPM Model includes the broadest number of observable atmospheric phenomena under the least number of postulates [7]. Therefore, the MPM Model relates measurable meteorological variables (temperature, pressure, etc) to propagation variables (attenuation, time delay and phase dispersion). Since wave parameters (signal strength, polarization, etc) are modified by the neutral atmosphere, a macroscopic approach to signal propagation is to model the atmosphere by a refractive index which gives a measure of the interaction between the electromagnetic wave and the atmospheric medium[7]. A general expression for a propagating plane wave is [22]:

$$E(x) = E_o \exp\left(-j\gamma x\right) \tag{A.1}$$

where the propagation constant γ is defined as a function of the complex refractive index, n

$$\gamma = 2\pi f \frac{n}{c} \tag{A.2}$$

Putting this result into equation A.1 results in a wave equation written as an explicit function of the refractive index n, as

$$E(x) = E_o \exp\left[\frac{-j2.\pi.f.x.n}{c}\right] \tag{A.3}$$

where

- E_o is the initial amplitude of signal
- c is the speed of light in vacuum
- f is the frequency of the wave
- x is the distance traveled by the wave

In above equation the index of refraction, n, is a function of frequency and atmospheric conditions. Although the changes in its value are small (in the order of 0.0005 for the real part and 0.001 for the imaginary part), a small difference in the real part reduces the propagation velocity to something less than c, while the associated imaginary part attenuates the signal amplitude. To make the study of refractivity more convenient, another measure is introduced called the complex refractivity, defined in units of parts per million (*ppm*) and given by [25] [13]:

$$N = (n-1)10^6 \qquad ppm \tag{A.4}$$

A.2 MPM Model

The seminal references for the MPM model are [7] [8]

A.2.1 Model Variables.

A.2.1.1 **Input Variables.** The input parameters for the MPM Model are:

1. Barometric pressure, P, in kPa

$$P = p + e \tag{A.5}$$

where p and e are partial pressures for dry air and water vapor, respectively.

2. Temperature, T_l, in $°C$ which is converted into a relative inverse temperature variable as

$$\theta = \frac{300}{(T_l + 273.15)} \tag{A.6}$$

3. Relative humidity, U_l, in $\%RH$

$$U_l = \left(\frac{e}{e_s}\right) 100 \tag{A.7}$$

where e_s water vapor saturation pressure. The water vapor concentration, v, in g/m^3 can be expressed in terms of the relative humidity as follows

$$v = 7.223e\theta = 1.73910^9 U_l \theta^5 \exp -22.64\theta \tag{A.8}$$

4. Suspended water droplet concentration, W_l, in g/m^3

5. Rainfall rate, R_l, in mm/h

6. Frequency, f, in Ghz

In summary, six atmospheric input variables (P_l, T_l, U_l, W_l and R_l) and frequency, f, are used in the MPM Model

A.2.1.2 **Output Variables.** The main output of the model is the complex refractivity in *ppm* as

$$N_t(f) = N_{ol} + N(f) = N_{ol} + N'(f) - jN''(f) \tag{A.9}$$

where N_{ol}, the nondispersive part, is real, positive and defined as

$$N_{ol} = N_1 + N_2 + N_3 + N_4 \tag{A.10}$$

where dry air contribution is defined as

$$N_1 = 2.588p\theta \tag{A.11}$$

water vapor contribution defined as

$$N_2 = (41.63\theta + 2.39)e\theta \tag{A.12}$$

water droplet contribution defined as

$$N_3 = W_l(3/2)[1 - 3/(\epsilon_o + 2)] \tag{A.13}$$

and rain contribution defined as

$$N_4 = R_l(3.7 - 0.012R)/k_r \tag{A.14}$$

The factor k_r is the imaginary rain refractivity coefficient which is a function of frequency, and drop size and shape. And N is, the dispersive part of refractivity, which is a function of frequency

and defined by

$$N = N' - jN'' = (N_l + N_d + N_c) + N_w + N_r \tag{A.15}$$

where N' and N'' are real and N_l, N_d, N_c, N_w, and N_r are complex in general.

The dispersive part of the complex refractivity is then converted to the following path specific variables: α the propagation loss in dB/km, β the phase dispersion in deg/km, and τ the dispersive delay in ps/km. These variables are related to the refractivity as follows

$$\alpha = 0.1820 f N''(f) \qquad \text{dB/km} \tag{A.16}$$

$$\beta = 1.2008 f N'(f) \qquad \text{deg/km} \tag{A.17}$$

$$\tau = 3.336 N'(f) \qquad \text{psec/km} \tag{A.18}$$

Since the dispersive part is important because it causes signal amplitude attenuation, signal phase dispersion, and signal delay as shown in equations A.17, A.18 and A.18, each of its elements will be discussed in detail next.

A.2.1.3 **Dispersive refractivity.** As shown above, dispersive refractivity consists of five parameters. these parameters will be defined and explained individually.

1. Moist air resonance contribution. N_l, (44 oxygen lines and 30 water vapor lines). The spectral line-by-line summation of two absorbing molecules, O_2 and H_2O, gives the resonance contribution

$$N_l = \sum_{i=1}^{44} S_i F(f)_i + \sum_{k=1}^{30} S_k F(f)_k \tag{A.19}$$

$$F = F' - jF'' \tag{A.20}$$

where S is the line strength in khz (see table A.1) and F is the line shape function in Ghz^{-1}. The shape function used was the Van Vleck-Weisskof as modified by Rosenkranz describing the pressure-induced line interference. The line absorption (F'') and dispersion refractivity (F') are given by

$$F''(f) = \frac{A}{X} + \frac{A}{Y} - \delta\left(\frac{f}{\nu_o}\right)\left[\frac{(\nu_o - f)}{X} + \frac{(\nu_o + f)}{Y}\right] \tag{A.21}$$

$$F'(f) = \frac{(B - f)}{X} + \frac{(B + f)}{Y} - \left(\frac{2}{\nu_o}\right) + \delta\left[\frac{A}{X} - \frac{A}{Y}\right] \tag{A.22}$$

respectively, where the following abbreviations were used

$$A = \gamma f / \nu_o \tag{A.23}$$

$$B = (\nu_o^2 + \gamma^2)/\nu_o \approx \nu_o \tag{A.24}$$

$$X = (\nu_o - f)^2 + \gamma^2 \tag{A.25}$$

$$Y = (\nu_o + f)^2 + \gamma^2 \tag{A.26}$$

The parameters in the above abbreviations are shown in table A.1 where ν_o is the line center

Symbol	O_2 lines in air (i)	H^2O lines in air (k)
S, khz	$a_1 10^{-6} p\theta \exp[a_2(1-\theta)]$	$b_1 e\theta^{3.5} \exp[b_2(1-\theta)]$
γ, Ghz	$a_3 10^{-3}(p\theta^{(0.8-a_4)} + 1.1e\theta)$	$b_3 10^{-3}(p\theta^{b4} + b_5 e\theta^{b_6})$
δ	$(a_5 + a_6\theta)10^{-3} p\theta^{0.8}$	0

Table A.1 The Line Parameters for Line Spectra of Absorption

frequency in Ghz and the spectrometric parameters a_1 through a_6 and b_1 through b_6 for the strength S , pressure broadened width γ, and pressure induced interference δ are listed in tables A.3 and A.4.

2. Dry air nonresonant refractivity, N_d, has a small effect at ground level pressure due to the Debye spectrum of oxygen below 10 Ghz and pressure-induced nitrogen absorption the effect of which become noticeable above 100 Ghz. The imaginary and real parts of the nonresonant refractivity term for dry air are defined as follows

$$N_d''(f) = \frac{S_d f}{\gamma_o}\left[1 + \left(\frac{f}{\gamma_o}\right)^2\right] + a_p f p^2 \theta^{3.5} \tag{A.27}$$

$$N_d'(f) = S_d\left(\frac{1}{[1 + (f/\gamma_o)^2]} - 1\right) \tag{A.28}$$

where the the Debye strength S_d and width γ_o, and continuum coefficient a_p are given by

$$S_d = 6.14.10^{-4} p\theta^2 \tag{A.29}$$

$$\gamma_o = 5.6.10^{-3}(p + 1.1e)\theta \tag{A.30}$$

$$a_p = 1.40(1 - 1.2.10{-}5 f^{1.5})10^{-10} \tag{A.31}$$

where p is the partial pressure for dry air in kPa and θ is defined in equation A.6.

3. Water-Vapor Continuum Contribution, N_c. The water-vapor continuum imaginary and real parts are defined as

$$N_c''(f) = f(b_s e + b_f p)10^{-5} e\theta^3 \tag{A.32}$$

$$N_c'(f) = f^2 b_o(1 - 0.20\theta)10^{-5} e\theta^{2.7} \tag{A.33}$$

where e is the partial pressure of water vapor in kPa. These are considered as an addition to enhance the local H_2O line contributions, where

$$b_s = 3.57\theta^{7.5}, \qquad b_f = 0.113, \qquad b_o = 0.998.$$

The three contributions discussed above are the total moist air contributions to the refractivity. The detailed structure of the MPM Model for moist air is shown graphically in figure A.1. It shows the variation in refractivity for a range of relative humidity levels which highlights the molecular resonance absorption at 60 Ghz, 119 Ghz, and higher due to O_2, and near 22 Ghz, 183 Ghz, and higher due to H_2O. This graph shows the importance of relative humidity to describe the water vapor effects of attenuation and dispersion.

4. Suspended Water Droplet Refractivity, N_w. Suspended water droplets account for the effects of haze, fog, and clouds which are good millimeter wave absorbers and scatterers. The real and imaginary parts of refractivity are defined as

$$N_w''(f) = W_l(9/2)[\epsilon''(1+\eta^2)]^{-1} \tag{A.34}$$

$$N_w'(f) = W_l(9/2)\left[\frac{1}{(\epsilon_o+2)} - \frac{\eta}{\epsilon''(1+\eta^2)}\right] \tag{A.35}$$

where $\eta = (2+\epsilon')/\epsilon''$; ϵ_o is the static ($f=0$) permitivity and ϵ', ϵ'' are the real and imaginary parts of of liquid water permitivity which are defined as

$$\epsilon''(f) = (\epsilon_o - \epsilon_1)(f/f_p)[1+(f/f_p)^2] + (\epsilon_1 - \epsilon_2)(f/f_s)[1+(f/f_s)^2] \tag{A.36}$$

$$\epsilon'(f) = \frac{(\epsilon_o - \epsilon_1)}{[1+(f/f_p)^2]} + \frac{(\epsilon_1 - \epsilon_2)}{[1+(f/f_s)^2] + \epsilon_2} \tag{A.37}$$

where $\epsilon_o = 77.66 + 103.3(\theta - 1)$, $\epsilon_1 = 5.48$, and $\epsilon_2 = 3.51$. And the principal and secondary relaxation frequencies in Ghz are $f_p = 20.09 - 142(\theta - 1) + 294(\theta - 1)^2$, and $f_s = 590 - 1500(\theta - 1)$.

5. Rain Effects. The refractivity of rain, N_r, is a function of the rain drop size. When the drop diameter is in the range of 0.1 to 5 mm, substantial interaction takes place between rain drops and electromagnetic waves. To count for the rain effect; the real and imaginary parts of rain refractivity are approximated as

$$N_r''(f) = k_r R_l^z \tag{A.38}$$

$$N_r'(f) = \frac{R_l(0.012R_l - 3.7)y^{2.5}}{[f_r(1 + y^{2.5})]} \tag{A.39}$$

where R_l = rainfall rate in mm/h, $y = f/f_r$ and $f_r = 53 - R_l(0.37 - 0.0015R_l)$, f_r and f are in Ghz. Also $k_r = x_1 f^{y_1}$ and $z = x_2 f^{y_2}$ where the values of x_1, x_2, y_1 and y_2 with respect to frequency, f, in Ghz are shown in table A.2. The effect of rain is shown graphically in figure

f Ghz	x_1	y_1	f GHz	x_2	y_2
$1 to 2.9$	$3.51.10^{-4}$	1.03	$1 to 8.5$	0.851	0.158
$2.9 to 54$	$2.31.10^{-4}$	1.42	$8.5 to 25$	1.41	-0.0779
$54 to 180$	0.225	-0.301	$25 to 164$	2.63	-0.272
$180 to 1000$	18.6	-1.151	$164 to 1000$	0.616	0.0126

Table A.2 Values of Regression Fit Variables x_1, x_2, y_1 and y_2

A.2. This figure shows attenuation and phase dispersion due to four levels of rainfall rate. It can be seen that rain has a major effect on signal propagation.

ν_o	a_1	a_2	a_3	a_4	a_5	a_6
50.474238	0.94	9.694	8.60	0	1.600	5.520
50.987749	2.46	8.694	8.70	0	1.400	5.520
51.503350	6.02	7.744	8.90	0	1.165	5.520
52.021410	14.14	6.844	9.20	0	0.883	5.520
52.542394	31.02	6.004	9.40	0	0.579	5.520
53.066907	64.10	5.224	9.70	0	0.252	5.520
53.595749	124.70	4.484	10.00	0	-0.066	5.520
54.130000	228.00	3.814	10.20	0	-0.314	5.520
54.671159	391.80	3.194	10.50	0	-0.706	5.520
55.221367	631.60	2.624	10.79	0	-1.151	5.514
55.783802	953.50	2.119	11.10	0	-0.920	5.025
56.264775	548.90	0.015	16.46	0	2.881	-0.069
56.363389	1344.00	1.660	11.44	0	-0.596	4.750
56.968206	1763.00	1.260	11.81	0	-0.556	4.104
57.612484	2141.00	0.915	12.21	0	-2.414	3.536
58.323877	2386.00	0.626	12.66	0	-2.635	2.686
58.446590	1457.00	0.084	14.49	0	6.848	-0.647
59.164207	2404.00	0.391	13.19	0	-6.032	1.858
59.590983	2112.00	0.212	13.60	0	8.266	-1.413
60.306061	2124.00	0.212	13.82	0	-7.170	0.916
60.434776	2461.00	0.391	12.97	0	5.664	-2.323
61.150560	2504.00	0.626	12.48	0	1.731	-3.039
61.800154	2298.00	0.915	12.07	0	1.738	-3.797
62.411215	1933.00	1.260	11.71	0	-0.048	-4.277
62.486260	1517.00	0.083	14.68	0	-4.290	0.238
62.997977	1503.00	1.665	11.39	0	0.134	-4.860
63.568518	1087.00	2.115	11.08	0	0.541	-5.079
64.127767	733.50	2.620	10.78	0	0.814	-5.525
64.678903	463.50	3.195	10.50	0	0.415	-5.520
65.224071	274.80	3.815	10.20	0	0.069	-5.520
65.764772	153.00	4.485	10.00	0	-0.143	-5.520
66.302091	80.09	5.225	9.70	0	-0.428	-5.520
66.836830	39.46	6.005	9.40	0	-0.726	-5.520
67.369598	18.32	6.845	9.20	0	-1.002	-5.520
67.900867	8.01	7.745	8.90	0	-1.255	-5.520
68.431005	3.30	8.695	8.70	0	-1.500	-5.520
68.960311	1.28	9.695	8.60	0	-1.700	-5.520
118.750343	945.00	0.009	16.30	0	-0.247	0.003
368.498350	67.90	0.049	19.20	0.6	0	0
424.763124	638.00	0.044	19.16	0.6	0	0
487.249370	235.00	0.049	19.20	0.6	0	0
715.393150	99.60	0.145	18.10	0.6	0	0
773.839675	671.00	0.130	18.10	0.6	0	0
834.145330	180.00	0.147	18.10	0.6	0	0

Table A.3 Local Line Data File of MPM Model for Moist Air (a_i for O_2)

ν_o	b_1	b_2	b_3	b_4	b_5	b_6
22.235	0.109	2.143	28.110	0.690	4.800	1.000
67.814	0.001	8.735	28.580	0.690	4.930	0.820
119.996	0.001	8.356	29.480	0.700	4.780	0.790
183.310	2.300	0.668	28.130	0.640	5.300	0.850
321.226	0.046	6.181	23.030	0.670	4.690	0.540
325.153	1.540	1.540	27.830	0.680	4.850	0.740
336.187	0.001	9.829	26.930	0.690	4.740	0.610
380.197	11.900	1.048	28.730	0.690	5.380	0.840
390.135	0.004	7.350	21.520	0.630	4.810	0.550
437.347	0.064	5.050	18.450	0.600	4.230	0.480
439.151	0.921	3.596	21.000	0.630	4.290	0.520
443.018	0.194	5.050	18.600	0.600	4.230	0.500
448.001	10.600	1.405	26.320	0.660	4.840	0.670
470.889	0.330	3.599	21.520	0.660	4.570	0.650
474.689	1.280	2.381	23.550	0.650	4.650	0.640
488.491	0.253	2.853	26.020	0.690	5.040	0.720
503.569	0.037	6.733	16.120	0.610	3.980	0.430
504.482	0.013	6.733	16.120	0.610	4.010	0.450
556.936	510.000	0.159	32.100	0.690	4.110	1.000
620.701	5.090	2.200	24.380	0.710	4.680	0.680
658.007	0.274	7.820	32.100	0.690	4.140	1.000
752.033	250.000	0.396	30.600	0.680	4.090	0.840
841.074	0.013	8.180	15.900	0.330	5.760	0.450
859.865	0.133	7.989	30.600	0.680	4.090	0.840
899.407	0.055	7.917	29.850	0.680	4.530	0.900
902.555	0.038	8.432	28.650	0.700	5.100	0.950
906.206	0.183	5.111	24.080	0.700	4.700	0.530
916.172	8.560	1.442	26.700	0.700	4.780	0.780
970.315	9.160	1.920	25.500	0.640	4.940	0.670
987.927	138.000	0.258	29.850	0.680	4.550	0.900

Table A.4 Local Line Data File of MPM Model for Moist Air (b_k for H_2O)

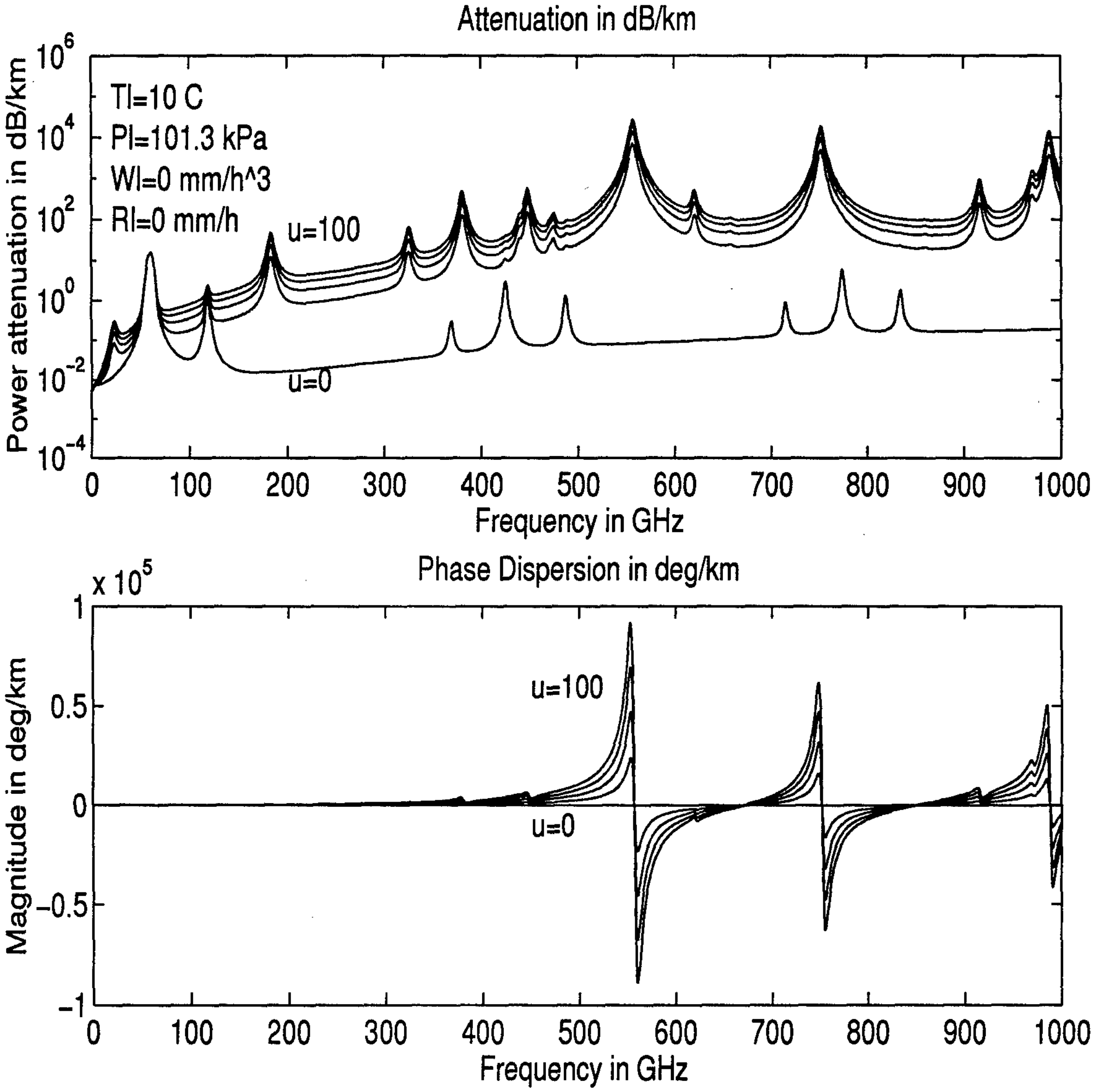

Figure A.1 Attenuation And Phase Dispersion At Various Relative Humidities, 0, 25, 50 and 100 RH

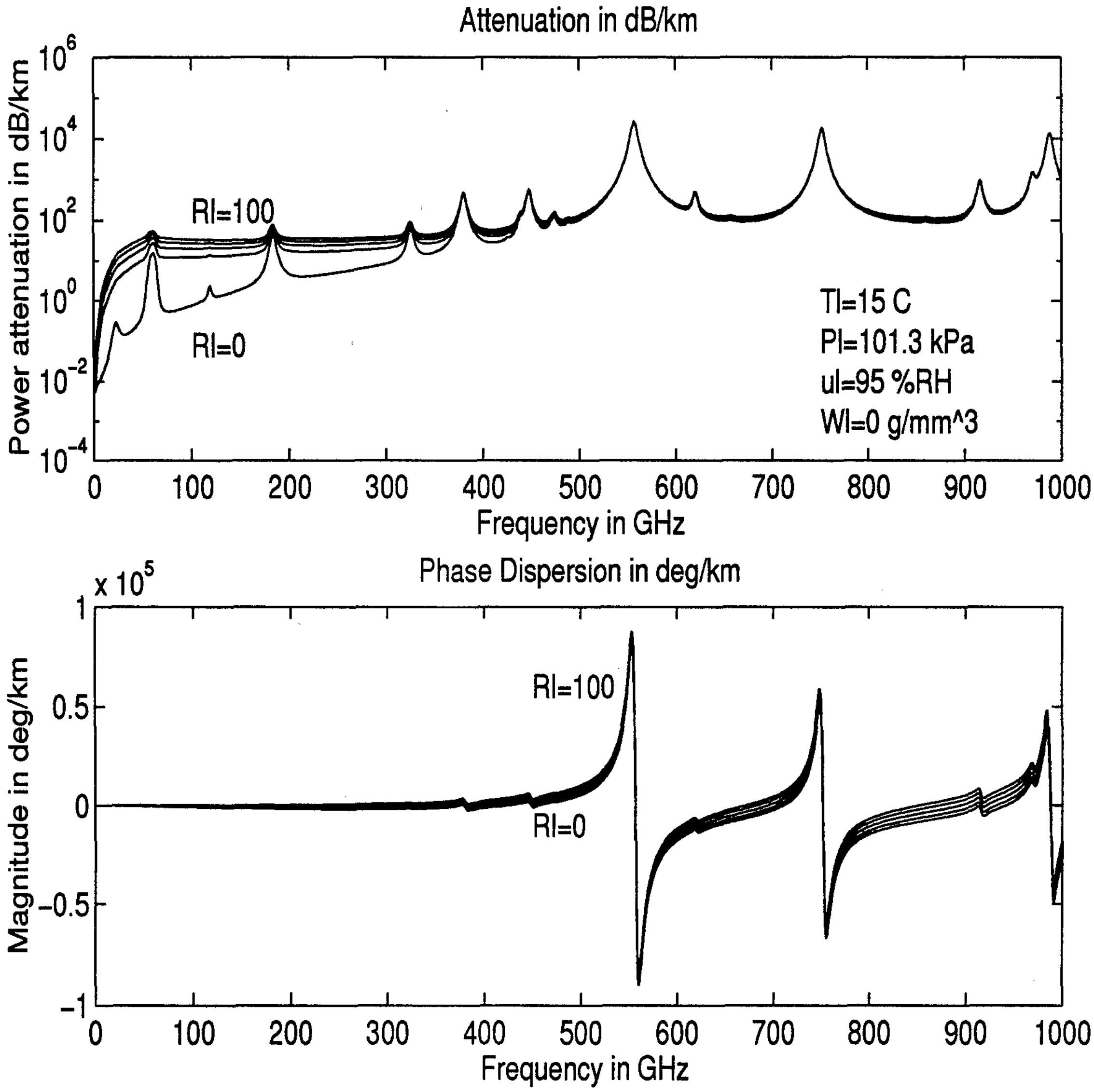

Figure A.2 Attenuation And Phase Dispersion For Various Rainfall Rates

Appendix B. Wideband Radiometer

A radiometer is a signal energy estimating device which detects the presence or absence of a signal within a given bandwidth, W, over an observation time, T. Normally, it is desirable to have W and T matched to those of the signal desired to be detected. The radiometer block diagram is shown in figure B.1.

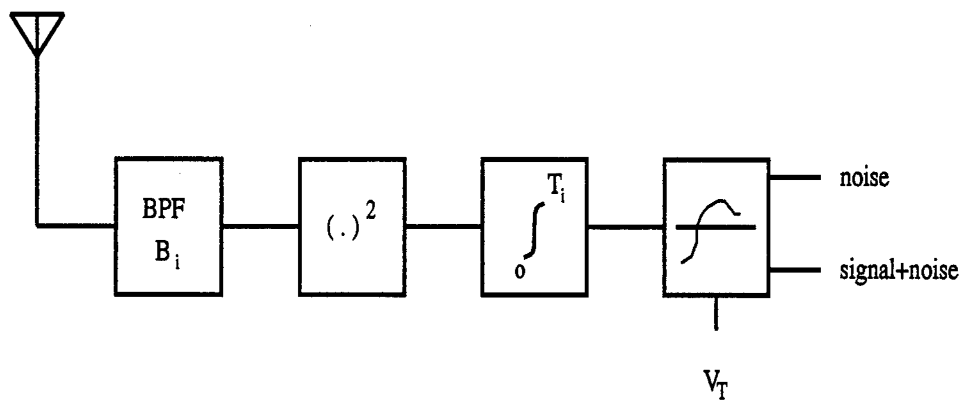

Figure B.1 Radiometer Block Diagram

The radiometer consists of a bandpass filter (BPF) with bandwidth B_i, followed by a squaring circuit, an integrating circuit over an observation period T_i, and a threshold detection circuit of threshold V_T. Now following the signal through the system analytically will yield a relationship between the radiometer parameters probability of detection P_d, probability of false alarm P_f, B_i, and T_i and the required signal-to-noise ratio(SNR) for detection. Assuming signal plus noise is present at the radiometer input, the BPF output, $x(t)$ is

$$x(t) = s(t) + n(t) \tag{B.1}$$

where

- $s(t)$ is the signal coming through the BPF of bandwidth B_i

- $n(t)$ is the noise (AWGN) coming through the BPF of bandwidth B_i This BPF output is then squared by the squaring circuit giving

$$y(t) = [s(t) + n(t)]^2 \tag{B.2}$$

The output of the squaring circuit is then integrated over a period T_i, giving

$$\begin{aligned}
v(t) &= \int_0^{T_i} y(t)dt &\text{(B.3)}\\
v(t) &= \int_0^{T_i} [s(t) + n(t)]^2 \, dt &\text{(B.4)}\\
v(t) &= \int_0^{T_i} \left[s(t)^2 + 2s(t)n(t) + n(t)^2\right] dt &\text{(B.5)}
\end{aligned}$$

Taking the expected value of $v(t)$ to get the energy, assuming $n(t)$ a zero-mean random process having a two-sided power spectral density (PSD) of $N_o/2$ and assuming the noise is uncorrelated with the signal, the following is obtained

$$\begin{aligned}
E[v(t)] &= \int_0^{T_i} E[s(t)^2 + 2s(t)n(t) + n(t)^2]dt &\text{(B.6)}\\
E[v(t)] &= \int_0^{T_i} \left[E[s(t)^2] + 2E[s(t)n(t)] + E[n(t)^2]\right] dt &\text{(B.7)}\\
E[v(t)] &= \int_0^{T_i} \left[E[s(t)^2]\right] dt + \int_0^{T_i} \left[E[n(t)^2]\right] dt &\text{(B.8)}\\
E[v] &= E_s + N_o T_i B_i &\text{(B.9)}
\end{aligned}$$

where E_s is the signal energy and $N_o T_i B_i$ is noise energy. Dividing the input signal energy by the input noise energy, one obtains the input signal-to-noise ratio SNR_{IN}

$$SNR_{IN} = \frac{E_s}{N_o T_i B_i} \tag{B.10}$$

The corresponding output SNR is given by [2]

$$SNR_{OUT} = \frac{SNR_{IN}^2 T_i B_i}{1 + 2SNR_{IN}} \tag{B.11}$$

For a radiometer, the SNR at the input is usually small which reduces equation B.11 to

$$SNR_{OUT} = SNR_{IN}^2 T_i B_i \tag{B.12}$$

the output SNR in equation B.12 is also known as the detectability factor, d^2. This factor can also be related to the radiometer performance parameters by

$$d^2 = \left[Q^{-1}(P_f) - Q^{-1}(P_d)\right]^2 \tag{B.13}$$

where Q^{-1} is the inverse error function. Now equating equation B.12 with equation B.13 gives

$$SNR_{IN} = \frac{d}{\sqrt{T_i B_i}} \tag{B.14}$$

but

$$SNR_{IN} = \frac{S_{IN}}{N_{IN}} = \frac{S_{IN}}{N_o B_i} = \frac{d}{\sqrt{T_i B_i}} \tag{B.15}$$

The input SNR is the minimum required for the radiometer to be able to detect the presence of a signal. Therefore, using equation B.15 the required SNR, SNR_{req}, can be defined as

$$SNR_{req} = \frac{S_{IN}}{N_o B_i} = \frac{d}{\sqrt{T_i B_i}} \tag{B.16}$$

Bibliography

1. Madden, C.B. *Effect of Jamming and Excision Filtering Upon Error Rate and Detectability of a Spread Spectrum Communications Systems.* MSEE Thesis, Air Force Institute of Technology, Wright Paterson AFB OH, December 1995.

2. Nicholson, D.L. *Spread Spectrum Signals Design: LPE and AJ systems*, Computer Science Press: Rockville, MD, 1988.

3. Gutman, L.L. and G.E. Prescott "System Quality Factors for LPI Communications," *IEEE Aerospace and Electronics Systems Magazine*,pp. 25-28, December 1989.

4. De Arcangelis, Mario *Electronic Warfare*, Blandford Press: UK. Dorset, 1985.

5. Vorst, V. and Vanhoenacker, D. "Propagation Limitations For Transionspheric Systems From 10 To 300 GHz," Advisory Group For Aerospace Research And Development (France) Technical Report AGARD-LS-172, June 1990.

6. Hall, M.P. *Effects of The Troposphere on Radio Communication*, Peter Pereginus Ltd: London, 1986.

7. Liebe, H.J. "MPM-An Atmospheric Millimeter-Wave Propagation Model," *International Journal of Infrared and Millimeter Waves*, Vol. 10, No. 6, pp. 631-650, 1989.

8. Liebe, H. J. "An Updated Model For Millimeter Wave Propagation In Moist Air," *Radio Science*, Vol. 20, No. 5, pp.1069-1089, September-October 1985.

9. Flock, W.L. *Propagation Effects on Satellite Systems at Frequencies Bellow 10GHz: A Handbook for Satellite System Design*, (Second Edition). National Aeronautics and Space Administration, 1987.

10. O'Brien, W.J., et.al. "On Achieving Network LPI for Spread Spectrum Communications," Army Research Office Technical Report ARO 21611.3-EL (NTIS AD-A 163 985), E-Systems, Inc., Fairfax, VA, October 1985.

11. Mills, R.F. *Detectability models and Waveform Design for Multiple Access Low-Probability-of-Intercept Networks.* PhD dissertation. University of Kansas, Kansas KA, 1994.

12. Mills, R.F. and Prescott, G. E. "A Comparison of Various Radiometer detection Models," *IEEE Transaction on Aerospace And Electronic Systems*, Vol. 32, No. 1, pp. 467-473, January 1996.

13. Boithias, L. *Radiowave Propagation*, McGraw-Hill: New York, 1987.

14. Sklar, B. *Digital Communications: Fundamentals and Applications*, Prentice-Hall: Englewood Cliffs, NJ, 1988.

15. Skolnik, M.I. *Introduction to Radar Systems*, (Second Edition). McGraw-Hill: New York, 1980.

    Egli J. J. "Radio Propogation Above 40 *Mc* over irregular terrain," *Proc. IRE*, Vol. 45, No. 10, 1957.

16. Parsons, D. *The Mobile Radio Propagation Channel*, Halsted Press: New York, 1992.

17. Parsons, D. and Gardiner, G. *Mobile Communication Systems*, Halsted Press: New York, 1989.

18. Delisle, G. Y., Lefevre J.P., Lecours, M. and Chourianrd J. Y. "Propagation Loss Prediction: A Comparative Study With Application to Mobile Radio Channel," *IEEE Trans.*, VT-34, No. 2, pp. 86-95, May 1985.

19. Levanon, N. *Radar Principles*, John Wiley and Sons: New York, 1988.

20. Kraus, J. D. *Antennas*, (Second Edition). McGraw-Hill: New York, 1988.

21. Griffiths, J. *Radio Wave Propagation And Antennas An Introduction*, Prentice-Hall: U.K. London, 1987.

22. Cheng, D. K. *Field and Wave Electromagnetics*, (Second Edition). Addison-Wesley: New York, 1990.

23. Feher, Kamilo *Wireless Digital Communications Modulation And Spread Spectrum Applications*, Prentice-Hall: NJ, 1995.

24. Kraus, J. D. *Elecromagnetics*, (Forth Edition). McGraw-Hill: New York, 1991.

25. Doviak, R. J. and Zrinc', D. S. *Doppler Radar and Weather Observations*, (Second Edition). Academic Press Inc:San diego, CA, 1993.

26. Peterson, R. L., Ziemer R. E.and Borth D. E. *Introduction to Spread Spectrum Communications*, Prentice-Hall: Englewood Cliffs, NJ, 1995.

27. Hata, M. "Empirical Formula for Propagation Loss in Land Mobile Radio Service," *IEEE TRANS. Vehicular Technology*, VT-29, No. 3, pp. 317-325, August 1980.

28. Mills R. F. Class Notes, EENG 673, "Applications of Communication Technology," School of Engineering, Air Force Institute of Technology, Wright-Patterson AFB OH, Summer Quarter 1995.

29. Gutman, L. L. Notes on Low-Probability-of-Intercept (LPI) Communications, EENG 700, "Seminar in Remote Sensing," School of Engineering, Air Force Institute of Technology, Wright-Patterson AFB OH, Winter Quarter 1995.

30. Shi, J. Zheng, Y. and Song, J. "A Set of New Radio Propagation Models Based on The Measurements in Chinese Environments," Proc. SPIE, Vol. 2556, pp. 58-68, 1995.

Vita

Ala B. Ghordlo [redacted] he joined the Royal Jordanian Air Force (RJAF), and was selected to study electrical and electronic engineering in the U.K. In June 1988, he graduated from The University of Nottingham/England with a Bachelor of Engineering Degree in Electrical and Electronic Engineering and was promoted to a Second Lieutenant in the RJAF and was subsequently promoted to First Lieutenant in June 1989 and Captain in June 1992. In March 1994 he was selected by the RJAF to earn his Masters of Electrical Engineering Degree at the Air Force Institute of Technology at Wright-Patterson AFB. After graduation, Capt. Ghordlo will be serving in the Communications Wing in the RJAF.

Permanent address: P.O. BOX 889
ZARKA-JORDAN
JORDAN

REPORT DOCUMENTATION PAGE

Form Approved
OMB No. 0704-0188

Public reporting burden for this collection of information is estimated to average 1 hour per response, including the time for reviewing instructions, searching existing data sources, gathering and maintaining the data needed, and completing and reviewing the collection of information. Send comments regarding this burden estimate or any other aspect of this collection of information, including suggestions for reducing this burden, to Washington Headquarters Services, Directorate for Information Operations and Reports, 1215 Jefferson Davis Highway, Suite 1204, Arlington, VA 22202-4302, and to the Office of Management and Budget, Paperwork Reduction Project (0704-0188), Washington, DC 20503.

1. AGENCY USE ONLY *(Leave blank)*

2. REPORT DATE
December 1996

3. REPORT TYPE AND DATES COVERED
Master's Thesis

4. TITLE AND SUBTITLE
Analysis of Multimode Low-Probability-of-Intercept (LPI) Communications With Atmospheric Effects

5. FUNDING NUMBERS

6. AUTHOR(S)
Ala Ghordlo
Captain, RJAF

7. PERFORMING ORGANIZATION NAME(S) AND ADDRESS(ES)
Air Force Institute of Technology, WPAFB OH 45433-6583

8. PERFORMING ORGANIZATION REPORT NUMBER
AFIT/GE/ENG/96D-03

9. SPONSORING/MONITORING AGENCY NAME(S) AND ADDRESS(ES)
Lawrence Gutman
WL/AAMI
2185 Avionics Circle
WPAFB, OH 45433-7301

10. SPONSORING/MONITORING AGENCY REPORT NUMBER

11. SUPPLEMENTARY NOTES

12a. DISTRIBUTION/AVAILABILITY STATEMENT
Approved for Public release; Distribution Unlimited

12b. DISTRIBUTION CODE

13. ABSTRACT *(Maximum 200 words)*
This research expanded Low-Probability-of-Intercept (LPI) communications in two areas. First, multimode communications was included to account for ground-to-ground and air-to-ground links in addition to the standard air-to-air links traditionally used in LPI analysis. Second, atmospheric conditions were included to account for atmospheric attenuation. In previous LPI analysis atmospheric effects were assumed negligible. Therefore, atmospheric attenuation had to be included to include scenarios where the communication and interception links are experiencing different and possibly fluctuating atmospheric conditions. The analyses and simulations performed on LPI links, including mode and atmospheric effects in LPI analysis clearly showed that these two factors play a dramatic role in LPI analysis.

14. SUBJECT TERMS
Low-Probability-of-Intercept (LPI) Communications, Atmospheric Effects, Propagation Modes, Communications Modes and Boundaries,Spread Spectrum

15. NUMBER OF PAGES
130

16. PRICE CODE

17. SECURITY CLASSIFICATION OF REPORT	18. SECURITY CLASSIFICATION OF THIS PAGE	19. SECURITY CLASSIFICATION OF ABSTRACT	20. LIMITATION OF ABSTRACT
UNCLASSIFIED	UNCLASSIFIED	UNCLASSIFIED	UL

GENERAL INSTRUCTIONS FOR COMPLETING SF 298

The Report Documentation Page (RDP) is used in announcing and cataloging reports. It is important that this information be consistent with the rest of the report, particularly the cover and title page. Instructions for filling in each block of the form follow. It is important to ***stay within the lines*** to meet ***optical scanning requirements***.

Block 1. Agency Use Only *(Leave blank)*.

Block 2. Report Date. Full publication date including day, month, and year, if available (e.g. 1 Jan 88). Must cite at least the year.

Block 3. Type of Report and Dates Covered. State whether report is interim, final, etc. If applicable, enter inclusive report dates (e.g. 10 Jun 87 - 30 Jun 88).

Block 4. Title and Subtitle. A title is taken from the part of the report that provides the most meaningful and complete information. When a report is prepared in more than one volume, repeat the primary title, add volume number, and include subtitle for the specific volume. On classified documents enter the title classification in parentheses.

Block 5. Funding Numbers. To include contract and grant numbers; may include program element number(s), project number(s), task number(s), and work unit number(s). Use the following labels:

C	-	Contract	**PR**	-	Project
G	-	Grant	**TA**	-	Task
PE	-	Program Element	**WU**	-	Work Unit Accession No.

Block 6. Author(s). Name(s) of person(s) responsible for writing the report, performing the research, or credited with the content of the report. If editor or compiler, this should follow the name(s).

Block 7. Performing Organization Name(s) and Address(es). Self-explanatory.

Block 8. Performing Organization Report Number. Enter the unique alphanumeric report number(s) assigned by the organization performing the report.

Block 9. Sponsoring/Monitoring Agency Name(s) and Address(es). Self-explanatory.

Block 10. Sponsoring/Monitoring Agency Report Number. *(If known)*

Block 11. Supplementary Notes. Enter information not included elsewhere such as: Prepared in cooperation with...; Trans. of...; To be published in.... When a report is revised, include a statement whether the new report supersedes or supplements the older report.

Block 12a. Distribution/Availability Statement. Denotes public availability or limitations. Cite any availability to the public. Enter additional limitations or special markings in all capitals (e.g. NOFORN, REL, ITAR).

DOD - See DoDD 5230.24, "Distribution Statements on Technical Documents."
DOE - See authorities.
NASA - See Handbook NHB 2200.2.
NTIS - Leave blank.

Block 12b. Distribution Code.

DOD - Leave blank.
DOE - Enter DOE distribution categories from the Standard Distribution for Unclassified Scientific and Technical Reports.
NASA - Leave blank.
NTIS - Leave blank.

Block 13. Abstract. Include a brief *(Maximum 200 words)* factual summary of the most significant information contained in the report.

Block 14. Subject Terms. Keywords or phrases identifying major subjects in the report.

Block 15. Number of Pages. Enter the total number of pages.

Block 16. Price Code. Enter appropriate price code *(NTIS only)*.

Blocks 17. - 19. Security Classifications. Self-explanatory. Enter U.S. Security Classification in accordance with U.S. Security Regulations (i.e., UNCLASSIFIED). If form contains classified information, stamp classification on the top and bottom of the page.

Block 20. Limitation of Abstract. This block must be completed to assign a limitation to the abstract. Enter either UL (unlimited) or SAR (same as report). An entry in this block is necessary if the abstract is to be limited. If blank, the abstract is assumed to be unlimited.